

**ANALYSIS OF TOTAL HARMONIC  
DISTORTION AND SWITCHING LOSSES OF  
PWM IN GRID-CONNECTED PHOTOVOLTAIC  
SYSTEM**

**SYAHIERAH ELIYA BINTI SABRI**

**UMP**

**MASTER OF SCIENCE**

**UNIVERSITI MALAYSIA PAHANG**

## UNIVERSITI MALAYSIA PAHANG

### DECLARATION OF THESIS AND COPYRIGHT

Author's Full Name : SYAHIERAH ELIYA BINTI SABRI  
Date of Birth : 30/12/1993  
Title : ANALYSIS OF TOTAL HARMONIC DISTORTION AND  
SWITCHING LOSSES OF PWM IN GRID-CONNECTED  
PHOTOVOLTAIC SYSTEM  
Academic Session : SEMESTER 2 2018/2019

I declare that this thesis is classified as:

- CONFIDENTIAL (Contains confidential information under the Official Secret Act 1997)\*
- RESTRICTED (Contains restricted information as specified by the organization where research was done)\*
- OPEN ACCESS I agree that my thesis to be published as online open access (Full Text)

I acknowledge that Universiti Malaysia Pahang reserves the following rights:

1. The Thesis is the Property of Universiti Malaysia Pahang
2. The Library of Universiti Malaysia Pahang has the right to make copies of the thesis for the purpose of research only.
3. The Library has the right to make copies of the thesis for academic exchange.

Certified by:

\_\_\_\_\_  
(Student's Signature)

931230-11-5416

\_\_\_\_\_  
New IC/Passport Number  
Date:

\_\_\_\_\_  
(Supervisor's Signature)

IR DR MUHAMAD ZAHIM  
BIN SUJOD

\_\_\_\_\_  
Name of Supervisor  
Date:

NOTE : \* If the thesis is CONFIDENTIAL or RESTRICTED, please attach a thesis declaration letter.

## SUPERVISOR'S DECLARATION

We hereby declare that we have checked this thesis and in our opinion, this thesis is adequate in terms of scope and quality for the award of the degree of Master of Science.

---

(Supervisor's Signature)

Full Name : IR DR MUHAMAD ZAHIM BIN SUJOD

Position : SENIOR LECTURER

Date :

---

(Co-supervisor's Signature)

Full Name : DR MOHD SHAWAL BIN JADIN

Position : SENIOR LECTURER

Date :

### **STUDENT'S DECLARATION**

I hereby declare that the work in this thesis is based on my original work except for quotations and citations which have been duly acknowledged. I also declare that it has not been previously or concurrently submitted for any other degree at Universiti Malaysia Pahang or any other institutions.

---

(Student's Signature)

Full Name : SYAHIERAH ELIYA BINTI SABRI

ID Number : MEE16010

Date :



UMP

ANALYSIS OF TOTAL HARMONIC DISTORTION AND SWITCHING LOSSES  
OF PWM IN GRID-CONNECTED PHOTOVOLTAIC SYSTEM



SYAHIERAH ELIYA BINTI SABRI

Thesis submitted in fulfillment of the requirements  
for the award of the degree of  
Master of Science

UMP

Faculty of Electrical & Electronics Engineering

UNIVERSITI MALAYSIA PAHANG

AUGUST 2019

## ACKNOWLEDGEMENTS

First and foremost, I would like to thank Allah SWT to enable me to complete my Master and thesis on “Analysis of total harmonic distortion and switching losses of PWM in grid-connected photovoltaic system”. Furthermore, He gives me the power to believe in my passion and pursue my dream.

I offer my sincerest gratitude to my supervisor, Ir. Dr. Muhamad Zahim and my co-supervisor, Dr. Mohd Shawal for the continuous support to complete the research, for their patience, advices, guides and immense knowledge which has motivated me in completing this research.

Last but not least, it is impossible to complete this research without support from my parents, family, Muhammad Amirul, and helps from my colleagues especially Noor Aisyah during my hard time.



UMP

## ABSTRAK

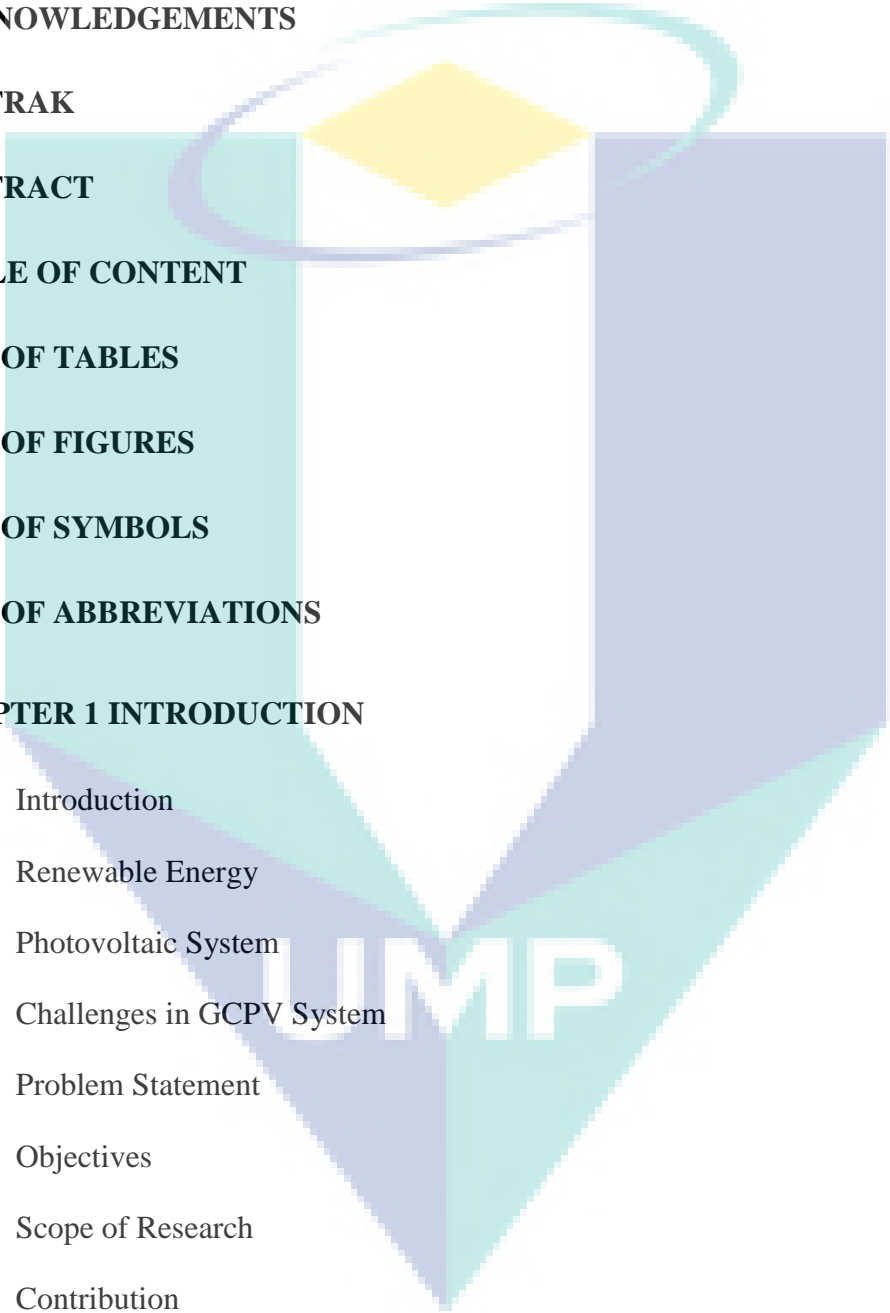
Sistem fotovoltaik (PV) menjadi pilihan tenaga alternatif terbaik untuk menjana elektrik yang boleh menggantikan sumber bahan api dan pada masa yang sama tidak memudaratkan persekitaran. Sistem PV yang disambung ke grid (GCPV) membekalkan tenaga arus ulang alik (AC) yang dijana ke grid utiliti untuk diagihkan kepada pengguna. Dalam sistem GCPV, penukar arus terus (DC) kepada AC adalah suatu kemestian tetapi merupakan beban tidak linear yang menjana lebih banyak jumlah herotan harmonik (THD) ke dalam sistem kuasa elektrik. Harmonik yang dijana oleh sistem PV akan menurunkan kualiti grid kuasa dan memberi kesan terhadap kebolehpercayaan dan keselamatan. IEEE Std 519-1992 dan piawaian Tenaga Nasional Berhad (TNB) menggariskan THD perlu kurang dari 5% dalam kadar keluaran penukar DC kepada AC pada kabel yang disambung ke titik gabungan sepunya (PCC). Disamping itu, tahap sinaran suria di Malaysia adalah berbeza sepanjang hari serta sepanjang tahun. Kesan tahap sinaran suria yang rendah akan menyebabkan keluaran susun atur PV rendah dan masukan penukar DC kepada AC secara relatif menjadi rendah. Penukar DC kepada AC menunjukkan tidak kelinearan yang besar apabila penukar DC kepada AC beroperasi dengan masukan kuasa rendah ketika sinaran suria berada pada tahap rendah. THD dalam sistem GCPV dipengaruhi oleh tahap sinaran suria kerana hubungan antara tahap sinaran suria dan THD adalah berkadar songsang. Tambahan pula, perkaitan utama yang lain dalam sistem GCPV adalah kehilangan pensuisan pada alat pensuisan dalam penukar DC kepada AC. Keberkesanan sistem boleh ditingkatkan dengan melaraskan kehilangan pensuisan serendah mungkin. Teknik Pemedulat Pulsa Lebar (PWM) mempunyai kelebihan tersendiri seperti mudah dilaksanakan dan dikawal, serasi dengan pemproses mikro masa kini, tiada komponen tambahan diperlukan bagi mengawal voltan keluaran dan akhir sekali, harmonik lebih rendah boleh dikurangkan atau dihapuskan. Dalam kajian ini, objektif utama adalah untuk mengendalikan kajian bagi mengurangkan harmonik dan kehilangan pensuisan dalam sistem GCPV. Model sistem GCPV MATLAB/Simulink dipilih sebagai platform untuk melaksanakan PWM berterusan (CPWM) dan PWM tidak berterusan (DPWM) dalam pengawalan penukar DC kepada AC bagi mengkaji kesan pilihan ulangan pensuisan PWM ke atas THD dan prestasi kehilangan pensuisan pada tahap sinaran suria yang berbeza. Bilamana teknik-teknik ini dibandingkan, didapati CPWM ternyata sebagai pilihan penyelesaian terbaik. Hal ini disebabkan oleh nilai THD yang rendah diperolehi apabila CPWM dilaksanakan dalam kawalan penukar DC kepada AC. Tambahan pula, THD apabila DPWM dilaksanakan adalah lebih tinggi berbanding CPWM pada semua tahap sinaran suria. Nilai ulangan pensuisan yang bersesuaian pada tahap sinaran suria yang berbeza yang memenuhi piawaian keperluan THD serta kehilangan pensuisan yang minimum dicadangkan dalam tesis ini. Nilai ulangan pensuisan yang bersesuaian bagi setiap julat tahap sinaran suria adalah  $f_{sw1} = 12600.00$  Hz semasa  $200 - 400 \text{ W/m}^2$ ,  $f_{sw2} = 5000.00$  Hz semasa  $401 - 600 \text{ W/m}^2$ ,  $f_{sw3} = 1746.00$  Hz semasa  $601 - 800 \text{ W/m}^2$  dan  $f_{sw4} = 1545.50$  Hz untuk  $801 - 1000 \text{ W/m}^2$  tahap sinaran suria. Sementara itu, DPWM memerlukan ulangan pensuisan yang tinggi bagi mencapai piawaian THD dan hasilnya adalah mendorong kepada kehilangan pensuisan yang tinggi dalam sistem. Penemuan utama dalam penyelidikan ini adalah pemilihan ulangan pensuisan PWM yang bersesuaian boleh mengurangkan THD pada tahap sinaran suria yang berbeza.

## ABSTRACT

Photovoltaic (PV) system becomes the best alternative energy choice to produce electricity that can replace fuel resource and at the same time not harmful to our environment. Grid-connected PV (GCPV) system supply the AC power generated to the utility grid then distributed to the consumer. In a GCPV system, an inverter is a mandatory, but it is a non-linear load that generates more total harmonic distortion (THD) into the electrical power system. Harmonic generated by the PV system may downgrade the quality of power grid and affect the reliability and safety. IEEE Std 519-1992 and the largest Malaysia electricity utility company Tenaga Nasional Berhad (TNB) standard stated that, THD should be less than 5 % in the rated inverter output of the cable connected to Points of Common Coupling (PCC). Moreover, the solar irradiance in Malaysia varies daily and also throughout the year. The consequence of low irradiance level is that the output of the PV array is low and thus the input of the inverter relatively becoming low. The inverter exhibit large non-linearity when the inverter is operating at low power input during the low level of solar irradiance. The THD in a GCPV system is influenced by the solar irradiance due to the inversely proportional relationship between solar irradiance and THD. In addition, other main concerns in the GCPV system are switching losses of the switching devices in the inverter. The effectiveness of a system can improve by keeping the switching losses as low as possible. Pulse Width Modulation (PWM) techniques has its own benefits such as easy to implement and control, compatible with today's digital microprocessor, no additional components needs to be added to obtain control of the output voltage and lastly, lower harmonics can be eliminated or minimized. In this research, the main objective is to carry out research to minimize harmonics and switching loss reduction in the GCPV system. A GCPV system model in MATLAB/Simulink is used as the platform to implement continuous PWM (CPWM) and discontinuous PWM (DPWM) in the inverter control to investigate the effect of PWM switching frequency selection on THD and switching losses performance at different level of solar irradiance. The techniques were compared and CPWM is suggested as the recommended solution. This is due to the lower THD value obtained when CPWM applied in the inverter control. Additionally, the THD when DPWM applied is higher compared to CPWM at all solar irradiance levels. The appropriate minimum switching frequency of the PWM at different solar irradiance level that meet the standard THD requirement with minimum switching losses is proposed in this thesis. The appropriate switching frequency value for each of the solar irradiance ranges are  $f_{sw1} = 12600.00$  Hz during 200 – 400 W/m<sup>2</sup>,  $f_{sw2} = 5000.00$  Hz when 401 – 600 W/m<sup>2</sup>,  $f_{sw3} = 1746.00$  Hz throughout 601 – 800 W/m<sup>2</sup> and  $f_{sw4} = 1545.50$  Hz for 801 – 1000 W/m<sup>2</sup> solar irradiance level. Meanwhile, DPWM required higher switching frequency to meet the standard THD and thus lead to higher switching losses in the system. The key finding in this investigation is the appropriate selection of switching frequency of the PWM may decrease the THD content at different solar irradiance level.



# TABLE OF CONTENT

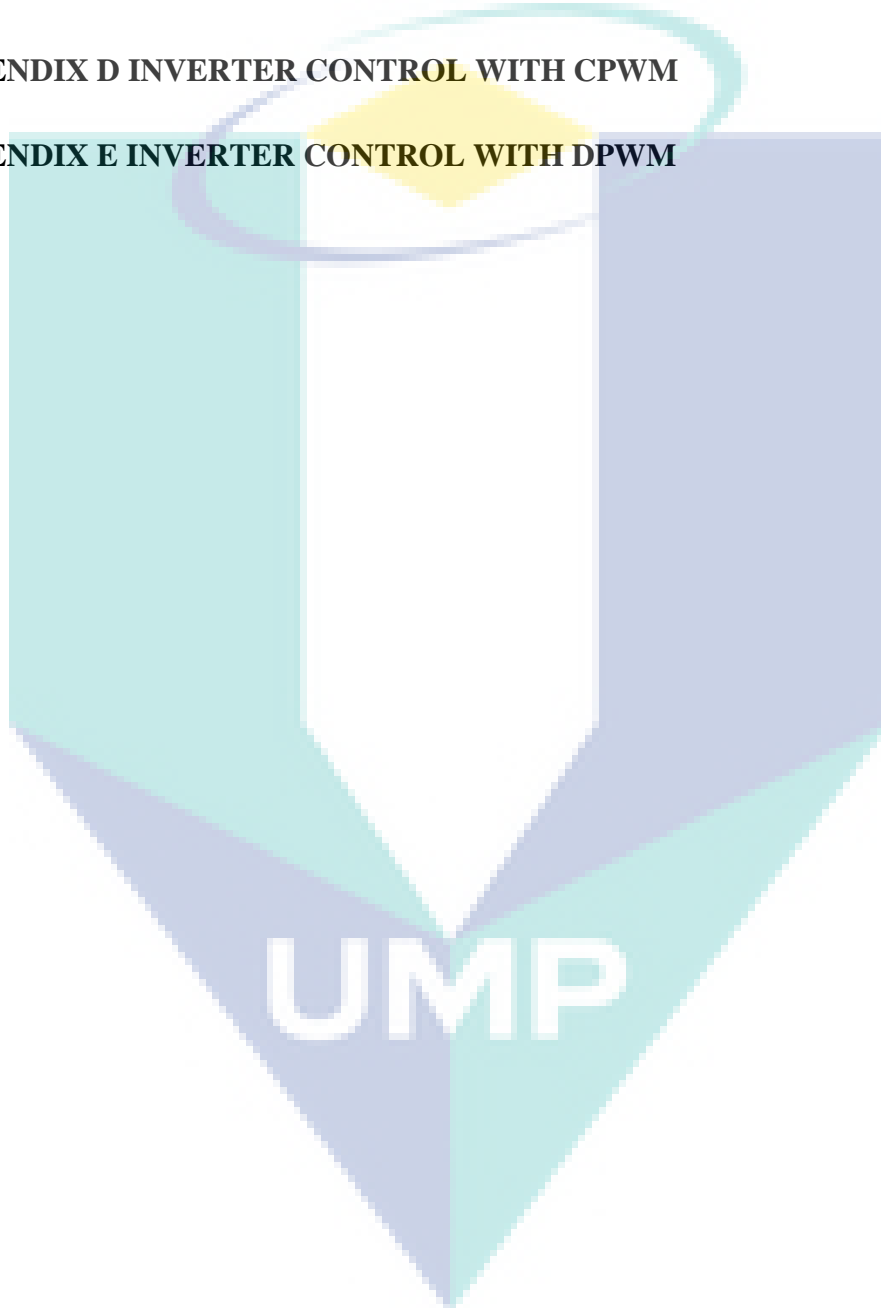


<b>DECLARATION</b>	
<b>TITLE PAGE</b>	
<b>ACKNOWLEDGEMENTS</b>	<b>ii</b>
<b>ABSTRAK</b>	<b>iii</b>
<b>ABSTRACT</b>	<b>iv</b>
<b>TABLE OF CONTENT</b>	<b>v</b>
<b>LIST OF TABLES</b>	<b>ix</b>
<b>LIST OF FIGURES</b>	<b>x</b>
<b>LIST OF SYMBOLS</b>	<b>xii</b>
<b>LIST OF ABBREVIATIONS</b>	<b>xiii</b>
<b>CHAPTER 1 INTRODUCTION</b>	<b>1</b>
1.1 Introduction	1
1.2 Renewable Energy	1
1.3 Photovoltaic System	4
1.4 Challenges in GCPV System	5
1.5 Problem Statement	6
1.6 Objectives	7
1.7 Scope of Research	8
1.8 Contribution	9
1.9 Thesis Organization	9

<b>CHAPTER 2 LITERATURE REVIEW</b>	<b>11</b>
2.1 Introduction	11
2.2 Photovoltaic System	11
2.2.1 Factors Effect the Solar Cell Performance	13
2.2.2 Principle of Operation of GCPV System	14
2.2.3 Designing GCPV Systems	16
2.3 History of Converter	16
2.4 Inverter	17
2.4.1 Voltage Source Inverter	20
2.4.2 PWM-VSI Circuit Design	20
2.4.3 Voltage Source Inverter Basic Operation	22
2.5 Switching Devices	25
2.6 Power Quality Issues	27
2.7 Harmonics	29
2.8 Switching Losses	30
2.9 Pulse Width Modulation	31
2.9.1 Process to Generate PWM	37
2.9.2 Continuous PWM Concept	38
2.9.3 Discontinuous PWM Concept	40
2.10 Passive Filter	43
2.11 Previous Research	45
2.12 Conclusion	50
 <b>CHAPTER 3 METHODOLOGY</b>	 <b>52</b>
3.1 Introduction	52
3.2 Research Methodology	53

3.2.1	GCPV System Configuration	55
3.2.2	PWM Implementation in GCPV System	58
3.2.3	Control of GCPV System Based on CPWM	61
3.2.4	Control of GCPV System Based on DPWM	63
3.2.5	FFT Analysis	64
3.2.6	Switching Losses Analysis	66
3.3	Conclusion	67
<b>CHAPTER 4 RESULTS AND DISCUSSION</b>		<b>68</b>
4.1	Introduction	68
4.2	Performance Analysis	68
4.2.1	Analysis of Output Power at Different Irradiance	69
4.2.2	Analysis THD at Different Irradiance	72
4.2.3	Analysis of Switching Frequency of PWM at Different Irradiance	78
4.2.4	Analysis of Switching Losses between PWM Techniques at Different Irradiance	86
4.3	Discussion	87
4.4	Conclusion	88
<b>CHAPTER 5 CONCLUSION</b>		<b>89</b>
5.1	Recommended Solution	91
5.2	Suggestion for Future Work	92
<b>REFERENCES</b>		<b>93</b>
<b>PUBLICATIONS</b>		<b>101</b>

<b>APPENDIX A LIST OF CPWM CARRIER SIGNAL TRIAL TO FIND STANDARD THD</b>	<b>102</b>
<b>APPENDIX B LIST OF DPWM CARRIER SIGNAL TRIAL TO FIND STANDARD THD</b>	<b>106</b>
<b>APPENDIX C GCPV SYSTEM MODEL MATLAB/SIMULINK CIRCUIT</b>	<b>112</b>
<b>APPENDIX D INVERTER CONTROL WITH CPWM</b>	<b>113</b>
<b>APPENDIX E INVERTER CONTROL WITH DPWM</b>	<b>115</b>



## LIST OF TABLES

Table 2.1	Summation of operation switches in 180° conduction modes	24
Table 2.2	Line to line voltages for 180° conduction mode	25
Table 2.3	Survey on the factors causes power quality problems	29
Table 2.4	Injection of zero sequence signals in the fundamental voltage of PWM	36
Table 3.1	Specification of SunPower SPR-X21-345-COM PV module	56
Table 3.2	Switching frequency selection based on solar irradiance range	58
Table 4.1	Average output current and power of the GCPV system model based on solar irradiance for CPWM and DPWM	70
Table 4.2	THD level for CPWM and DPWM based on different solar irradiance level at 1 kHz switching frequency	73
Table 4.3	Minimum switching frequency of the PWM and THD at different level of solar irradiance	84
Table 4.4	Results of increasing 33 % of CPWM and decreased 33 % of DPWM switching frequency to analyse switching losses	87
Table 5.1	Recommended switching frequency selection based on solar irradiance range	91


UMP

## LIST OF FIGURES

Figure 1.1	Global top 10 solar PV markets total installed shares by the end of 2017	3
Figure 1.2	I-V curve of a PV module	5
Figure 1.3	Frequency occurrence of the global completely clear sky index	8
Figure 2.1	A typical SAPV system configuration	12
Figure 2.2	A typical GCPV system configuration	12
Figure 2.3	Temperature effect on voltage and current output of solar cell	13
Figure 2.4	Solar irradiance effect on voltage and current output	14
Figure 2.5	The main circuit topology of VSI	19
Figure 2.6	The main topology of CSI	19
Figure 2.7	Power converter structures of PWM-VSI	21
Figure 2.8	Three-phase VSI circuit with three-phase balance load connected	22
Figure 2.9	Line to neutral voltage for 180° conduction mode waveform	24
Figure 2.10	Line to line voltage waveform for 180° conduction mode	25
Figure 2.11	IGBT symbol	26
Figure 2.12	Output characteristic of IGBT	27
Figure 2.13	Noise free sinusoidal wave shape of voltage and current of a linear load	28
Figure 2.14	Non-sinusoidal wave shape with power quality problem for a non-linear load	28
Figure 2.15	Two groups of pulses involves in PWM	32
Figure 2.16	The process to generate PWM signal	33
Figure 2.17	Output signal of CPWM and DPWM	34
Figure 2.18	PWM types and categories	35
Figure 2.19	Graph of THD against $m_i$ for CPWM and DPWM signals ( $V_a = \text{SPWM}$ , $V_{a1} = \text{TTHIPWM}$ , $V_{a2} = \text{THIPWM}$ , $V_{a3} = \text{DPWM1}$ , $V_{a4} = \text{DPWM2}$ )	36
Figure 2.20	Process to generate PWM	38
Figure 2.21	Three-phase THIPWM modulated wave	39
Figure 2.22	The process to produce a modulated modulating signal for TTHIPWM	39
Figure 2.23	The process to produce a modulated modulating signal for DPWM0, DPWM1 and DPWM2	41
Figure 2.24	Low pass filter response	44
Figure 2.25	High pass filter response	44

Figure 2.26	Low pass filter circuits	45
Figure 2.27	High pass filter circuit	45
Figure 3.1	Methodology flowchart	55
Figure 3.2	General block diagram of the research	56
Figure 3.3	PWM switching frequency selection	57
Figure 3.4	TTHIPWM modulating signal	59
Figure 3.5	DPWM2 modulating signal	59
Figure 3.6	Comparison between modulation and carrier signal of TTHIPWM	59
Figure 3.7	Comparison between modulation and carrier signal of DPWM2	60
Figure 3.8	TTHIPWM output signal	60
Figure 3.9	DPWM2 output signal	60
Figure 3.10	CPWM (TTHIPWM) subsystem	61
Figure 3.11	DPWM (DPWM2) subsystem	63
Figure 3.12	Powergui FFT analysis tool	66
Figure 4.1	Average output current of the GCPV system model based on solar irradiance for CPWM and DPWM control techniques	71
Figure 4.2	Average output power of the GCPV system model based on solar irradiance for CPWM and DPWM control techniques	72
Figure 4.3	$THDi$ level for CPWM and DPWM based on different solar irradiance level at 1 kHz switching frequency	74
Figure 4.4	One cycle output current waveform for CPWM control technique	75
Figure 4.5	One cycle output current waveform for DPWM control technique	77
Figure 4.6	Harmonic spectrum of the current at PCC using CPWM control at different solar irradiance level	81
Figure 4.7	Harmonic spectrum of the current at PCC using DPWM control at different solar irradiance level	84
Figure 4.8	Minimum switching frequency of CPWM and DPWM carrier signal to obtain in standard $THDi$ at different level of solar irradiance	85
Figure 5.1	Block diagram of proposed CPWM as the recommended solution to meet the standard THD and minimize switching losses in a GCPV system	92

## LIST OF SYMBOLS



$\omega$	Angular Frequency
$^{\circ}\text{C}$	Degree Celsius
%	Percentage
C	Capacitor
R	Resistor
L	Inductor
V	Voltage
I	Current
N	Neutral
Z	Impedance
A	Ampere
s	Second
t	Time
u	Instantaneous Voltage
i	Instantaneous Current
a, b, c	Three-phase Quantities
GW	Giga-Watt
GWp	Giga-Watt Peak
MW	Mega-Watt
MWp	Mega-Watt Peak
kWp	Kilo-Watt Peak
km	Kilo-meter
kHz	Kilo-Hertz
MHz	Mega-Hertz
$\text{W}/\text{m}^2$	Watt per Square Meter
$V_s$	Voltage Source
$V_{\text{dc}}$	Direct Current Voltage



## LIST OF ABBREVIATIONS

APOD	Alternative Phase Opposition Displacement
BIPV	Building Integrate Photovoltaic
BJT	Bipolar Junction Transistor
BOS	Balance of System
c	Collector Terminal
CBSVPWM	Carrier Base Pulse Width Modulation
CPWM	Continuous Pulse Width Modulation
CSI	Current Source Inverter
DPWM	Discontinuous Pulse Width Modulation
DPWM2	Discontinuous PWM with $\pi/3$ Modulation Phase Angle
e	Emitter Terminal
FACTS	Flexible AC Transmission System
$f_{co}$	Cut Off Frequency
$f_s$	Switching Frequency
FFT	Fast Fourier Transform
FiT	Feed-in Tariff
g	Gate Terminal
G	Solar Irradiance
GC	Grid-connected
GCPV	Grid-connected Photovoltaic
GTO	Gate Turn-Off Thyristor
GUI	Graphical User Interface
HVDC	High Voltage Direct Current
IGBT	Insulated Gate Bipolar Transistor
IGCT	Integrated Gate-Commutated Thyristor
$I_{sc}$	Short-circuit Current
$m_i$	Modulation Index
MOSFET	Metal Oxide Silicon Field Effect Transistor
MPP	Maximum Power Point
MPPT	Maximum Power Point Tracker
NEM	Net Energy Metering

PCC	Point of Common Coupling
PCS	Power Conditioning System
PD	Phase Disposition
PF	Power Factor
POD	Phase Opposition Displacement
PV	Photovoltaic
RMS	Root Mean Square
PVPP	Photovoltaic Power Plant
SA	Stand-alone
SAPV	Stand-alone Photovoltaic
SEDA	Sustainable Energy Development Authority
SMPS	Switch-Mode Power Supplies
SPD	Surge Protection Device
SPWM	Sinusoidal Pulse Width Modulation
STC	Standard Test Condition
THD	Total Harmonic Distortion
THIPWM	Third Harmonic Injected Pulse Width Modulation
TNB	Tenaga Nasional Berhad
TTHIPWM	$\frac{1}{4}$ Peak Value of Triangular Third Harmonic Injection Pulse Width Modulation
UPS	Uninterruptible Power Supply
$V_c$	Carrier Waveform Magnitude
$V_{oc}$	Open-circuit voltage
$V_m$	Modulated Waveform Magnitude
VSI	Voltage Source Inverter
VSPWM	Variable Structure PWM

## CHAPTER 1

### INTRODUCTION

#### 1.1 Introduction

The first chapter of this thesis begins with the background of the study and further describes the photovoltaic (PV) system as the chosen renewable energy to be focus of this research and the challenges in a PV system. This is followed by the research problem statement, research objectives, scope of research and contribution of this research. This chapter concludes with the organization of the thesis.

#### 1.2 Renewable Energy

Our earth is unwell due to the problems such as pollution and global warming. Energy demand in this decade is increasing due to the rapid growth of industrialization. Moreover, technology advancement also contributes to the increment of the energy demand. In order to fulfil the energy demand required, the usages of the fossil fuel get larger from year to year. The effects are fossil fuel resources reduced and these conventional sources can cause pollution happens when generating the electricity.

Apart from that, it is difficult to transport fuels to a remote area and the cost to distribute the electricity produced is high due to the long transmission line need to be used (Selvam, 2014). This problem can be solved by generating electricity using the non-conventional sources and it is our responsibility so that the next generation can live in the clean environment. There are several available non-conventional or renewable energy sources that can replace fossil fuel use such as solar, wind, rain, tides, waves and geothermal heat (Penkey, Alhajeri, & Johnson, 2016) (Rajasekaran, Thulasi, & Glenn, 2016) (Abdool & Alwanna, 2014).

Solar and wind are the most popular and preferable renewable energy sources since both sources are eco-friendly and easy to obtain the sources (Shaari, Omar, Haris, & Sulaiman, 2010b). The world energy demands are capable of being fulfilled if the PV technology is properly utilized (Nordin & Rahman, 2015). Besides that, the average cost of PV components and the cost of solar technique power generation are constantly decreased (Ayub, Gan, & Kadir, 2014). Not to mention, the improvement of solar cell efficiency together with the development of the manufacturing technology in the past few years (Sunny & Anto, 2013).

In 2016, the prices of PV modules are expected to decrease no less than 5 %. This can be another profit if solar energy is chosen since the PV system can be more economically feasible (Penkey et al., 2016) (Rajasekaran et al., 2016). For the last decades, the PV technology increasing 40 % per year and many countries permitted, encourage and funded solar technology in their country nowadays (Nordin & Rahman, 2015) (Kumar, Saha, Dey, & Barman, 2015). Furthermore, fossil fuel produced the energy released less than the solar radiation that reaching the earth's surface which is 1000 times greater and it is an effective solution to reduce the Global warming (Oh & Sunwoo, 2008).

The main advantage of renewable energy is not harming the environment since it is clean energy and noise free (Oh & Sunwoo, 2008). Meanwhile, in term of sources, renewable energy is cheap to operate least expensive sources of energy and secure energy source (Penkey et al., 2016). The first stage to produce the electrical power is to build the power harvesting station. The location to build will require more land and also costly to build. For example, the capital cost of the PV system is high compared to conventional energy sources (Khatib, Mohamed, & Sopian, 2012). These unfavourable circumstances only during the early stage of the construction of renewable energy.

The technology of direct conversion of sunlight energy to electrical energy by the p-n junction semiconductor device is recognized as PV (Selvam, 2014) (Kamal EL-Sayed, 2017). Phenomenon to convert light into electricity discovered by Henri Becquerel in 1893 while Albert Einstein explained the principle of PV effect in 1905 (Shaari et al., 2010b). Starting 1970's and 80, the PV industry starting to expand due to the oil crisis (Sopian et al., 2007). Total cumulative PV installation amounted at the end

of 2015 including off grid is 242 GWp with Europe and China contribution is 40 % and 21 % respectively.

In 2017, a total of 99.1 GW of grid-connected (GC) solar was installed. It is 30 % year-on-year growth over the 76.6 GW added in 2016. Apart from that, the year 2017 was a landmark for solar PV since the world added more capacity from solar PV than from any other type of power generating technology and it is more than total of fossil fuels and nuclear power combined. The top five nation market was China which is the dominated global solar market demand in 2017, the United State, India, Japan and Turkey. The list of the top five responsible for 84 % of newly installed capacity. Meanwhile, the next five were Germany, Australia, the Republic of Korea, the United Kingdom and Brazil. China alone operates nearly 1/3 of the world’s solar power generation capacities as shown in Figure 1.1.

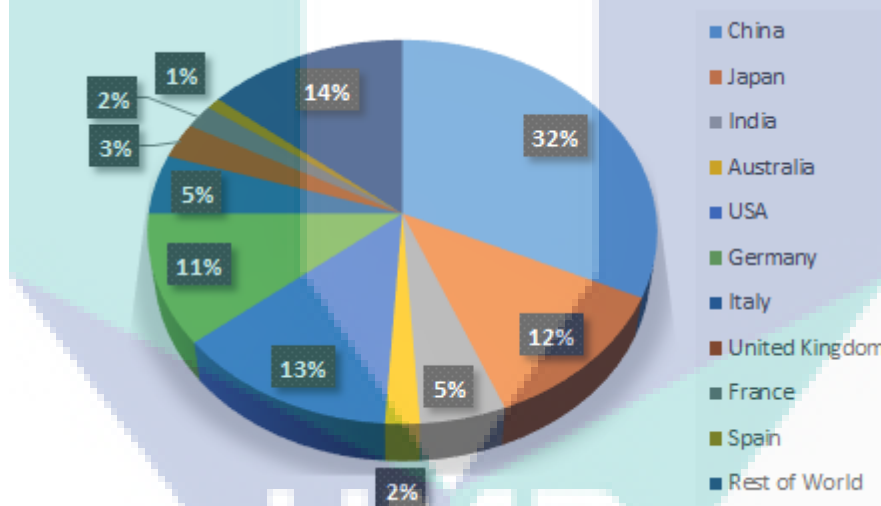


Figure 1.1 Global top 10 solar PV markets total installed shares by the end of 2017

Advances in balance of system (BOS) technologies helped improve installation and overall performance. Besides that, increasing competitiveness of solar PV, rising demand for electricity in developing countries and increasing awareness of solar PV potential to reduce pollution give impact to the market expansion. Global solar market demand in 2017 was dominated by China where the PV installed in China was 53.3 %, more than half of the world’s solar capacity in one year. According to (SolarPower Europe & Schmela, 2018), China is expected to significantly increase the solar demand again to around 40 GW in 2020, 45 GW in 2021 and 55 GW in 2022. Moreover, the rest of the world will continue to play a stronger role in the solar sector. It is assumed that

global demand to increase 17 % to 125.2 GW in 2020, 12 % to 140.4 GW in 2021 and 157.8 GW in 2022.

10th Malaysia Plan (2011-2015) introduced Renewable Energy Act 2010 and the Sustainable Energy Development Authority (SEDA) Act 2011 was proving that the government has made a long term commitment towards renewable energy growth. A new Malaysian Standard for PV integrated and retrofitted application was published in February 2012 which is “Design, installation, maintenance and inspection of PV mounting system – code of practice” – MS2440:2012 (Mahyudin & Abdul Malek, 2012). By the end of August 2018, PV system with more than 378 MW of capacity received the Feed-in Tariff (FiT) according to SEDA, just 0.5 MW than at the end of 2017. Under net energy metering (NEM) programme, Malaysia aims to implement 500 MW of PV capacity between 1 November 2016 and 2020. Up to the present, the progress of the programme is rather slow (Jäger-Waldau, 2018).

### **1.3 Photovoltaic System**

Generally, the PV system configuration can be categories into GC and stand-alone (SA) (Khatri & Kumar, 2017). GC system integrates PV technology with the main grid and it is an interconnected network where electrical power from the generating power station will be transmitted to the substation through the high voltage transmission lines then the consumer received the electricity via distribution lines. Meanwhile, SA system is an off grid system (Nordin & Rahman, 2015). This system is most suitable to be used in a rural area where the utility grid is out of reach (Sopian et al., 2007) (Badi, Zakaria, Nordin, & Mustapa, 2014).

Everything has its pros and cons, same goes for the PV system. The merits of a PV system are inexhaustible, clean energy source, environmentally friendly, cost reduction, less maintenance, requires little maintenance, a secure energy source, silent since there are no rotating parts involve and size-independent electricity conversion efficiency (S.I. Sulaiman, Rahman, Musirin, & Shaari, 2011) (Renu & Surasmi, 2014) (Mohammad Bagher, Abadi Vahid, & Mohsen, 2015). The drawbacks of the PV system are PV array experience large variations of its output power during bad weather such as heavy rain. The capital cost or installation cost is high (Khatib et al., 2012) (Fezzani, Mahammed, Drid, & Chrifi-alaoui, 2015).

The major challenge of using PV resource is the non-linear output characteristics. This problem happens since the output of the PV system depends on the temperature and solar irradiance (Oh & Sunwoo, 2008) (Fezzani et al., 2015). As the PV cell temperature increase, the output voltage drops. Meanwhile, solar irradiance and output current are directly proportional to each other. Maximum power can be obtained by track and control with maximum power point tracker (MPPT) to guarantee the PV modules operated at its maximum power point (MPP) and optimize the power produce so that the power cost can be reduces when the power generation of the PV system increased (Abdool & Alwanna, 2014) (Cai, Ren, Jiao, Cai, & Cheng, 2011).

The non-linear output of a PV module is represented in Current-Voltage (I-V) curve as shows in the Figure 1.2 below. Short-circuit current ( $I_{sc}$ ), Open-circuit voltage ( $V_{oc}$ ) and MPP are points along the curve.  $I_{sc}$  is the possible maximum current and  $V_{oc}$  is the maximum possible voltage generated by the cell or module and measured when an external circuit with no resistance is connected. MPP is the operating point when a PV panel delivers maximum output power (Ehmidat, 2013). Maximum power operating current ( $I_{mp}$ ), maximum power voltage ( $V_{mp}$ ) and MPP are specified at the knee of the I-V curve. The information required to form PV system that can be operated as close as possible to its MPP are provided by the I-V curve.

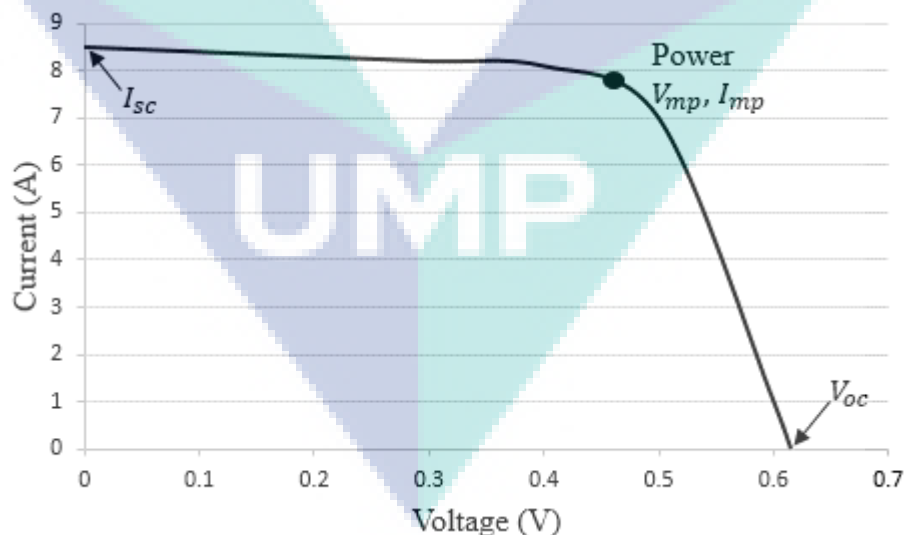


Figure 1.2 I-V curve of a PV module

#### 1.4 Challenges in GCPV System

In a power system, power quality is the grid's ability to supply a clean and stable power supply. The main aim in three phase power system is to produce the noise-free

sinusoidal wave shape and within the voltage and frequency tolerance. Same goes to grid-connected PV (GCPV) system which is designed with the main aim to inject the sinusoidal current to the grid with low total harmonic distortion (THD) level (Renu & Surasmi, 2014). However, any power system cannot avoid involvement in power quality problems. There are 9 most popular power quality problems which are voltage sags, very short and long interruption, voltage spike, voltage swell, harmonic distortion, voltage fluctuation, noise and voltage unbalance (Portal, 2014).

In this research, the harmonic distortion is highlighted. Increase use of many non-linear loads such as inverter leads to power system harmonics issues (Padure, Haraguta, Vintea, & Ghita, 2014). This issue is a big issue and many researches have been done on power system harmonics. Important to realize that the output current for a GCPV system is depends on the solar irradiance. Malaysia solar irradiance is not constant throughout the year hence the output is inconstant. Thus, the THD also will increase when the solar irradiation is decreased and vice versa (Al-Shetwi & Sujod, 2017) (Hicks, Baghzouz, & Haddad, 2018).

IEEE 519-1992 defines harmonics as a sinusoidal component of a periodic wave that having frequencies that multiple of a power system fundamental frequency. Besides that, it also can be defined as voltage or current waveforms that are non-sinusoidal shape. Classic sources of harmonics are DC brush motors, arc furnaces and welding machines. Together with the largest non-linear loads specifically inverter, rectifier, chopper and AC-AC converter that connected to the electrical power system which then produce non-sinusoidal currents. In that case, the supply voltage distorted at point of common coupling (PCC). Under those circumstances, the ordinary consequences of harmonic problem are overheating of all cables and equipment, resonance occurrence, neutral overload in 3-phase systems, proximity and skin effects (Portal, 2014).

## **1.5 Problem Statement**

In case of large GCPV power plant, the inverter which is non-linear load generates more THD into electrical power system. Harmonic generated may downgrade the quality of the power grid and affect the reliability and safety. IEEE Std 519-1992 and Tenaga Nasional Berhad (TNB) standard stated that, THD should be less than 5 % at the rated inverter output of the cable connected to PCC. In Malaysia, the solar



irradiance varies throughout the year being dependent on the seasons. Furthermore, it also varies daily depending on the position of the sun and the weather. These changes can influence the THD in a GCPV system since the irradiance and THD are inversely proportional. The consequence of low irradiance level is that the output of the PV array is low and thus the input of the inverter relatively becoming low. It is reported that, the inverter exhibits large non-linearity when the inverter is operating at low power input during the low level of solar irradiance.

The output voltage changes according to the power consumption of the load and irradiance in a standard inverter without pulse width modulation (PWM) technology. PWM technology able to correct the output voltage and reduces the THD simultaneously. Besides that, THD can be avoided in the system using an additional filter circuit. High switching frequency need to be used to reduce the THD grandly, but the effect is switching losses proportionally increase. It is thus worth to investigate the performance of Continuous PWM (CPWM) and Discontinuous PWM (DPWM) as inverter control by analyse THD and switching losses for varies solar irradiance level at different switching frequency of the PWM carrier signal. Therefore, this research proposes the minimum switching frequency where the THD still in standard requirement even if the irradiance is low and reduce the switching losses with suitable choice of PWM technique implemented.

## **1.6 Objectives**

The main objective is to carry out research to minimize harmonics and switching losses in the GCPV system. The research, however, will deeply focus on the following aspects:

- (i) To implement CPWM and DPWM in a GCPV system model.
- (ii) To investigate the effect of switching frequency on THD and switching losses performance at different solar irradiances.
- (iii) To propose a control method of switching frequency in order to maintain THD within the standard requirement during different range of irradiances.

## 1.7 Scope of Research

The scope area of study is the PV system in Malaysia environment. The study aims to implement PWM techniques in a GCPV system model to investigate the effect of switching frequency on THD and switching losses performance at different solar irradiance. In Malaysia, there is potential to install a PV system since the average solar irradiation per month is 400-600 W/m<sup>2</sup>. Malaysia is located in the equatorial region, which is the strategic location and solar energy can be one of the significant renewable energy sources (Yunus, Koingud, Kutty, & Yaakub, 2014).

Furthermore, the abundant solar irradiance, mean daily sunshine hours in Malaysia ranges between 4 to 8 hours per day and zero clear sky in Malaysia as shown in Figure 1.3 make the PV system become the dominant renewable energy sources (Jianhui Wong, 2014). The maximum solar irradiance tested in the simulation of this research is 1000 W/m<sup>2</sup> which is the peak solar irradiance while the minimum solar irradiance tested is 200 W/m<sup>2</sup>. In Malaysia, the PV array experience large variations of its output power during bad weather such as heavy rain.

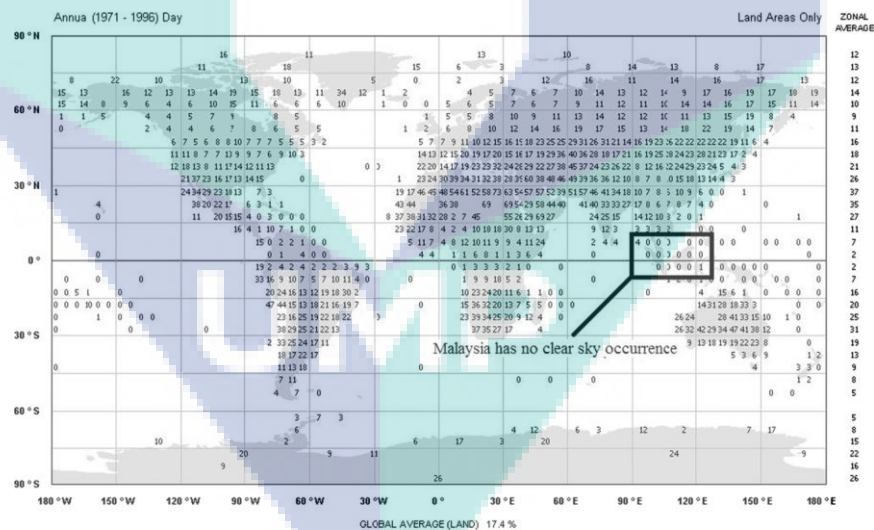


Figure 1.3 Frequency occurrence of the global completely clear sky index  
Source: Jianhui Wong (2014)

Lower harmonic can be eliminated or minimize by using PWM technique. There are two general types of PWM technique which are CPWM and DPWM. Both of the PWM has its own advantage such as CPWM able to minimize the harmonic distortion and DPWM able to minimize switching losses in a system. In this research, one type of

each one of the CPWM and DPWM techniques that has better performance compared to the other type are chosen for further research. For CPWM,  $\frac{1}{4}$  peak value of triangular third harmonic injection PWM (TTHIPWM) is chosen since it generates the precise pulses required by the inverter if compared with the other PWM, can increase the fundamental output by 15 % and able to reduce harmonic content. Meanwhile, discontinuous PWM with  $\pi/3$  modulation phase angle (DPWM2) from DPWM type is chosen. Basically, performance of DPWM is the same and only contain slightly different. DPWM2 has the better performance according to the previous research where the harmonic distortion is the lowest compared to the other DPWM types.

## **1.8 Contribution**

The contribution of this research is analysing the performance of the inverter with the application of two types of PWM to find which PWM type used that capability to give the optimal performance with less THD and follow the standard which is THD less than 5 %. Moreover, power system with less power quality issue may guarantee the safety and reliability of the electrical equipment. In addition, this research proposes the minimum switching frequency of the PWM carrier signal according to the solar irradiance since Malaysia has wide-ranging solar irradiance throughout the year. Lastly, a GCPV system with optimal performance in THD and switching losses with a suitable PWM type with minimum switching frequency can be proposed.

## **1.9 Thesis Organization**

This thesis is organized into five chapters. The brief overview about renewable energy and mainly of PV energy is in Chapter 1. Besides that, the main focus of this research which is the problem statement, objectives and contribution of the research are stated in this chapter.

Chapter 2 provides details of PV system. Furthermore, the facts about inverter, power quality issues, PWM and previous researches that have the same purpose with this research is included.

The main idea of this research is to design GCPV system model with THD in standard value and less switching losses. Chapter 3 explains the overall research plan for this research which includes the PWM generation, GCPV system configuration in

flowchart and block diagram forms and control of the system based on PWM techniques.

The results of the investigation are presented in Chapter 4. The results are analysed based on the electrical parameters based on the solar irradiance level, THD effect based on solar irradiance level and minimum switching frequency of the PWM carrier signal required to obtain in standard THD are proposed. In addition, the switching losses analyses also presented. The PWM techniques are compared and the recommended solution is suggested at the end of this chapter.

Chapter 5 concludes the overall research from the previous chapter, whether the GCPV system can meet the standard or not. Lastly, recommendation to upgrade this research is elaborated.



UMP

## CHAPTER 2

### LITERATURE REVIEW

#### 2.1 Introduction

In this research, the main aim is to produce a GCPV system where THD remain in the standard level and low switching losses by design a GCPV system that has less power quality issue with the utilizing PWM technique in the inverter control for that purpose. Solar irradiance is the key variable in this research to observe what happened to the THD in different solar irradiance level. Therefore, review of the theoretical and empirical literature together with the summary of the previous research and how it related to this study are included.

#### 2.2 Photovoltaic System

PV system uses solar irradiance that strikes the solar array. Next, DC power is generated. An inverter is utilized to convert the DC power to AC power (Rajasekaran et al., 2016) (Shahril Irwan Sulaiman, Rahman, Musirin, Shaari, & Sopian, 2012) (Zhao & Liu, 2012). Inverter plays an important role in a PV system operation. An inverter is used to interface the PV system with the AC network and to ensure that the PV module is operated at MPP with sinusoidal current transferred to the electric grid (Renu & Surasmi, 2014) (Aamri, Maker, Mouhsen, & Harmouchi, 2015). The significant contrast between SA and GC is the system integrates with the main grid or not. In this section, the comparison of the system application and system component between SA and GC is further discussed respectively.

Firstly, stand-alone PV (SAPV) system applications are providing power for domestic systems in rural area since the location is farther and not connected to grid utility. Besides that, this system also suitable to use in a diverse range of non-domestic

application for example telecommunications. Unlike GCPV system, this system has two principal applications which are distributed system and centralised system (Khatri & Kumar, 2017). The system that provides power produced directly to grid connected consumers or directly to the electricity network is known as a distributed system. Meanwhile, centralised system does not link with consumer and produces power in bulk (Shaari et al., 2010b).

The main component in any PV system is the PV modules that will be connected either in series or parallel to produce PV arrays. Inverter, cables, breakers and other protection devices such as surge protection device (SPD) or fuses and structure for mounting the PV modules or array are the lists of the important and the BOS components that both SAPV and GCPV system required. However, to complete the SAPV system, a few components need to be added to the system to make the system complete. Other typical BOS components of the SAPV system are generator set, rectifier, transformer and switches (Kamal EL-Sayed, 2017). Figure 2.1 and Figure 2.2 below show the configurations of SAPV and GCPV respectively (Shaari et al., 2010b). GCPV is more important due to the total volumes of PV required in a related network system and various advantages compared to SAPV (Badi et al., 2014).

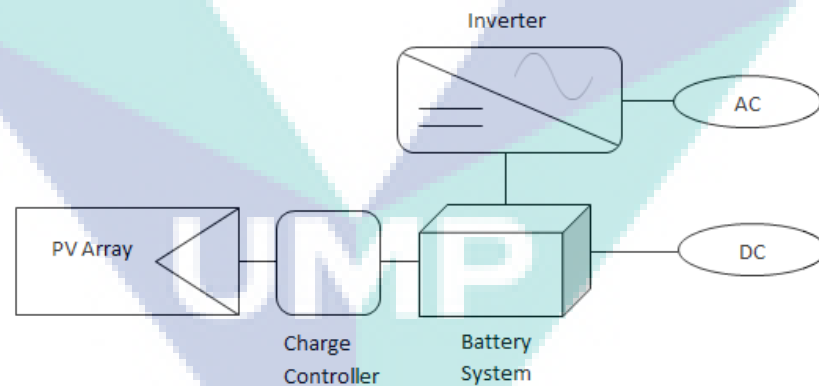


Figure 2.1 A typical SAPV system configuration

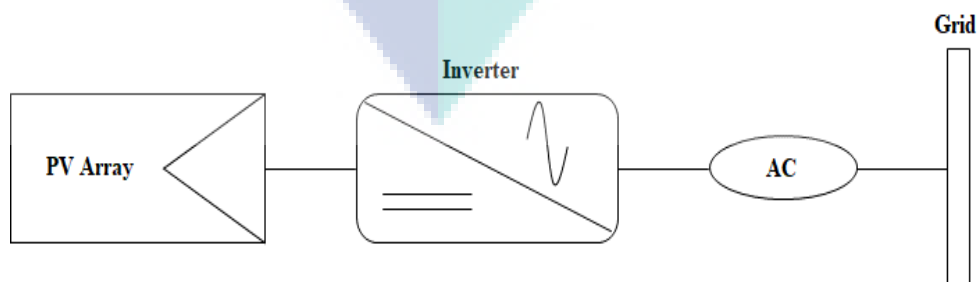


Figure 2.2 A typical GCPV system configuration

### 2.2.1 Factors Effect the Solar Cell Performance

Factors that affect the performance of the PV system are temperature and solar radiation (Oh & Sunwoo, 2008) (Renu & Surasmi, 2014). The average Malaysia temperature is typically 30 °C to 35 °C. The recommended highest cell operating temperature is set at 75 °C meanwhile the recommended lowest cell operating temperature is at 20 °C. Figure 2.3 below shows the relation on how temperature affects the I-V curve. At 25 °C, the voltage output is at an optimal level compared when the temperature at 75 °C as the voltage reduced 0.5 % per °C when the temperature increased above 25 °C. This can be concluded that the performance of the solar cell does not increase when the temperature increase. The only parameter affected by an increase in temperature is mostly in the open circuit voltage while the short circuit current roughly constant as the temperature changed (Shaari et al., 2010b).

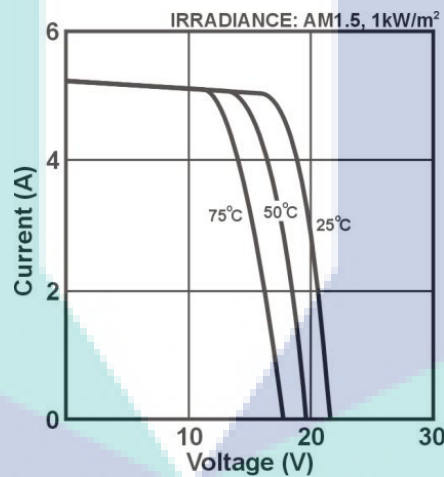


Figure 2.3 Temperature effect on voltage and current output of solar cell

Solar radiation is discussed in terms of irradiance which is defined as the intensity of solar power at a point of observation and the conventional unit of solar irradiance is watt per meter square,  $W/m^2$  (Pradhan, Ali, & Jena, 2013). Among factors that affect the solar irradiance are geographic, meteorological, time of the day, local weather (Cheng, Cao, & Ge, 2012) and movement of the clouds (Zambri, Aras, Khamis, & Hairi, 2016). The solar radiation that reaches the Earth's surface can be discussed in three components of the irradiance.

The components include  $G_{direct}$  which is the component of solar radiation that has travelled in a straight path from the sun to the point of observation but shed a

shadow when there are objects in the path of the solar radiation and the second component is  $G_{diffuse}$  that can be defined as the solar radiation that reach the point of the observation after scattering due to particles in the atmosphere (Salim, Mohammed Najim, & Mohammed Salih, 2013) (Khatri & Kumar, 2017). The sum of these two components arrive at the point of observation will form  $G_{global}$  and the equation for this is expressed in equation 2.1.

$$G_{global} = G_{direct} + G_{diffuse} \quad 2.1$$

According to Figure 2.4, when irradiance increases, thus the amperage output increase while the voltage does not have a lot of change (Ehmidat, 2013) (Phap, Yamamura, Ishida, & Nga, 2017). MPP also affected as the irradiance changes (Aamri et al., 2015). Solar irradiance that reaches the top of the earth's atmosphere at the point of 30 km normal to the surface of the average earth curvature is  $1367 \text{ W/m}^2$  (Shaari et al., 2010b). This research takes solar irradiance in count to observe and analyse the performance of the PV system. Previous research proved that solar irradiance and THD are inversely proportional (Al-Shetwi & Sujod, 2017).

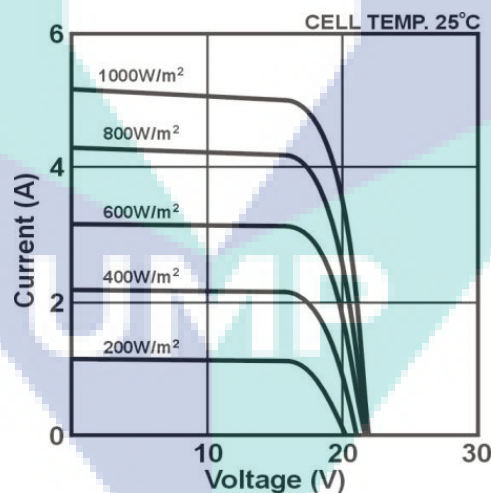


Figure 2.4 Solar irradiance effect on voltage and current output

### 2.2.2 Principle of Operation of GCPV System

In the early stage, PV system was used only for small scale load such as household purposed (Penkey et al., 2016). In recent years, PV system has become one of the alternative ways to produce electricity, especially the GCPV system since this system can provide power to the end user building located in urban and sub-urban with



utility grid highly available via a transmission line (S.I. Sulaiman, Rahman, Musirin, et al., 2011) (S.I. Sulaiman, Rahman, & Musirin, 2010). This system has two typical types which are central and distributed.

As for central system, the operation is similarly with the central power stations that use various types of fossil fuels where the power stations directly connect to the transmission or distribution system to be distributed to the end consumer. Normally, the small central GCPV system is 50 kWp, while the system can be as large as several MWp that already been installed in recent years. Central system can generate more power and it needs to be installed in higher radiation place. In contrast, wide area is a must for this type of system, more transmission losses and high maintenance (Shaari, Omar, Haris, & Sulaiman, 2010a).

Commercial and domestic or residential are the main application for a distributed system. Both system usually used building integrate photovoltaic (BIPV) system where the PV modules itself are part of the building and the power generated will be consumed by the load in the house first where normally during the evening, the peak power demand. In the commercial system, it will provide typically greater than 10 kWp power to the load within the building attached to the PV system and no power exported to the grid but it will possibly export during the weekend when the building such as office blocks or retail shops are closed. The residential system power range is commonly 1 to 5 kWp.

Power of the distributed system will be generated mostly during the afternoon and the excess power will be exported to the grid. The owner receives credit for the energy provided to the grid. Good points of having GCPV system are able to reduce the dependency on grid power (Abdool & Alwanna, 2014). The positives for this system are no cost in buying the land to set up this system, transmission losses lower because of the simplicity of this system implementation where the system is installed near to the point of load (S.I. Sulaiman, Rahman, Musirin, et al., 2011) and low maintenance compared to the commercial system. The drawbacks of this system are need own financial assistance and long payback period (Shaari et al., 2010a). Besides that, during night time or bad weather the user still can have the electricity from the grid and the owner can have saving on electricity bill based on the exported electricity to the grid (S.I. Sulaiman et al., 2010).

### **2.2.3 Designing GCPV Systems**

Technical sizing procedure and economic sizing procedure are the most crucial issues in designing GCPV system. Technical sizing procedure includes the selection of the type of PV modules and matched inverter. First of all, the designer needs to identify the constraint involve in that particular project for example designed for space, designed for energy requirement or designed for a budget. Then, the designer is required to determine the PV array size and configuration. Both of the procedures will be considered in the design process to determine the expected technical performance indicator and economic performance indicator of the proposed system.

It is important to get the accurate sizing to avoid over or under sizing and definitely will give impact the investment, the system will not function well and perform below the expectation. By considering the meteorological condition and accurate selection of the component can help the designer to get the proper sized for the proposed system. Sizing process can be done using a manual method and intelligent method such as Genetic Algorithm (S.I. Sulaiman, Rahman, Musirin, et al., 2011), Evolutionary Programming (S.I. Sulaiman et al., 2010) and Artificial Immune (S.I. Sulaiman, Rahman, & Musirin, 2011). Software frequently used to compare the results of manual sizing process (Nordin & Rahman, 2015) (Shahril Irwan Sulaiman et al., 2012).

### **2.3 History of Converter**

The early invention of the machine by Ferraris and Tesla in 1885 and 1887 respectively was DC machine, synchronous machine, induction machine and squirrel cage machine by Dobrowolsky later in 1890. This invention had mainly been implemented in the industry due to its high performance control method and cost reduction as the results of continuous progress, improved structure and performance characteristic. Furthermore, the developments of the electric machine and control method which are controller and power sources with controllable characteristic are in parallel in the twentieth century and continue at an increasing rate (Ahmet M. Hava, 1998).

Some of the early power converters invented in the middle of the century are mercury valve rectifier, thyratrons, metal tank rectifiers, cycloconverters, load

commutated inverter and current source and voltage source inverter (VSI). The highest performance and cost effective device from all power converters listed is VSI. Furthermore, the development of the modern power electronic switches such as bipolar junction transistor (BJT), metal oxide silicon field effect transistor (MOSFET) and insulated gate bipolar transistor (IGBT) boost the application of the power converter especially IGBT, the most widely utilized devices then revolutionized PWM-VSI (Ahmet M. Hava, 1998).

Power conversion in electronics can be done with power electronics technology. The converter is the power electronics technology and the application of the converter is to transform one form of electrical energy to another form of electrical energy which is AC or DC. There are typically four types of converter category. First, AC to DC known as rectifiers where a diode rectifier circuit converts AC input into a fixed DC voltage. Second, chopper is a converter that converts fixed DC input voltage to a controllable DC output voltage. Third, AC to AC converter is called AC Voltage Controllers and it is utilized to convert fixed AC input voltage directly into variable AC output voltage at the same frequency. Lastly, the converter that widely used in induction motors, uninterruptible power supply (UPS) and high voltage direct current (HVDC) is known as inverter. It converts fixed DC voltage to a variable AC voltage.

Large amount of low frequency harmonic voltage or current of the power converter in the early stage of the invention was due to the typically low switching frequency. This problem was solved by increasing the frequency capability of a solid state semiconductor device and therefore the power electronic converter able to transfer energy to load in controlled quantity. PWM or intelligent power electronic switching algorithm was invented by Kirnnich, Heinrick and Bowes in early 1960's is developed (Abd Halim, 2013) in parallel with the semiconductor device and control theory development.

## **2.4 Inverter**

In the context of power electronics, inverter power conversion circuit operate from a stiff DC source and generate AC output. The sources for the inverter can be a DC voltage source or DC current source (Fang, Cui, Liu, & Cao, 2011). If the input is fed with a constant DC voltage source and supported by a relatively large capacitor feed

the main inverter circuit, then the inverter is known as VSI while if the source is fed with a DC current source, then the inverter is called current source inverter (CSI). The VSI circuit has direct control over output AC voltage whereas CSI circuit directly controls output AC current.

The main converter circuit of a VSI is fed with capacitor supported the DC voltage source as shown in Figure 2.5. DC voltage source for VSI can be a battery bank. Another source of DC voltage source is a solar PV cells (Abd Halim, 2013). It is not fixed that only DC voltage source can be the source for VSI. This is explained by the fact that the AC voltage source after being rectified into DC voltage source also can be the source for VSI (Kharjule, 2015). The voltage source is assumed as stiff since the source voltage magnitude does not depend on load connected (Parikh, 2017). On the other hand, DC inductor that is fed with a voltage source such as a battery, fuel-cell stack, diode rectifier or thyristor converter is the supply for the CSI and the output voltage depending on the load impedance (Peng, 2003). The main circuit of CSI is shown in Figure 2.6.

Single-phase VSI apply half-bridge and full-bridge forms. Applications of single-phase VSI are for power supplies and single-phase UPSs. An application that requires sinusoidal voltage waveform will use three-phase VSI. The examples of the three-phase VSI application are UPS, Adjustable Speed Drive (ASD), flexible AC transmission system (FACTS) devices such as STATCOM, active filter for power quality improvement and renewable energy. As a matter of fact, almost all of the appliances and machines today operate with AC power, commercial inverter units can be used when the AC supply interrupted for a limited time period. This can be done by using the battery supply as the DC voltage source. Next, the inverter converted to AC voltage of the desired frequency and supply the output for domestic purpose (Parikh, 2017).

Commonly for three inverter legs CSI, six semiconductors switching device that consists of reverse block capacity such as IGBT, GTO and a power transistor with the unidirectional current flow and bidirectional voltage blocking used in the main circuit. During the operation of the three phase CSI, at least one of upper three devices and one of the lower three devices should be on by reason of the upper and lower devices of each phase leg cannot be gated at the same time (Peng, 2003) (Jayanth, Boddapati, &

Geetha, 2018). Basically the application of CSI is related to speed control that is AC induction motors.

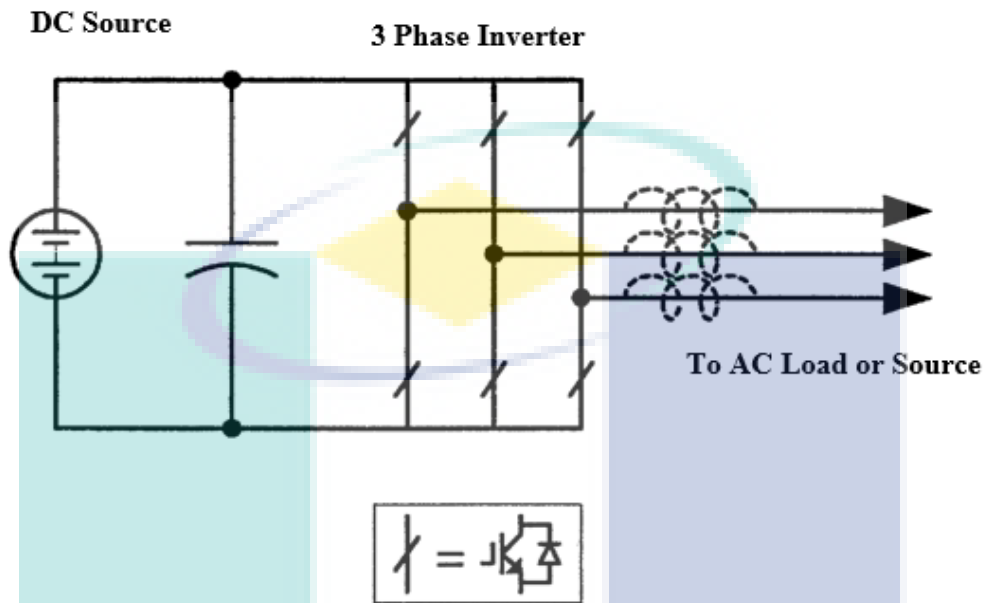


Figure 2.5 The main circuit topology of VSI  
Source: Peng (2003)

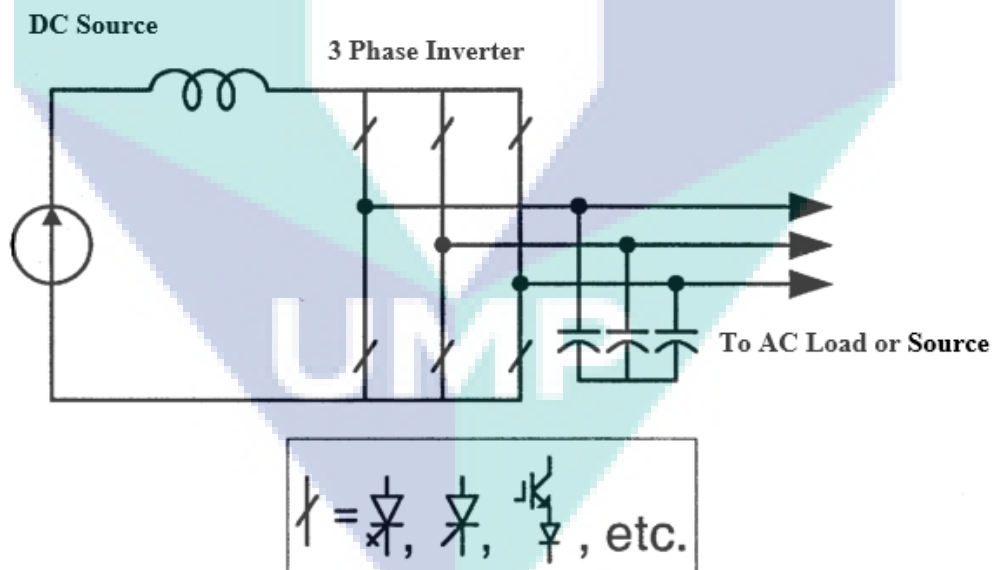


Figure 2.6 The main topology of CSI  
Source: Peng (2003)

The main circuit for both of the inverter is non-interchangeable. This is due to fact that the main circuit of the VSI is supported by the capacitor while the inductor supported the circuit of the CSI. Therefore, it is impossible for the VSI main circuit to be operated for CSI and oppositely (Peng, 2003). Besides that, the concept for VSI is

the AC output voltage must be less than the DC voltage source. Theoretically, the VSI is the buck inverter for DC to AC power conversion. One of the disadvantages of VSI is difficult to protect against short circuit and if that happens, the voltage source and the switches will possibly damage. Next, CSI is basically a boost inverter since the AC output voltage need to be more than the DC voltage that fed the inductor in the main circuit. The current source and switches may be damaged if an open circuit occurs. In brief, VSI and CSI can be either buck or boost converter respectively (Fang et al., 2011). Short circuit and open circuit may disturb the inverter operation of the VSI and CSI (Nozadian, Ebrahimzadeh, Babaei, & Asl, 2017). In this research, only VSI is considered further.

#### **2.4.1 Voltage Source Inverter**

The general topology of VSI is quite simple which is involved an overwhelming level of technology and intelligence. It consists of six power semiconductor switches with anti-parallel feedback diodes. It has separate circuit modes for each of the switch states that generating the correct frequency and magnitude output voltage. IGBT that operating at high frequency (kHz – MHz) is the commonly used as the semiconductor power switching devices. The power rating of VSI is from a fraction of a kW to MW level (Ahmet M. Hava, 1998).

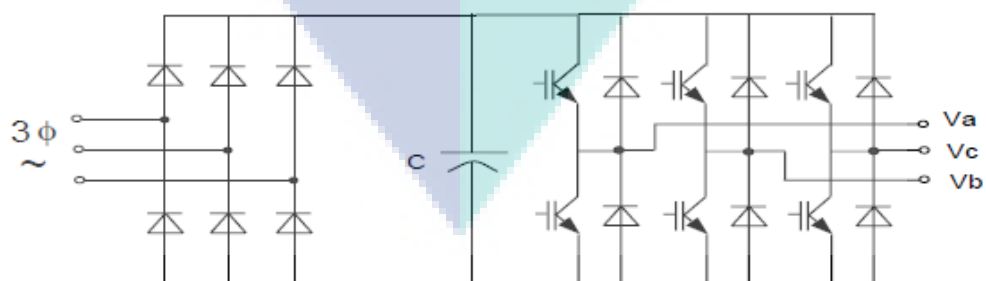
Furthermore, VSI is utilized with the PWM method that will result in inverter output voltage approximates the reference value through high frequency switching. PWM choice will influence the inverter energy efficiency, waveform quality and voltage linearity. In PWM-VSI, the drive control algorithm generates a voltage reference signal and modulator programs the inverter switching device gate logic signal. Then, the logic signal will be the source of the power switching devices which later applied to the inverter switch gates (Khan, Siraj, Khan, Mahboob, & Haque, 2017). The switches communicate and an inverter output voltage that approaches the reference voltage over a predetermined carrier cycle is generated (Ahmet M. Hava, 1998).

#### **2.4.2 PWM-VSI Circuit Design**

There is a variety of PWM-VSI drive exists due to its wide range applications. The main function of all PWM-VSI drives is to generate three-phase voltage with

controllable magnitude and frequency from a DC voltage source. Moreover, each of the applications may use different PWM-VSI. These differences create many sizes, cost, performance and the power rating of the PWM-VSI. The power circuit design of PWM-VSI is determined by the voltage and current ratings required. In addition, the voltage and current ratings can choose the power circuit topology, type of switching device, passive filtering components, cooling method and the drive hardware protection circuit complexity. Overall complexity of the drives is relying on the power rating and bandwidth requirement. When both of the factors are high, the complexity also increases. PWM-VSI typically designed with minimum component count and complexity (Ahmet M. Hava, 1998).

The structure of PWM-VSI hardware is particularly depending on the application. As an example, in the application of AC motor drive application, two structures of PWM-VSI are briefly discussed. The basic power converter structure of PWM-VSI drive as shown in Figure 2.7 (a) where the components that involve are three-phase diode bridge circuit that will rectify the AC input voltage, DC link capacitor to filter the rectified voltage which later formed the stiff DC voltage source and lastly the PWM-VSI to convert DC voltage to three-phase AC voltage. PWM method can offer controllable magnitude and frequency. Power semiconductor switching device such as IGBT that utilize in the VSI with a high switching frequency that can be as high as many tens of kilohertz. Another structure of PWM-VSI is illustrated in Figure 2.7 (b). All the components are the same with the addition of an inductor or a DC reactor series with the rectifier (Ahmet M. Hava, 1998). The benefit is the harmonic content on both AC line and DC capacitor can be lowered (Parikh, 2017).



(a)

Figure 2.7 Power converter structures of PWM-VSI

Source: Ahmet M. Hava (1998)

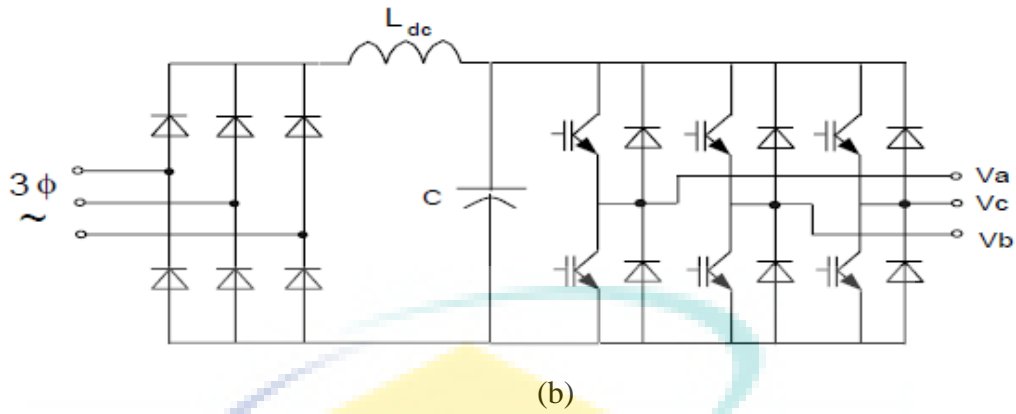


Figure 2.7 Continued

### 2.4.3 Voltage Source Inverter Basic Operation

Three-phase inverter converts a DC input into three-phase AC output. The three-phase two-level VSI consists of three inverter legs, thus the output from each inverter leg produces the three-phase voltage (Kharjule, 2015). Figure 2.8 shows the circuit for a three-phase two-level VSI with three-phase balanced load connected.

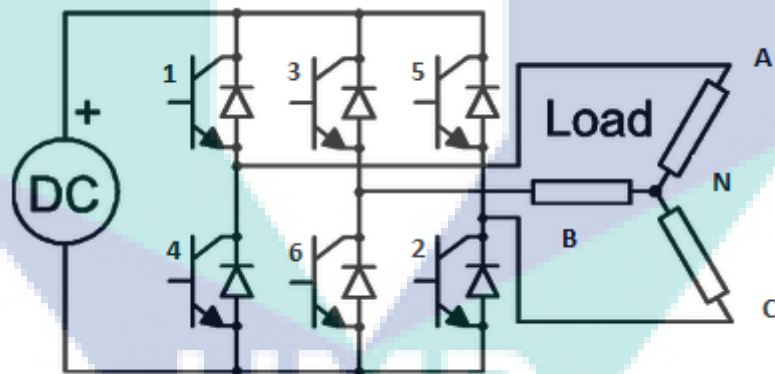


Figure 2.8 Three-phase VSI circuit with three-phase balance load connected

The terminal of the VSI legs A, B and C are connected to the load in three-phase delta or star connection. The conduction mode will be discussed is  $\pi$  radians or  $180^\circ$  time period where the thyristor triggered after an interval of  $\pi/3$  radians or  $60^\circ$  and will remain ON for  $180^\circ$ . After  $60^\circ$ , one of the conducting switches will turn OFF and the other switch will start conducting. At any instant of time, the switches will conduct simultaneously. Two of the conducting switches are from one group either upper or lower three and the other one conducting switch is from the other group (Parikh, 2017).



The operation of the VSI with balanced star connected load is explained. The points S1, S5 and S6 are in conduction mode for the period  $0^\circ$  to  $60^\circ$ . The terminal A and C of the load is connected to the positive point of the source while terminal B connected to the negative point of the source. Each load has its impedance and the impedance between the positive terminal and neutral are  $\frac{Z}{2}$  since the resistance for points A and C are parallel to each other while the impedance between the negative terminal and neutral is Z. Therefore, the total impedance and the current in this conduction mode are in equation 2.2 below. If  $i_1$  is the current that flow in the close circuit, the value of current is given by divided the total voltage,  $V_s$  by the total impedance as shown in equation 2.3 below (Xplanator, 2017).

$$\text{Total impedance: } Z + \frac{Z}{2} \quad 2.2$$

$$\text{Total current, } i_1: \frac{V_s}{Z + \frac{Z}{2}} = \frac{2 V_s}{3 \cdot Z} \quad 2.3$$

The total voltage drop across each of the impedance will be total current,  $i_1$  multiply with the total impedance. The line to neutral voltage will be  $V_{AN}$ ,  $V_{BN}$  and  $V_{CN}$  as shown equation 2.4 – 2.6 below.

$$V_{AN} = i_1 \cdot \frac{Z}{2} = \left[ \frac{2}{3} \cdot \frac{V_s}{Z} \right] \frac{Z}{2} = \frac{V_s}{3} \quad 2.4$$

$$V_{BN} = i_1 \cdot Z = \left[ \frac{2}{3} \cdot \frac{V_s}{Z} \right] Z = \frac{2V_s}{3} \quad 2.5$$

$$V_{CN} = i_1 \cdot \frac{Z}{2} = \left[ \frac{2}{3} \cdot \frac{V_s}{Z} \right] \frac{Z}{2} = \frac{V_s}{3} \quad 2.6$$

Table 2.1 is the summation of each of the operation of switches in  $180^\circ$  conduction mode and the line to neutral voltage of each of the intervals, not to mention Figure 2.9 shows the line to neutral or phase voltage of  $180^\circ$  conduction modes waveform.

Table 2.1 Summation of operation switches in 180° conduction modes

Interval	Duration	Conducting Switches			Line to Neutral Voltage		
					$V_{AN}$	$V_{BN}$	$V_{CN}$
1	60°	S1	S5	S6	$\frac{V_s}{3}$	$-\frac{2V_s}{3}$	$\frac{V_s}{3}$
2	60°	S1	S2	S6	$\frac{2V_s}{3}$	$-\frac{V_s}{3}$	$-\frac{V_s}{3}$
3	60°	S1	S2	S3	$\frac{V_s}{3}$	$\frac{V_s}{3}$	$-\frac{2V_s}{3}$
4	60°	S2	S3	S4	$-\frac{V_s}{3}$	$\frac{2V_s}{3}$	$-\frac{V_s}{3}$
5	60°	S3	S4	S5	$-\frac{2V_s}{3}$	$\frac{V_s}{3}$	$\frac{V_s}{3}$
6	60°	S4	S5	S6	$-\frac{V_s}{3}$	$-\frac{V_s}{3}$	$\frac{2V_s}{3}$

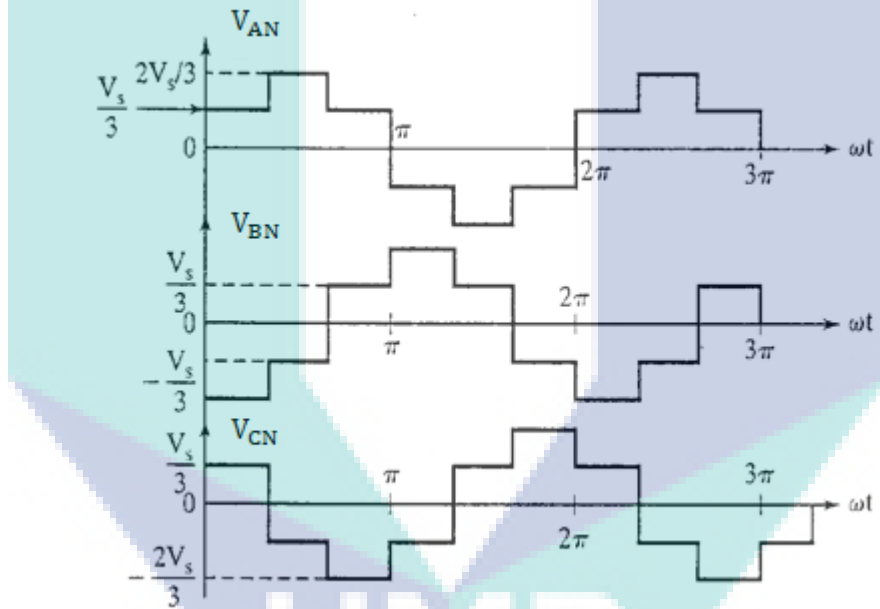


Figure 2.9 Line to neutral voltage for 180° conduction mode waveform

For obtaining line to the line plot for the waveform, the equations are as follows. Meanwhile, Table 2.2 is the summation of all the line to line voltage for 180° conduction mode. Figure 2.10 presents the line to line voltage waveform for 180° conduction mode.

$$V_{AB} = V_{AN} - V_{BN} \quad 2.7$$

$$V_{BC} = V_{BN} - V_{CN} \quad 2.8$$

$$V_{CA} = V_{CN} - V_{AN} \quad 2.9$$

Table 2.2 Line to line voltages for 180° conduction mode

Interval	$V_{AB}$	$V_{BC}$	$V_{CA}$
1	$V_s$	$-V_s$	0
2	$V_s$	0	$-V_s$
3	0	$V_s$	$-V_s$
4	$-V_s$	$V_s$	0
5	$-V_s$	0	$V_s$
6	0	$V_s$	$V_s$

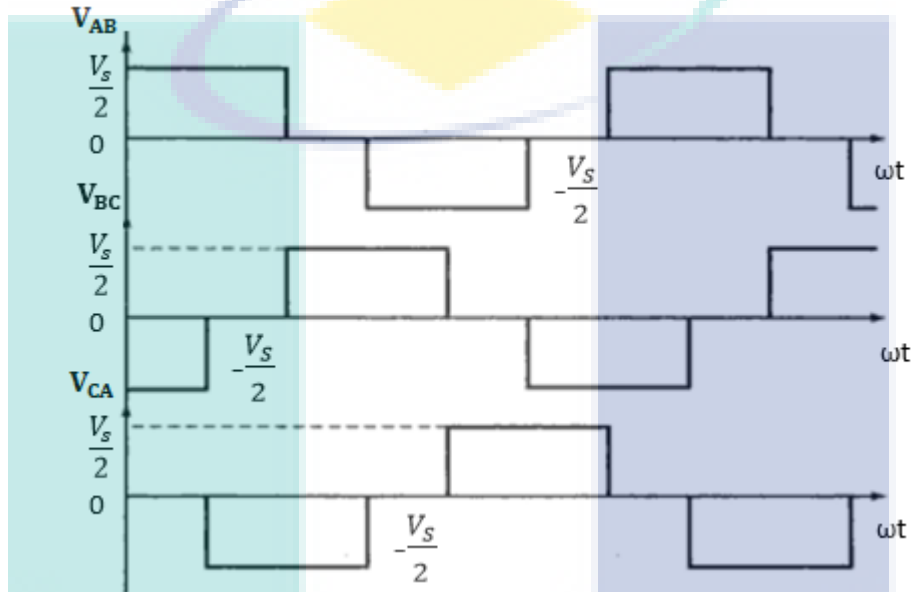


Figure 2.10 Line to line voltage waveform for 180° conduction mode

The most widely used power semiconductor devices are including IGBT's and gate turn-off thyristor's (GTO). The performance of VSI is depending on the switching device gate pulse pattern generation method. Other than the components stated above, the inverter drive typically involves overcurrent detector, DC link overvoltage detector, switching device saturation voltage detector, ground fault detector and line voltage surge suppressor. All the components are a must for an inverter to rapidly interrupt the drive and protect the PWM-VSI after a fault condition (Ahmet M. Hava, 1998).

## 2.5 Switching Devices

Metal Oxide Semiconductor Field Effect Transistor (MOSFET), IGBT, GTO and integrated gate-commutated thyristor (IGCT) are the example of power semiconductor that function as a switching device. A three-terminal semiconductor device called IGBT that was introduced since 1988 is suitable to be applied for moderate speed, high voltage application in power electronics, particularly in PWM,

UPS and switch-mode power supplies (SMPS), solar powered DC-AC inverter, various converter topologies and frequency converter applications operating in the hundreds of kHz range (Sujod, 2014).

The IGBT is the three-terminal electronic component which the terminals are known as emitter (e), collector (c) and gate (g) as shown in Figure 2.11. Terminal for the conductance are e and c while the g terminal is linked to its control. IGBT is a unidirectional device that can only switch current in the forward direction. Triggering and disabling its g terminal can simply switch ON and OFF an IGBT and provide full controllability at a wide range of switching frequencies. It only requires a small voltage to maintain the conduction through the device. This device will continue in ON state when a constant positive input signal across g and e terminal. Deduction of input signal will cause the IGBT to turn OFF (Sujod, 2014) (“Insulated Gate Bipolar Transistor or IGBT Transistor,” 2013).

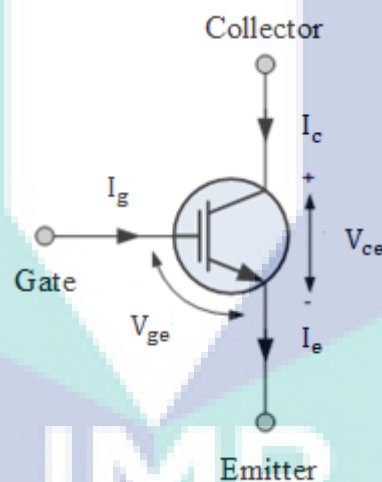


Figure 2.11 IGBT symbol

Source: “Insulated Gate Bipolar Transistor or IGBT Transistor” (2013)

The characteristic is similar as BJT and MOSFET. This is obviously shown that IGBT is the hybrid combination of low conduction loss of a BJT and high switching power of the MOSFET. The principle of operation of the IGBT is similar to the N-channel power MOSFET. The basic difference is that the resistance is much smaller in the IGBT when the current flow through the device in its ON. Based on Figure 2.12, this semiconductor switching device is controlled like a MOSFET but has the output

characteristics of BJT (“IGBT Structure and Circuit Working with Applications,” 2015).

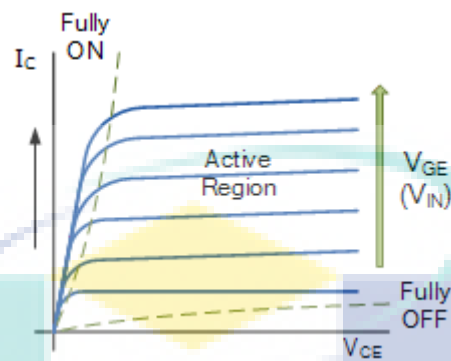


Figure 2.12 Output characteristic of IGBT

Source: “IGBT Structure and Circuit Working with Applications” (2015)

Compared to BJT and MOSFET, the benefit of the IGBT is the fact that it provides greater power gain than standard bipolar type transistor combined with the higher voltage operation and lower input losses of the MOSFET. The advantages of IGBT compared to the other switching device are low ON resistance, high voltage capacity, fast switching speed, ease of drive and joined with zero gate drive current creates a good option for sensible speed and various high voltage applications. Meanwhile, the drawbacks of IGBT are the speed of switching is lower to a power MOSFET and higher to BJT (“Insulated Gate Bipolar Transistor or IGBT Transistor,” 2013) (“IGBT Structure and Circuit Working with Applications,” 2015).

## 2.6 Power Quality Issues

Power quality had become the main concern for electric utilities and consumer since late 1980s. There are four main factors that cause concern about power quality which is user’s awareness of power quality issues, increasing demand for power supply efficiency, newer generation of generators and things interconnected in a network (Dugan, McGranaghan, Santoso, & Beaty, 2004). Power quality can be defined as the grid’s ability to supply a clean and stable power supply. Figure 2.13 shows the main aim of the power system is to produce the noise-free sinusoidal wave shape and within the voltage and frequency tolerance.

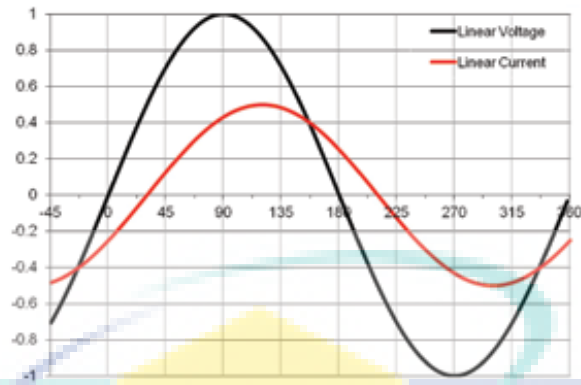


Figure 2.13 Noise free sinusoidal wave shape of voltage and current of a linear load  
Source: Shah (2013)

Therefore, any power problem manifested in voltage, current or frequency deviation that results in failure or misoperation of customer equipment are power quality problem definitions used in (Dugan et al., 2004). The example of a power supply with a power quality problem is shown in Figure 2.14 where the wave shape is non-sinusoidal and the load is non-linear.

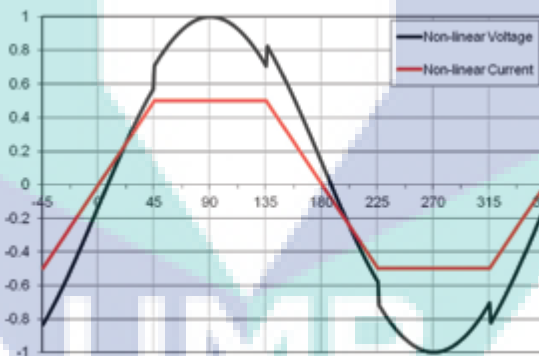


Figure 2.14 Non-sinusoidal wave shape with power quality problem for a non-linear load

Source: Shah (2013)

The utility and consumer opinion about the causes of power quality problems is shown in Table 2.3 below. This data was collected by Georgia Power Company. Both utility and consumer give different judgment while both agree that two-thirds of the problems are from events on natural phenomena (Dugan et al., 2004).

Table 2.3 Survey on the factors causes power quality problems

Power Quality Problem Factor	Customer Perception	Utility Perception
Natural	60 %	66 %
Utility	17 %	1 %
Customer	12 %	25 %
Neighbour	8 %	8 %
Other	3 %	2 %

Source: Dugan et al. (2004)

## 2.7 Harmonics

Some of the power quality issues such as THD will give a negative impact on the system since the quality of the power grid is decreased plus the reliability and safety of electrical equipment are affected (Zhao & Liu, 2012) (Kharjule, 2015). IEEE 519-1992 defines that harmonics as a sinusoidal component of a periodic wave of quantity having a frequency that is an integral multiple of the fundamental frequency.

A linear load can be easily defined as the load that obeys Ohm's law while the non-linear load is the load that has impedance change with applied voltage. Thus, current produce is non-sinusoidal and contains harmonics and create voltage distortion (Hicks et al., 2018). Referring to IEEE Std 519-1992 and TNB Technical Guidebook on Grid-interconnection of Photovoltaic Power Generation System to LV and MV Networks, the harmonic current requirement must not exceed 5 % in GC renewable energy generation systems (Abdool & Alwannan, 2014) (Oh & Sunwoo, 2008) (Zhao & Liu, 2012).

The main non-linear load that connected in an electrical power system is a static power converters for example inverter, rectifier, chopper and AC-AC converter. All of these converters produce non-sinusoidal current. Harmonic voltage and current in an electric power system are the result of non-linear load (Zambri et al., 2016) (Khatri & Kumar, 2017). According to IEEE 519-1992, THD is the ratio of root mean square (RMS) of the harmonic content to the RMS value of the fundamental quantity and expressed as a percent of the fundamental.

The quality of the AC current and voltage are measured by THD and the closer the wave to sinusoidal, the smallest the THD (Kharjule, 2015) (Rahimi, Mohajeryami, & Majzoobi, 2016). Besides that, other harmonic definition is mathematics ways of

describing distortion to a voltage or current waveform occurs at an integer multiple of the fundamental frequency. THD of the voltage at the PCC and THD of current can be calculated using equation 2.10 and equation 2.11 respectively. The point where the utility grid and the GCPV system are connected is known as PCC (Al-Shetwi & Sujod, 2017). Additionally, value of  $V_{rms}$  and  $I_{rms}$  can be found using equation 2.12 and equation 2.13 accordingly.

$$\% \text{ THD}_{V_{PCC}} = \frac{\sqrt{\sum_{h=2}^{\infty} V_{PCC}^2}}{V_1} \times 100 \quad 2.10$$

$$\% \text{ THD}_I = \frac{\sqrt{\sum_{h=2}^{\infty} I_h^2}}{I_1} \times 100 \quad 2.11$$

Where:

$V_{PCC}$  = voltage at PCC

$I_h$  = magnitude of individual harmonic components

$h$  = harmonic order

$$V_{rms} = V_{1,rms} \sqrt{1 + \left(\frac{\text{THD}_V}{100}\right)^2} \quad 2.12$$

$$I_{rms} = I_{1,rms} \sqrt{1 + \left(\frac{\text{THD}_I}{100}\right)^2} \quad 2.13$$

The quality of the power grid may be downgraded when there are harmonic current in the system. Besides that, it also gives impact to the reliability and safety of electrical equipment such as increase the machine heats due to increase iron and copper losses especially for generator since it typically has 3 to 4 times of the source of impedance, the increase in core losses due to increase in iron losses which are Eddy current and hysteresis and PR losses in the cable will dissipate as heat when carrying harmonic current (Zhao & Liu, 2012).

## 2.8 Switching Losses

Power electronic switching losses are one of the reasons that can contribute to total system losses. When a switch ON or OFF then instantaneously generates the alternating current level, switching losses occur (A. M. Hava, Kerkman, & Lipo, 1998).



For switching losses in IGBT, the switching losses occur when there is a turn-on and a turn-off signal at IGBT's gate and correspondingly load current, DC link voltage and switching frequency are the factor that will determine the switching losses. Switching losses can be defined as in equation 2.14 and equation 2.15 (Sujod, 2014).

$$P_{SWloss_T} = E_{on} + E_{off} \quad 2.14$$

$$P_{SWloss_D} = E_{rr} \quad 2.15$$

Where:

$E_{on}$  = turn-on losses on IGBT

$E_{off}$  = turn-off losses on IGBT

$E_{rr}$  = turn-off losses due to the reverse recovery in diode

Furthermore, low switching losses can produce less thermal stress of switching devices and the size of the heat sink in the compact power converter can be reduced. Apart from that, inverter cannot operate at very high switching frequencies because the switching losses can be increased (Asiminoaei, Rodriguez, & Blaabjerg, 2008). Large errors regarding the total losses switching losses will occur if not include the calculation or weighting the conduction losses by an estimated factor to take into account for switching losses since the transitions from on-state to off-state and vice versa do not occur instantaneously. The losses will more accurately with many points be considered in the calculation.

## 2.9 Pulse Width Modulation

PWM technique becomes the centre of attraction in this research due to the fact that it has benefits such as low power dissipation, easy to implement and control, no temperature variation, high power handling capacity, compatible with today's digital microprocessor, no additional components needs to be added to obtain control of the output voltage and lastly, lower harmonics can be eliminated or minimized. The downsides of PWM technique are switching frequency increase exceedingly which then lead the switching devices face greater stress and therefore derating those devices, attenuation of the wanted fundamental component of waveform and generation of high-frequency harmonic (Kharjule, 2015) (Singh, Kumar, Singh, & Patel, 2014).

Next, general theory of PWM technology is explained in two main aspects which are pulses involve and the main principle of PWM technique. Firstly, there are two groups of pulses involves at the inertial link input as shown in Figure 2.15. The pulses are two different waveforms known as modulated waveform and carrier waveform. The typical PWM controller receives three modulated waveforms and each of the modulated signal is 120° out of phase with the other two modulated signal and triangle carrier signal is used. Both of pulses have same impulse area and also same effectiveness.

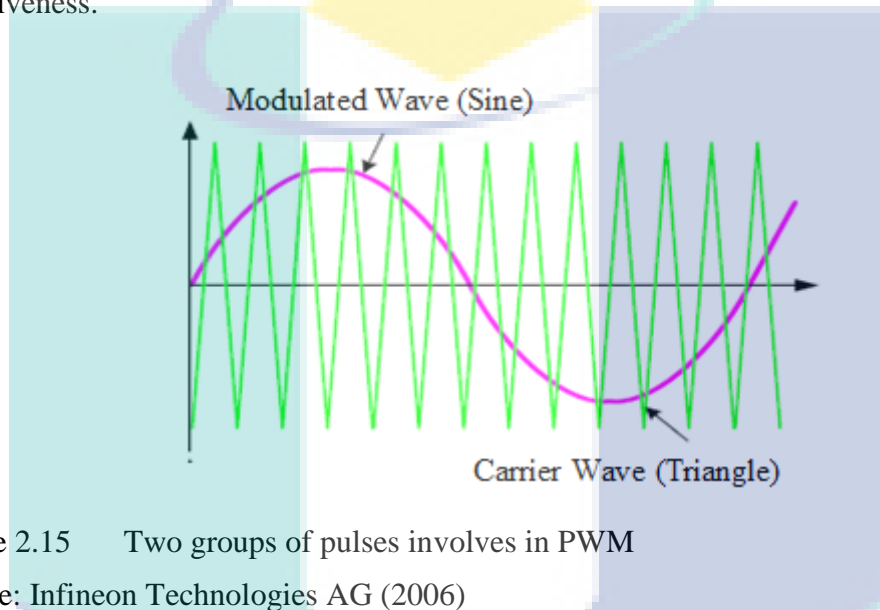


Figure 2.15 Two groups of pulses involves in PWM  
Source: Infineon Technologies AG (2006)

The triangular carrier signal is compared with the sinusoidal modulating signal. The triangular carrier wave determines the desired switching frequency with the simple equation as in equation 2.16 where  $T$  is the time for 1 cycles. When the modulating signal is greater than the carrier pulse, then the PWM output pulse is high (1) and it becomes low (0) when the condition between the two pulses are vice versa. The PWM output pulse can be observed in Figure 2.17.

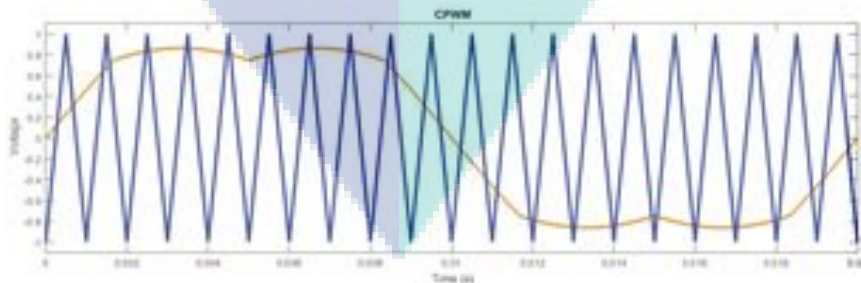
$$f_{sw} = \frac{1}{T} \quad 2.16$$

Modulation index ( $m_i$ ) can be defined as the ratio of the peak modulated waveform ( $V_m$ ) and carrier waveform ( $V_C$ ) magnitude. The  $m_i$  can be expressed in equation 2.17 (Kharjule, 2015).

$$m_i = \frac{V_m}{V_C} \quad 2.17$$

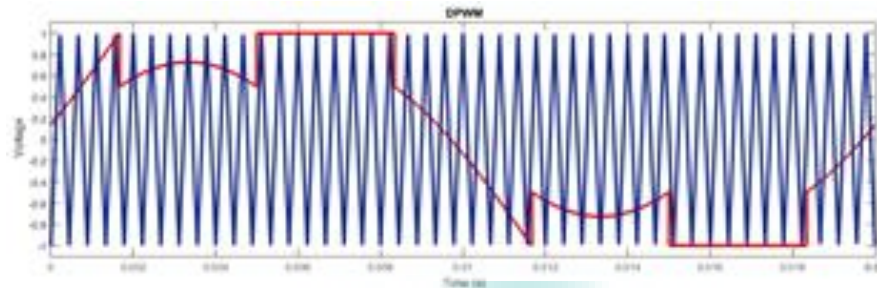
Normally the  $m_i$  preferred in PWM techniques is  $0 < m_i < 1$  or can never be more than unity (Prajapati, Ravindran, Sutaria, & Patel, 2014) where the carrier waveform has higher peak magnitude than modulated magnitude (Infineon Technologies AG, 2006) (Subsingha, 2016). The linear relationship between input and PWM output voltage is maintained and good quality output voltage produced (Prajapati et al., 2014). Meanwhile, over modulation can occur when  $m_i > 1$  or when the modulated waveform peak magnitude is higher than the carrier waveform peak magnitude. Over modulation is not preferred since linear mode cannot be kept and increment fundamental voltage magnitude will decrease the quality of output waveform (A. M. Hava et al., 1998).

Generally, CPWM and DPWM are two types of PWM. One of the PWM type is called CPWM because continuous throughout the modulating signal cycle (Wu, Shafi, Knight, & McMahon, 2011). The other type which is DPWM is purposely set equal to peak carrier signal so that switching does not take place at least 40 % carrier signal cycles (A. M. Hava et al., 1998). One phase switch is not switching, while the other two phases remain sinusoidal line to line voltage. Figure 2.16 shows an example of generating of the PWM signal for CPWM and DPWM. The type of PWM is differentiated based on the modulated waveform. The modulated waveform is generated based on the equation as shown in section 2.9.2 and section 2.9.3 for CPWM and DPWM respectively.



(a) CPWM

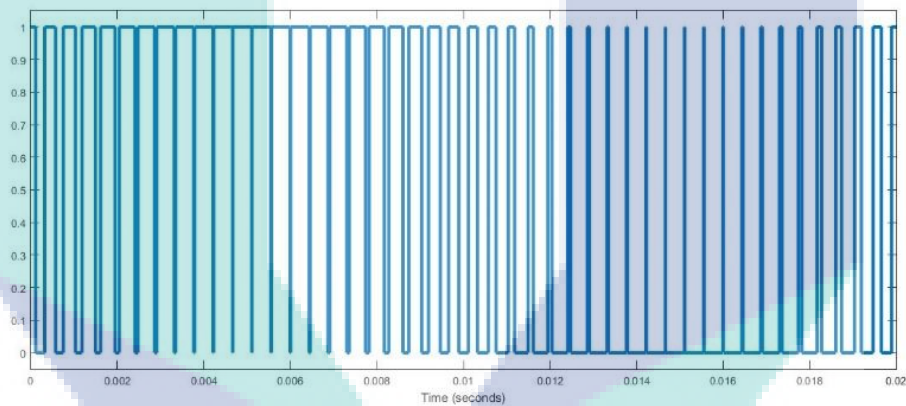
Figure 2.16 The process to generate PWM signal



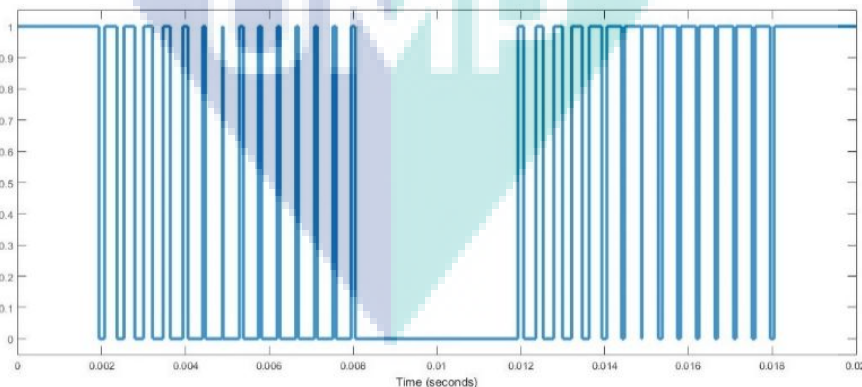
(b) DPWM

Figure 2.16 Continued

Figure 2.17 shows the differences between CPWM and DPWM output signal. The figures below show that DPWM has less output signal, hence less switching losses compared to CPWM with about 33 % reduction in the same switching frequency (Asiminoaei et al., 2008). Therefore, the usage of DPWM in inverter control could reduce power losses in the inverter and is preferred for size reduction of the inverter.



(a) CPWM output signal



(b) DPWM output signal

Figure 2.17 Output signal of CPWM and DPWM

Some of the examples of CPWM types are sinusoidal pulse width modulation (SPWM), third harmonic injected pulse width modulation (THIPWM) and TTHIPWM

or also known as carrier base space vector PWM (CBSVPWM), while DPWM types are DPWM0, DPWM1, DPWM2, DPWM3, DPWMMIN and DPWMMAX (Sujod, 2014). Types of CPWM and DPWM are shown in Figure 2.18.

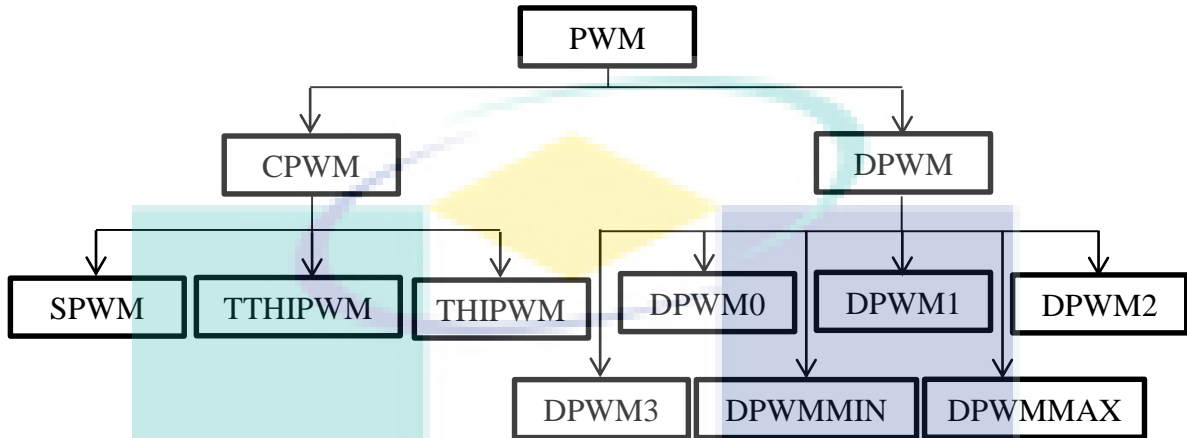


Figure 2.18 PWM types and categories

The basic type of PWM is SPWM where the sinusoidal modulated wave is directly compared with the triangle carrier wave (Subsingha, 2016). The other types of PWM encounter a process where zero sequence signal is injected in the fundamental voltage before compared the modulating reference signal with the carrier wave. The zero sequence signal is third harmonics with frequency three times of the fundamental voltage. PWM types that further discussed in this paper are SPWM, TTHIPWM, DPWM0, DPWM1 and DPWM2.

The diversity of the modulating reference signal depends on the different waveform of the third harmonic injected to the fundamental voltage (Sujod, 2014) (A. M. Hava et al., 1998). The merits of the third harmonic injection are it brings down the peak magnitude of the resultant modulating waveform and 15.5 % can improve the converter output voltage compared to SPWM (Zahim & Erlich, 2012). Furthermore, the instantaneous magnitude modified modulating signal is less than or equal to the peak magnitude carrier wave (Infineon Technologies AG, 2006). Table 2.4 below is the summation of the PWM types and the injection of zero sequence signals in the fundamental voltage.

Table 2.4 Injection of zero sequence signals in the fundamental voltage of PWM

PWM types		Injection of Zero Sequence Signal
CPWM	SPWM	
	THISPWM	✓
	TTHIPWM	✓
DPWM	DPWM0	✓
	DPWM1	✓
	DPWM2	✓
	DPWM3	✓
	DPWMMIN	✓
	DPWMMAX	✓

THD and switching losses are the main performance characteristics that are comparable between CPWM and DPWM. At low  $m_i$ , the THD for CPWM is low (Oh & Sunwoo, 2008). Meanwhile, greater THD occurs when low modulation DPWM is used. This is because harmonic is produced when the pulses are being modified when the PWM controller modifies the modulating signal as a function of third harmonic signal on per carrier cycle. Figure 2.19 below shows a graph that illustrating the THD against  $m_i$  for each of the PWM types (A. M. Hava et al., 1998). From the graph, when the  $m_i$  is from 0 until approximately 0.5, DPWM signals have higher THD than CPWM signals. After the  $m_i$  passes 0.5 and above, the CPWM signals show an increment in THD.

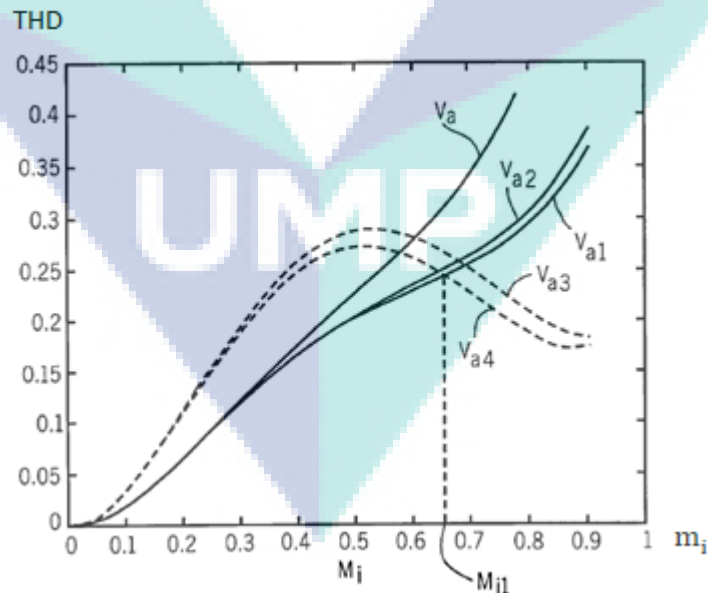


Figure 2.19 Graph of THD against  $m_i$  for CPWM and DPWM signals ( $V_a =$  SPWM,  $V_{a1} =$  TTHIPWM,  $V_{a2} =$  THIPWM,  $V_{a3} =$  DPWM1,  $V_{a4} =$  DPWM2)

Source: A. M. Hava et al. (1998)

Clearly, it is known that CPWM signal causes less THD compared to DPWM at low  $m_i$  but vice versa when the  $m_i$  is greater. For all CPWM types, the switching losses are same and independent of all load current phase angle while, the switching losses for DPWM is influenced by modulation types and load power factor (PF) (Zahim & Erlich, 2012) and able to minimize converter switching losses (Asiminoaei et al., 2008). In contrast to the fact stated above, according to (A. M. Hava et al., 1998) DPWM can overcome many weaknesses of CPWM such as switching losses where theoretically the switching losses of DPWM is reduced by average of 33 % reduction compared to CPWM (Asiminoaei et al., 2008). DPWM can minimize the switching losses since the switching is discontinuous during at least some of the portion of each modulating cycle (A. M. Hava et al., 1998) (Nguyen, Nguyen, & Lee, 2011).

### **2.9.1 Process to Generate PWM**

PWM is a fancy term used to describe a type of digital signal which has the ability to control voltage and frequency at one stage (Singh et al., 2014). Furthermore, THD and switching losses can be minimized with PWM (Ruban, Hemavathi, & Rajeswari, 2012). This technique can maximize the system gain at high modulating index values and the linear range of the system operation. PWM is used for controlling the amplitude of digital signals in order to control devices and applications requiring power or electricity. In inverter, the PWM signal is applied to the gate of the power transistor. This signal determines the on and off intervals of the transistors (Singh et al., 2014).

In order to produce the PWM output signal, desired frequency of three phases modulated signals are compared with high frequency triangular carrier signal by using a comparator (Prajapati et al., 2014) (Mohanty & Sahoo, 2010) as shown in Figure 2.20. As the result, the process generates the logical signal which is six pulses and later become the switching instant of inverter (Sathishkumar & Parthasarathy, 2016). Secondly, the main principle of PWM is ON/OFF control on semiconductor switching component of the output with generated pulses with the same amplitude but different width (Singh et al., 2014).

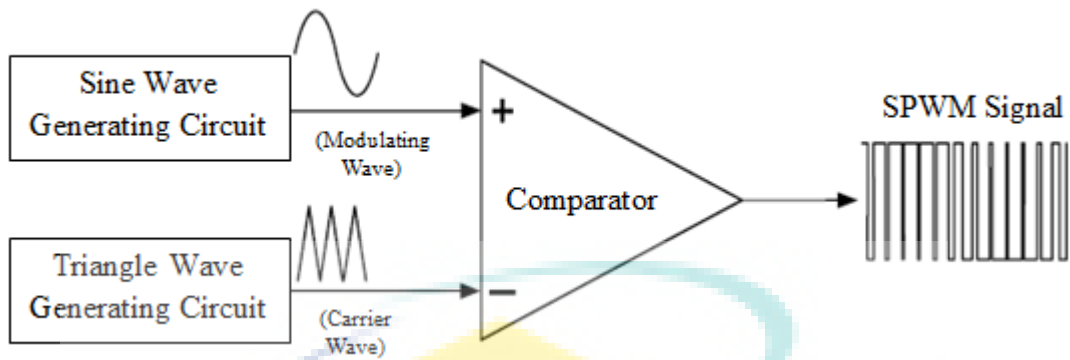


Figure 2.20 Process to generate PWM

Source: Infineon Technologies AG (2006)

### 2.9.2 Continuous PWM Concept

From all of the PWM types listed in Figure 2.18, the basic type of the PWM is referred to SPWM. It is the most popular and simplest to generate where sine-triangle wave comparison method is applied in this technique (Infineon Technologies AG, 2006) as shown in Figure 2.15. The high frequency of the triangular carrier voltage signal is compared with sinusoidal modulating signal (Prajapati et al., 2014) to produce the output signal the same as Figure 2.17 (a). For this reason, harmonic reduction using SPWM is most commonly used in industry (Subsingha, 2016).

In addition to SPWM, a third harmonic signal whose frequency is three times of the fundamental frequency injected into sinusoidal modulated wave and saddle-like modulated wave is produced as shown in Figure 2.21. The modified modulating signal is compared with the triangle carrier wave. This CPWM is called THIPWM and it is an optimized PWM method with advantages such as bringing down the peak magnitude of the resultant modulating waveform. Mixed third-harmonic in the PWM can 15.5 % improved the converter output voltage compared to SPWM and at the same time able to give better THD performance (Zahim & Erlich, 2012) (Nguyen et al., 2011).

TTHIPWM generates the precise pulses required by the inverter if compared with the other PWM and it is one of the most current trends in pulse generation (Sathishkumar & Parthasarathy, 2016). It has the same technique with THIPWM but different implementation method. This technique can increase the fundamental output



by 15 % and able to reduce harmonic content in line-to-line voltage (Singh et al., 2014) (Grigoletto, Stefanello, Silva, & Pinheiro, 2016).

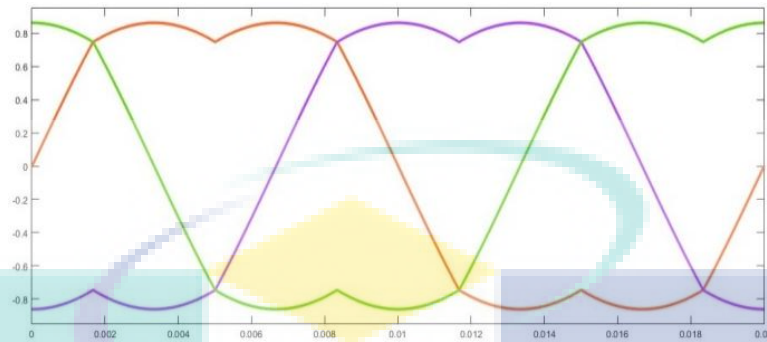


Figure 2.21 Three-phase THIPWM modulated wave

Moreover, TTHIPWM has a wide range of modulation, less switching losses and lower harmonic distortion compared to SPWM (Jayanth et al., 2018). Therefore, TTHIPWM is chosen as the CPWM technique to be implemented in the inverter control of the GCPV system for further studies and to minimize the THD and switching losses in the system according to the above statement and based on the result shown in Figure 2.19 where TTHIPWM has the lowest THD level compared to the other CPWM type.

Figure 2.22 below shows how the modulated modulating signal of TTHIPWM is produced where  $u_a, u_b$  and  $u_c$  are three fundamental voltages,  $u_a^*$  is the modulated modulating signal for 'phase a' and  $u_{no\_PWM}$  is the third harmonics that injected into the fundamental signal to produce the modulated modulating signal. The injection of the third harmonics for TTHIPWM is according to the equation 2.18 below (Sujod, 2014).

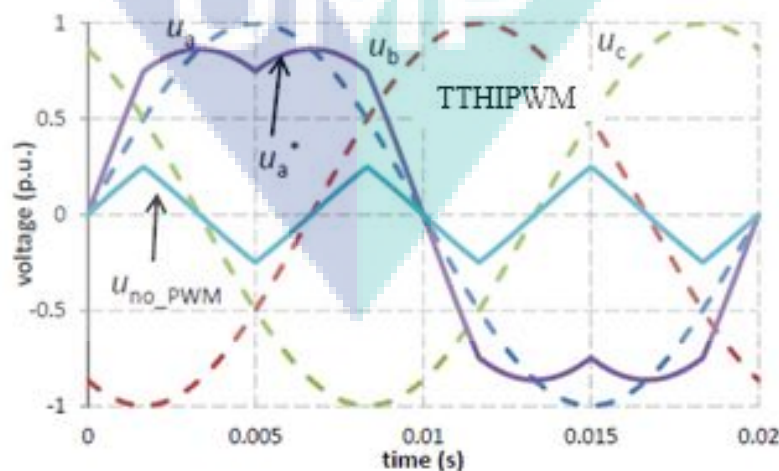


Figure 2.22 The process to produce a modulated modulating signal for TTHIPWM  
Source: Sujod (2014)

$$\text{If } |u_a| \leq |u_b| \text{ and } |u_a| \leq |u_c| \rightarrow u_{\text{no\_PWM},1} = 0.5 \times u_a$$

$$\text{If } |u_b| \leq |u_a| \text{ and } |u_b| \leq |u_c| \rightarrow u_{\text{no\_PWM},2} = 0.5 \times u_b$$

$$\text{If } |u_c| \leq |u_a| \text{ and } |u_c| \leq |u_b| \rightarrow u_{\text{no\_PWM},3} = 0.5 \times u_c$$

$$\text{Else } u_{\text{no\_PWM},1}, u_{\text{no\_PWM},2}, u_{\text{no\_PWM},3} = 0$$

$$u_{\text{no\_PWM}} = u_{\text{no\_PWM},1} + u_{\text{no\_PWM},2} + u_{\text{no\_PWM},3}$$

2.18

### 2.9.3 Discontinuous PWM Concept

DPWM types are included DPWM0, DPWM1, DPWM2, DPWM3, DPWMMIN and DPWMMAX. In this paper, DPWM0, DPWM1 and DPWM2 are explained further. All of the DPWM types mentioned are the techniques generated by adding the third harmonic signal to each of the modulating signal (A. M. Hava et al., 1998). Figure 2.23 shows the modulating signal of DPWM0, DPWM1 and DPWM2. The dotted lines are the three fundamental voltages  $u_a, u_b$  and  $u_c$ , while the purple colour is the modulated signal for 'phase a',  $u_a *$  after mixed with the third harmonic signal,  $u_{\text{no\_PWM}}$  that three times than the fundamental frequency. The injection of the third harmonic for DPWM0, DPWM1 and DPWM2 are referring to the equation 2.19, 2.20 and 2.21 respectively (Sujod, 2014).

As mentioned in section 2.9, according to (A. M. Hava et al., 1998) DPWM can overcome many weaknesses of CPWM such as switching losses where theoretically the switching losses of DPWM are reduced by average of 33 % reduction compared to CPWM. DPWM can minimize the switching losses since the switching is discontinuous during at least some of the portion of each modulating cycle. The switching losses for DPWM are influenced by modulation types and load PF (Zahim & Erlich, 2012) and able to minimize converter switching losses. Basically, all the DPWM types have the same characteristic when it comes to switching losses. In that case, the selection of which DPWM chosen to be implemented is by referring the THD performance of the DPWM. The result of the research by (Sujod, 2014) conclude that DPWM2 has the

lowest THD value compared to DPWM0 and DPWM1 and as well as the graph in Figure 2.19.

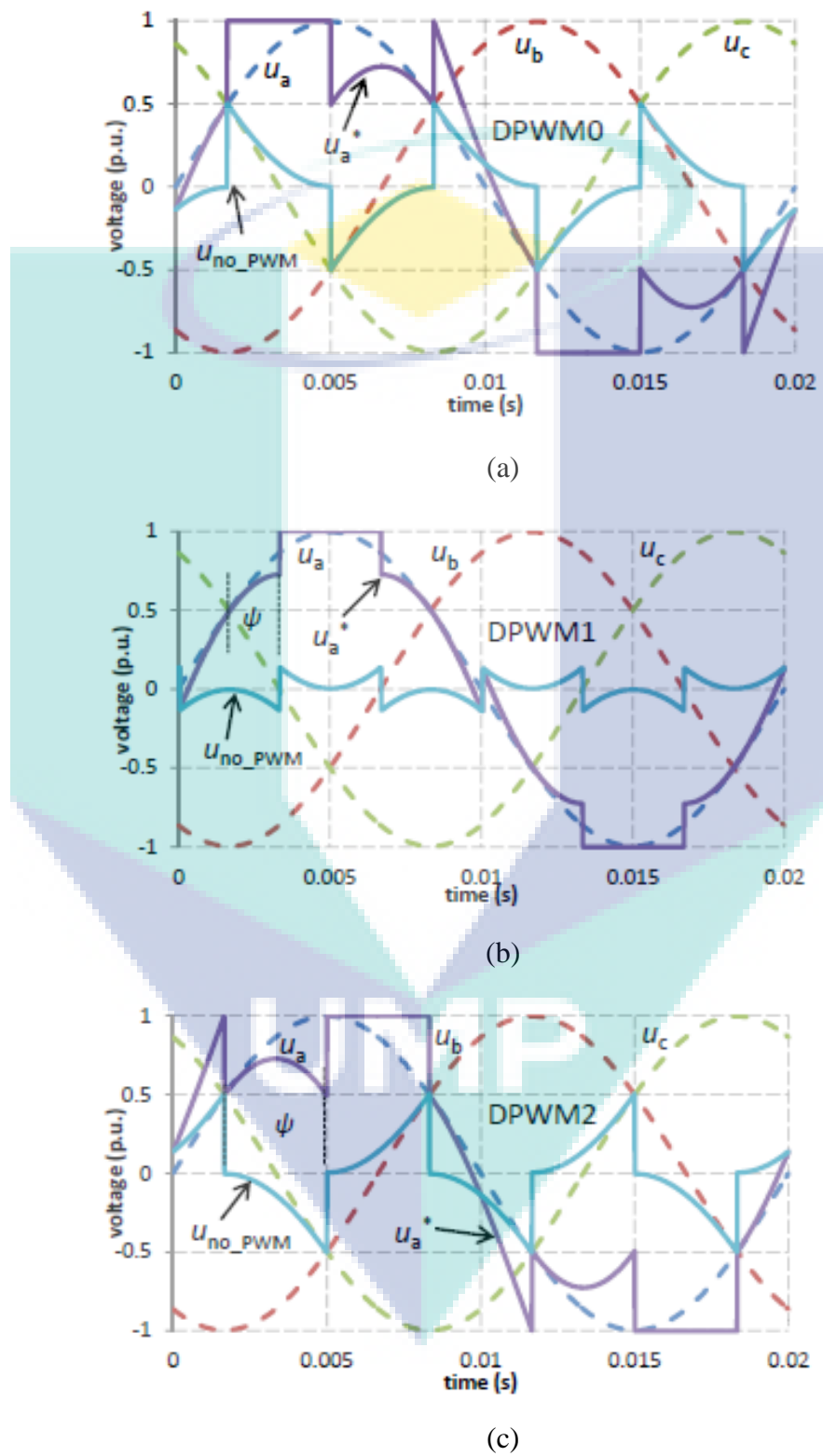


Figure 2.23 The process to produce a modulated modulating signal for DPWM0, DPWM1 and DPWM2

Source: Sujod (2014)

DPWM0:

$$\text{If } |u_c| \leq |u_a| \text{ and } |u_c| \leq |u_b| \rightarrow u_{\text{no\_PWM},1} = \text{sign}(u_a) - u_a$$

$$\text{If } |u_b| \leq |u_c| \text{ and } |u_b| \leq |u_a| \rightarrow u_{\text{no\_PWM},2} = \text{sign}(u_b) - u_b$$

$$\text{If } |u_a| \leq |u_b| \text{ and } |u_a| \leq |u_c| \rightarrow u_{\text{no\_PWM},3} = \text{sign}(u_c) - u_c$$

$$\text{Else } u_{\text{no\_PWM},1}, u_{\text{no\_PWM},2}, u_{\text{no\_PWM},3} = 0$$

$$u_{\text{no\_PWM},1} = u_{\text{no\_PWM},1} + u_{\text{no\_PWM},2} + u_{\text{no\_PWM},3}$$

2.19

DPWM1:

$$\text{If } |u_b| \leq |u_a| \text{ and } |u_c| \leq |u_a| \rightarrow u_{\text{no\_PWM},1} = \text{sign}(u_a) - u_a$$

$$\text{If } |u_a| \leq |u_b| \text{ and } |u_c| \leq |u_b| \rightarrow u_{\text{no\_PWM},2} = \text{sign}(u_b) - u_b$$

$$\text{If } |u_a| \leq |u_c| \text{ and } |u_b| \leq |u_c| \rightarrow u_{\text{no\_PWM},3} = \text{sign}(u_c) - u_c$$

$$\text{Else } u_{\text{no\_PWM},1}, u_{\text{no\_PWM},2}, u_{\text{no\_PWM},3} = 0$$

$$u_{\text{no\_PWM}} = u_{\text{no\_PWM},1} + u_{\text{no\_PWM},2} + u_{\text{no\_PWM},3}$$

2.20

DPWM2:

$$\text{If } |u_b| \leq |u_a| \text{ and } |u_b| \leq |u_c| \rightarrow u_{\text{no\_PWM},1} = \text{sign}(u_a) - u_a$$

$$\text{If } |u_c| \leq |u_b| \text{ and } |u_c| \leq |u_a| \rightarrow u_{\text{no\_PWM},2} = \text{sign}(u_b) - u_b$$

$$\text{If } |u_a| \leq |u_c| \text{ and } |u_a| \leq |u_b| \rightarrow u_{\text{no\_PWM},3} = \text{sign}(u_c) - u_c$$

$$\text{Else } u_{\text{no\_PWM},1}, u_{\text{no\_PWM},2}, u_{\text{no\_PWM},3} = 0$$

$$u_{\text{no\_PWM}} = u_{\text{no\_PWM},1} + u_{\text{no\_PWM},2} + u_{\text{no\_PWM},3}$$

2.21

## 2.10 Passive Filter

Filter circuit is also known as frequency-selective is a building block in a system that the function is passed to the output only the input signals that are in the desired range of frequencies while rejecting another. The frequencies that in the desired range are called band pass while the frequencies that outside the range of frequencies are known as stop pass. The band pass and stop pass for different types of filter are not the same as another depending on the function of the filter itself. In short, filters are employed in a system to alter the unwanted frequency components from the signal (Lacanette, 1991) (Winder, 2002).

Filter types are included passive filter, active filter, analog filter, digital filter, high pass filter, low pass filter, band pass filter, band stop filter, discrete time filter, continuous time filter, linear filter, non-linear filter, infinite pulse response filter and finite pulse response filter (Winder, 2002). Passive filter works well at high frequency. This feature is the most important in this research since the switching frequency that needs to reduce the THD is high because the switching frequency and THD are inversely proportional to each other (Abd Halim, 2013). Passive filter does not require any external power supply. The simplest passive filter types are RC and RL filter where it consist only one reactive element with no active components for example transistor.

One of the passive filter type is a low pass filter where it passes frequencies that below a cut off frequency ( $f_{co}$ ) and attenuates those above (Khanfara, Bachtiri, Hammoumi, & Boussetta, 2016) as shown in Figure 2.24. The  $f_{co}$  is the frequency that between pass and stop band pass. Meanwhile, the other passive filter type that passes frequencies above the critical frequency but rejects those below as shown in Figure 2.25 is a high pass filter. Besides that, band pass filter allows signal that in between the range of the pass band to pass through and attenuates signal with frequencies outside the range (Lacanette, 1991).

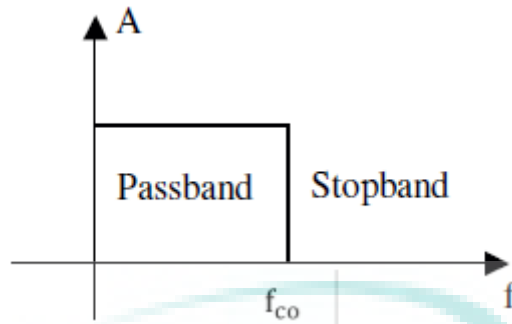


Figure 2.24 Low pass filter response

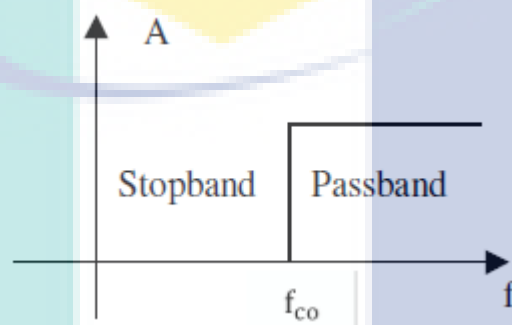
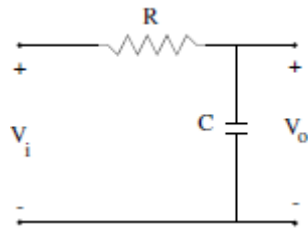
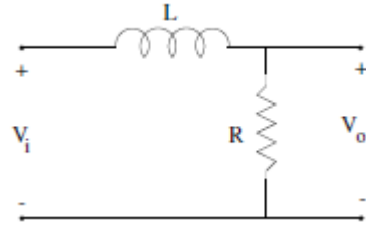


Figure 2.25 High pass filter response

Both of the filters consist only one reactive element RC or RL. The position of the component in the circuit can determine the filter type. The low pass RC filter and low pass RL filter circuit are shown in Figure 2.26. RC low pass filter operation is based on the principle of capacitive reactance and RL low pass filter operation is based on the principle of inductive reactance. Referring to Figure 2.27, the position of the components is switched and this makes the filters are operated with high pass characteristics. The equation to determine the  $f_{co}$  for each filter is included below and it turns out that the equation for low pass RC filter is the same as a high pass RC filter. Same goes to low pass RL filter and high pass RL filter, the equation to determine the  $f_{co}$  for both is also the same (Al-Shetwi & Sujod, 2017).

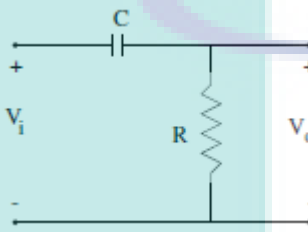


(a) Low pass RC filter

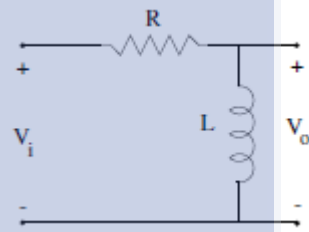


(b) Low pass RL filter

Figure 2.26 Low pass filter circuits



(a) High pass RC filter



(b) High pass RL filter

Figure 2.27 High pass filter circuit

Equation to determine  $f_{co}$  for low pass and high pass RC filter:

$$f_{co} = \frac{1}{2\pi RC} \quad 2.22$$

Equation to determine  $f_{co}$  for low pass and high pass RL filter:

$$f_{co} = \frac{R}{2\pi L} \quad 2.23$$

## 2.11 Previous Research

Many researchers around the world show interest in research on PWM-VSI drives since it has high demand in the market. Furthermore, many years of research and improving of the PWM-VSI have led to a positive impact on the PWM-VSI in terms of cost effective, efficient, compact and reliable high performance PWM-VSI drives. A number of literature related to PWM methods and drive control algorithm is published. A few research papers that have a common objective with this research are listed and

elaborate in this section. The results of the previous researches are considered as the reference and to be compared with the results obtained from this research.

In industry and electrical power system, it is more preferably use multi-level inverter because of the high performance of the inverter plus the THD and switching losses are low. In the meantime, increasing levels of inverter output voltage will increase the number of diodes which cause more switching losses. The purpose of this paper is to study the output voltage of the five level diode clamp inverter either no load or R-L load a 1 kW and with  $PF = 0.8$  with SPWM and THIPWM modulating signal. The modulating techniques applied in this research are phase disposition (PD), phase opposition displacement (POD) and alternative phase opposition displacement (APOD). Simulation was done with MATLAB/Simulink. The conclusion of the paper stated that the PD carrier signal generated the lowest THD for both THIPWM and SPWM. In addition, another conclusion can be made is PWM that injected with third harmonic will produce less THD than PWM that not injected with the third harmonic in the modulation signal (Subsingha, 2016).

Paper by (Kamal EL-Sayed, 2017) study the impact of PV system tied to the grid to power quality problem which is THD. The PSCAD software simulation environment was used to perform the research on the impact of PV inverter configuration, central and string with different controlling methods on inverter such as SPWM and space vector modulation. The simulation of harmonic distortion was applied at the PCC and the results were compared with IEEE Std 519-1992 standards. String inverter is the best choice compared to central inverter since all the PV modules affected by shading and output power decrease when using central inverter but only a certain number of PV modules affected by shading if using a string inverter. In addition, this research proves that central inverter produces less THD than string inverter in both cases using SPWM and space vector PWM control method. Meanwhile, string inverter shows better performance than central inverter when subjected to shadow effect. Lastly, space vector PWM produces less THD than SPWM.

One of the papers discussed PWM-VSI concentrates on the variable structure of the PWM controller for high efficient PV inverter (Oh & Sunwoo, 2008). Irradiance and temperature can affect the performance of the PV array output voltage. PV power conditioning system (PCS) should operate in a wide range of  $m_i$  since the MPP range of



a medium or high power PV PCS are normally  $450\sim 830 V_{dc}$  or  $300\sim 600 V_{dc}$ . Trade-off occurs between low harmonic currents and high efficiency. This issue can be solved when used PV PCS that can optimally satisfy both requirements with the proposed PWM converter system. The problem statement in this paper is PV PCS should satisfy the harmonic current requirement where total demand distortion (TDD) must be not greater than 5 % and must operate with high efficiency at all load ranges. Therefore, this research aimed to propose a PWM strategy for the medium or high power PCS. This paper compared and analyse appropriate PWM scheme for the PV PCS in the viewpoints of conversion efficiency and current harmonics and to minimize the switching losses of 3-phase PWM converter system.

Some of the PWM used are SVPWM, DPWMMIN and DPWM1 and the proposed PWM strategy are variable structure PWM (VSPWM) controller which selects the SVPWM, DPWMMIN and DPWM1 comparing the input PV power with power level functions depending on the  $m_i$ . This research was carried out with an experiment under some conditions and the inductive load is assumed as delta connected. Results that recorded in this experiment were efficiency, THD of grid current and PF. All the data were measured by using a precision power meter LMG500. The findings in this research are DPWM produce high THD and harmonic losses than CPWM for some switching frequency. The objective is achieved since the proposed method is appropriate for medium or high power PV PCS connected to the grid (Oh & Sunwoo, 2008).

Move to a paper that discussed the power losses for VSI based on the effects of CPWM and DPWM (Wu et al., 2011), it is proved that DPWM scheme has the lowest losses. The comparison of the PWM effect in this paper was investigated on VSI for induction motor drives where about two third of all electricity for industry in Europe and the United States apply the motor drive system. Losses in inverter depend on the form of PWM used to control the inverter switching to achieve a variable voltage and variable frequency output. The objective of this paper is to provide details of a quantitative study of the comparative inverter losses of SPWM and DPWM. A complete inverter model incorporating PWM excitation models and the Hefner IGBT model has been used to model a 4-kVA voltage-source inverter of the type commonly used in VSDs. Three PWM schemes have been considered in this paper which is SVPWM and

DPWM with SPWM as the benchmark. The heat generated by the devices is directly measures using calorimeter method. The power losses simulation was conducted in Pspice. Accurate inverter loss measurement is crucial in this paper. DPWM gives better performance than CPWM in term of reducing switching and therefore, DPWM able to simplify the thermal management issues and this has potential to reduce the inverter size and cost.

The effect of irradiance and temperature were analysed and discussed in (Pradhan et al., 2013) to observe how solar cell performance changes with the change in the mentioned factors. The results were presented in this paper after a number of experiments were conducted. P-N junctions are used in solar PV cells to convert sunlight energy into electrical power. I-V curve is a curve that shows the relationship between current and voltage. I-V curve will change since there is variation of the environmental conditions where the irradiance level and temperature changes. Thus, the MPP will also change. The solar irradiance will keep on changing throughout the day and this will varies I-V and P-V characteristics. Open circuit voltage and short circuit current increase with increasing solar irradiance and the MPP also varies. Besides that, the rate of photon generation increase when the temperature increase and thus reverse saturation current increase rapidly and this reduce the band gap. In conclusion, solar cells give full performance on cold and sunny days compared to hot and sunny weather.

A practical simulation of the sun radiation effect on the output performance of PV module introduced in (Salim et al., 2013) and the results showed that the output of the PV module increases as the simulated sun radiation increases. The simulation was conducted by using the Solara-130 PV module. In this paper, the performance of the PV model was evaluated practically by using a solar model tester (SMT). The SMT can generate solar irradiance from 100 W/m<sup>2</sup> until 1050 W/m<sup>2</sup> and I-V and P-V curves can be automatically plotted SMT by using the software controlling program. Besides that, the study of the impact of solar irradiance to current and voltage THD using a model developed in Simulink are discussed in (Ayub et al., 2014). The PV model was developed using the real solar irradiance data taken from UTeM laboratory and the results from the simulation will be compared with the measurement results obtained from the laboratory. The simulation and experiment result were taken based on clear day solar irradiance data. The results obtained from the study shows that the PV system

output power is proportional to the solar irradiation variance while the generated voltage of the PV system does not have a significant impact. The study shows that current THD has significant effect when the solar irradiance level changes but voltage THD not effect much.

One problem with a PV system that many become chosen topics by researchers is the distortion into the grid that contains some harmonics that are the results from usage of non-linear load such as inverter. The inverter is necessary in a Grid-tied operation system to convert the PV array's DC current to the electrical grid's AC current that is implemented by PWM. PV inverter rated current is limited to 5 % according to IEEE Std. 519-2014 and IEEE Std. 1547 in order to limit these harmonic emissions since inverters supply currents that are highly distorted when operating under low solar irradiance. In addition, current THD increase sharply under very low solar irradiance and depend on the quality of the power supply, types of inverter and its internal controls. (Hicks et al., 2018) study a 5.94 kW array that consists of 2 parallel strings, each containing 11 panels that were rated at 270 W under standard test condition (STC). The current harmonic content of the PV inverter during the late afternoon hours of a clear day were analysed with Fluke-3 Model 1735 analyzers that installed at its terminals. The conclusion can be made from this paper is THD increases under low power generation due to the inverse relation with the fundamental current.

A paper that study about the harmonic and voltage unbalance for photovoltaic power plant (PVPP) for Malaysian grid (Al-Shetwi & Sujod, 2017) discussed a research of the 1.5 MW capacity PVPP connected to the medium voltage level of distribution network by using VSI and RL filter connected to the low voltage of AC grid. This system was simulated using MATLAB/Simulink. The aim of this paper is to analyse the effects of installing the large PVPP system based on the Malaysian standard requirement at different level of solar irradiance to investigate current and voltage THD and voltage unbalance of distortion network. The outcome of this research is by using the inverter filter and PWM carrier frequency, the THD of the current and voltage at PCC has been decreased within the standard limit. Next, the relationship between solar irradiance and THD is inverse while direct relationship for solar irradiance and voltage unbalance.

A research was conducted with the aim to eliminate the 3<sup>rd</sup> and 5<sup>th</sup> harmonics by using five-level inverter and two different filters to fulfil the standard where the THD must be <5 %. In this research, a simulation of single phase inverter in a PV system was simulated in Psim software. This research was conducted in three steps which are the 3<sup>rd</sup> and 5<sup>th</sup> harmonics were eliminated by using five-level inverter, 7<sup>th</sup> harmonics is eliminated by using resonant filter and lastly the harmonics that over the threshold frequency were mitigated by using a low-pass filter to block the unwanted harmonics and allow certain frequency range to be transmitted. The objective of this research has been achieved since the THD level result is 3.8 % by using the low-pass filter (Khanfara et al., 2016).

Reduction of THD by switching frequency optimization in a three-level NPC inverter (Dawidowski, Stosur, Szewczyk, & Balcerek, 2014) paper presents the effect of switching frequency selection for three-level NPC inverter and its impact on the quality of output waveform for different cable lengths connecting the inverter with motor. An optimal switching frequency proposed by the authors to limit the THD. Efficiency improvement can be made by keeping the power losses as low level as possible. In this paper, other most often techniques to limit the THD such as LC filters, common mode (CM) chokes, common mode transformer, PWM modifications, and active compensation system of CM voltage were reviewed to be compared with the proposed method. This research was conducted with MATLAB/Simulink model to evaluate the effects of switching frequency changes in harmonic content in the cable with a range of the switching frequency investigated was 2 kHz and 8 kHz. As the conclusion from the results in this paper, the suitable selection of switching frequency of the inverter and cable length can decrease the harmonic content of the output waveforms in the cable.

## **2.12 Conclusion**

Previous research discusses the performance of the PWM types in terms of THD only, switching losses only or both. Meanwhile, others research connects the PWM to the converter or multi-level inverter in order to investigate the PWM performance by using different types of converter. Besides that, there are researches that implement the PWM in a system to reduce the THD to make it in the standard level or to reduce the switching losses of the system. In addition, many researchers focus on the relation between solar irradiance and THD levels in the PV system. An idea to investigate solar

irradiance effect on the THD level in a GCPV system crucial. Only few studies has been done in investigating the THD level and adjusting the switching frequency of the PWM carrier signal in order to maintain the THD at allowable percentage during different level of solar irradiance. Thus, the main objective of this research is to implement PWM techniques and investigate extensively the effect of switching frequency on THD.

In GCPV system, harmonic voltage and current in an electric power system which is the result of non-linear load decreases the quality of the power grid and hence affect the reliability and safety of electrical equipment. A control method of switching frequency selection is proposed in order to maintain THD within the standard requirement during solar irradiance changing since solar irradiance in Malaysia varies daily and also throughout the year. Both CPWM and DPWM type are implemented and investigated in this research.

Current and voltage waveforms at the PCC with the power grid contain harmonic distortion that may exceed recommended standard. MATLAB/Simulink environment was used to simulate the GCPV system model that used PWM as the inverter control to minimize the THD in the system. After the simulation has been done, the fast fourier transform (FFT) analysis was proceeded to obtain the THD of the system at the PCC when CPWM and DPWM was implemented in the inverter control at different level of irradiance. The switching frequency carrier signal is adjusted until the THD is less than 5 %. According to IGBT Infineon Technologies IRG4PH40UDPbF datasheet, the switching frequency can be optimized for high operating frequencies up to 40 kHz in hard switching.

## CHAPTER 3

### METHODOLOGY

#### 3.1 Introduction

This chapter discussed in details about the research method used to conduct this research. Three main steps are taken to complete this research which are a continuous study of PWM characteristics, conducts the experiment using PWM switching frequency selection in MATLAB/Simulink R12015a version and analyse the results. MATLAB software was chosen since it has powerful capabilities in numerical computation, data analysis and visual.

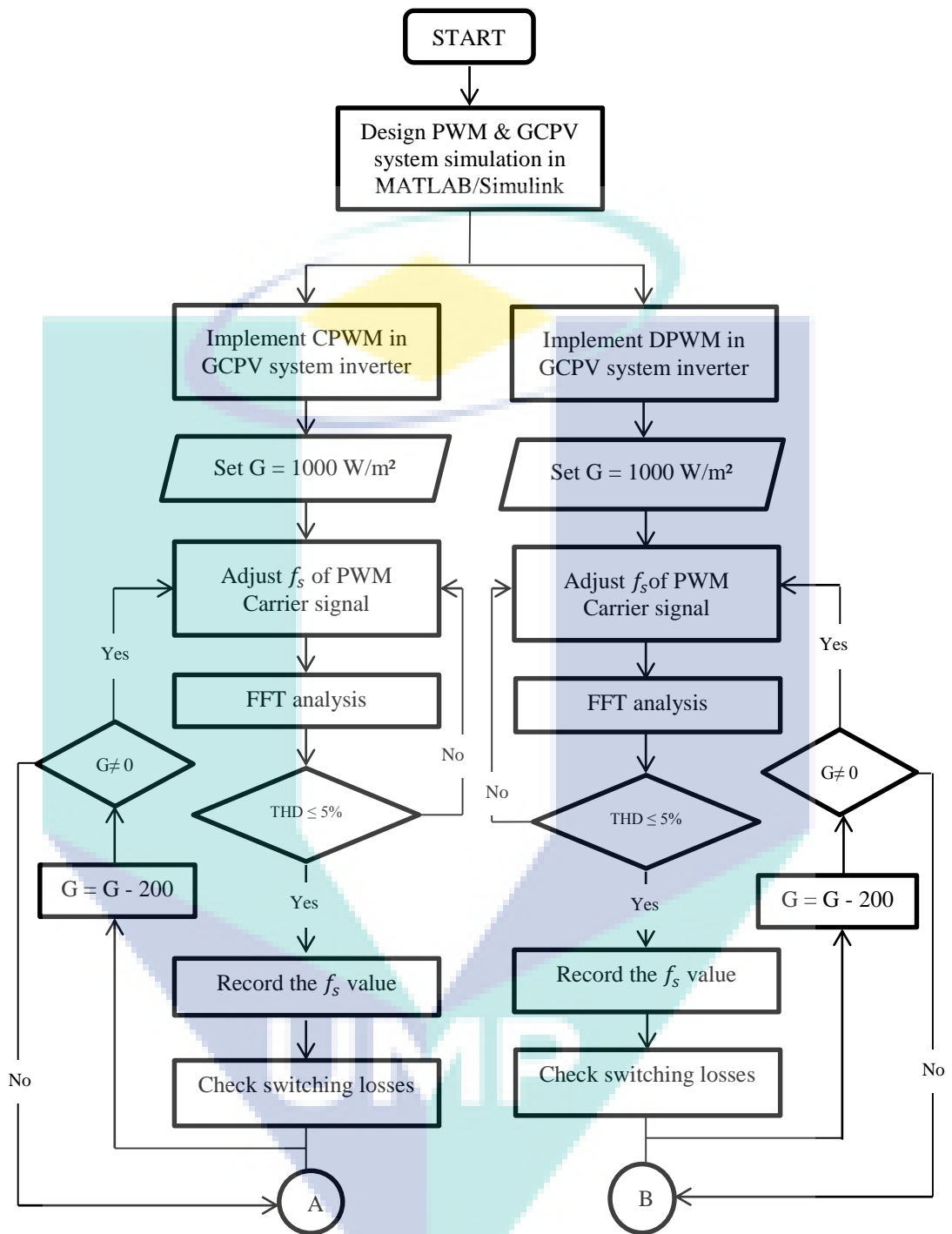
The outcome of the study on PWM characteristics from the previous research can be concluded that TTHIPWM and DPWM2 are chosen as the PWM used in controlling the inverter depending on the performance of the PWM type in term of THD and switching losses discussed in the Literature Review chapter under section 2.4.

As stated in the objective, the main goal of this research is to minimize THD level and switching losses in the GCPV system by proposing the minimum switching frequency for PWM inverter in the designed GCPV system that results the THD level less than 5 % according to IEEE Std 519-1992 and TNB Technical Guidebook on Grid-interconnection of Photovoltaic Power Generation System to LV and MV Networks. In the meantime, this research suggests the minimum switching frequency which then result in minimum switching losses, based on the fact that the switching losses increased when the inverter is operated at high switching frequency (Dawidowski et al., 2014).

### 3.2 Research Methodology

This research was implemented and analysed using MATLAB/Simulink R2015a version. The first step before proceeding with the simulation was the study of various PWM types. The PWM types that focussed on this research are SPWM, THIPWM and TTHIPWM for CPWM and DPWM0, DPWM1 and DPWM2 for DPWM. After the research of the characteristics of the PWM types was done, one PWM type for each CPWM and DPWM that has the best characteristic in respect of low THD was chosen for further analysis. TTHIPWM and DPWM2 are the PWM has chosen from CPWM and DPWM categories respectively since these two PWM are injected with the third harmonic to the fundamental voltage and able to improve the output voltage.

Figure 2.19 is the main reference for the previous research that prove which PWM types from both categories has the lowest THD compared to the other types which then implemented in the MATLAB/Simulink for further analysis. TTHIPWM and DPWM2 are designed using the MALTAB/Simulink to obtain three-phase pulses of PWM output signals. The PWM output signals were used as the inverter logic gate signal (Zahim & Erlich, 2012). This was the first step that should be done so that the designed PWM can be used as the controller in the inverter later in the GCPV system model. The research then proceeds with FFT analysis to obtain the THD of TTHIPWM and DPWM2 with different level of irradiance. The steps taken to complete this research are shown in the flowchart repeated in Figure 3.1 and referring to the flowchart below,  $G$  is solar irradiance and  $f_s$  is switching frequency. In the next sections, details about the research methodology to complete this research is explained.





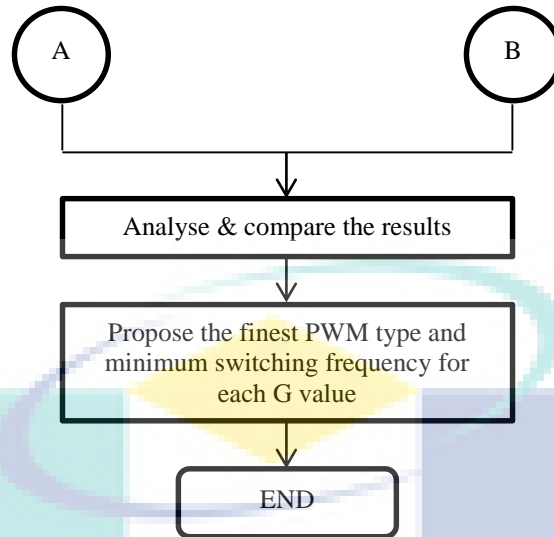


Figure 3.1 Methodology flowchart

### 3.2.1 GCPV System Configuration

The main aim of this research is to carry out a research to minimize the harmonic and the switching losses in a GCPV system. This can be achieved by investigating the effect of CPWM and DPWM as the inverter logic gate signal in the GCPV system model in MATLAB/Simulink in the aspect of THD and switching losses at different level of irradiance which is from  $1000 \text{ W/m}^2$  -  $200 \text{ W/m}^2$ . At the same time, the switching frequency of the CPWM and DPWM carrier signal are adjusted until the THD is less than 5 %.

For this purpose, it was necessary to develop a GCPV system model with 50 Hz fundamental frequency where the irradiance level and the switching frequency of the CPWM and DPWM can be changed during the simulation to observe the output waveform and record the THD level using FFT analysis tool at different operating condition. An overview of three-phase single-stage GCPV modelling scheme designed for this research is illustrated in Figure 3.2. This scheme includes PV array, DC-link capacitors that connects to the output terminal of the PV array and to reduce output power ripple, three-phase two-level IGBT VSI with PWM control and a three-phase transformer was used to connect the VSI to the utility grid. In addition, the harmonics generated by the IGBT Bridge were filtered by using the inverter choke RL and a small harmonics filter C hence decreasing the THD (Khan et al., 2017). This research MATLAB/Simulink circuit is presented in Appendix C.

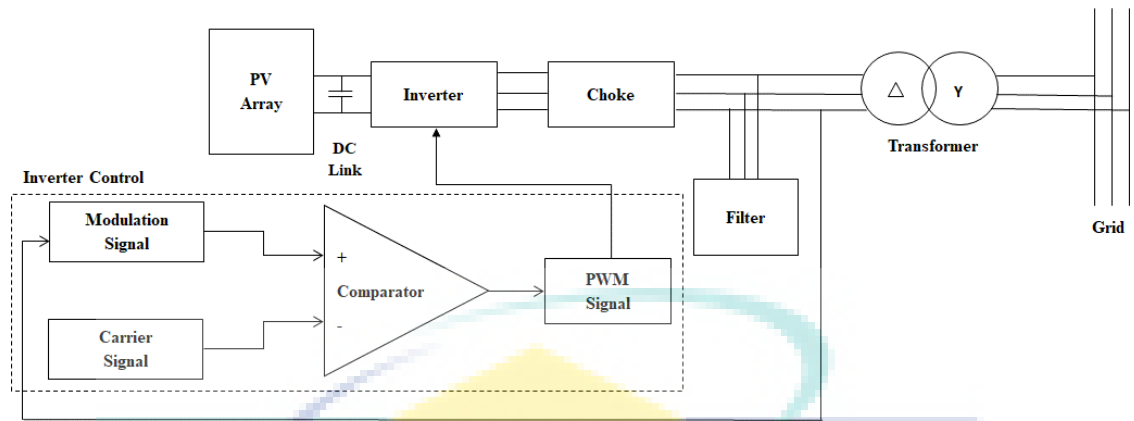


Figure 3.2 General block diagram of the research

In any PV system the most important components are PV module to absorb the solar irradiance and inverter to convert the DC output from the PV module to AC output voltage (Rahimi et al., 2016). If a PV system is connected to the grid, the compulsory component in the system is the inverter. The system is mainly composed of a matrix of the PV array. As for this research, the combination of 88 parallel strings and 7 series-connected modules per strings of SunPower SPR-X21-345-COM solar module with a capacity of 250 kW PV array were presented. Some of the parameters of STC from datasheet of the PV modules are shown in Table 3.1.

Table 3.1 Specification of SunPower SPR-X21-345-COM PV module

Parameter at STC	SunPower SPR-X21-345-COM
Cells per module (Ncell)	128
MPP	414.801 W
$I_{sc}$	6.09 A
$V_{oc}$	85.30 V
$I_{mp}$	5.69 A
$V_{mp}$	72.90 V
Temperature Coefficient of $I_{sc}$	0.030706 % / °C
Temperature Coefficient of $V_{oc}$	-0.229 % / °C

Besides that, the solar irradiance received by the system can be adjusted in the simulation. This is due to the irradiance received by the system became a variable to observe the effect of the THD corresponding to the irradiance. Meanwhile, in this research the temperature was kept constant at 25 °C by the reason of solar cell performance is absorbing sunlight at this peak of the optimum temperature range of the solar panel at a maximum.

The inverter is the most important part of the GCPV system. In this research, three-phase two-level inverter controlled IGBT Bridge was used in the designed system

to perform the power conversion of the output from the PV array. The input of the inverter was connected to the solar modules. As the solar irradiance level keeps changing throughout the day, consequently changes input of the VSI (Khan et al., 2017).

In the simulation, a Universal Bridge block with 3 numbers of bridge arms and IGBT as the power electronic device was connected between the PV arrays and choke RL was used as the inverter. IGBT Infineon Technologies IRG4PH40UDPbF was used as the reference in this research. As mentioned before, this research is to observe the effect of CPWM and DPWM when applied in the inverter control in the GCPV system. Therefore, both PWM were implemented in the inverter as shown in Appendix D and Appendix E for CPWM and DPWM respectively. In order to make sure the THD and switching losses are in the standard range.

In order to limit the generated THD below the standard requirement during the variance of solar irradiance, PWM switching frequency selection was proposed as shown in Figure 3.3. The switching frequency of the carrier signal was adjusted based on output from Table 3.2 that depend on the solar irradiance range. The values of switching frequencies were defined after the GCPV system is run in the simulation by manually adjusted the solar irradiance.

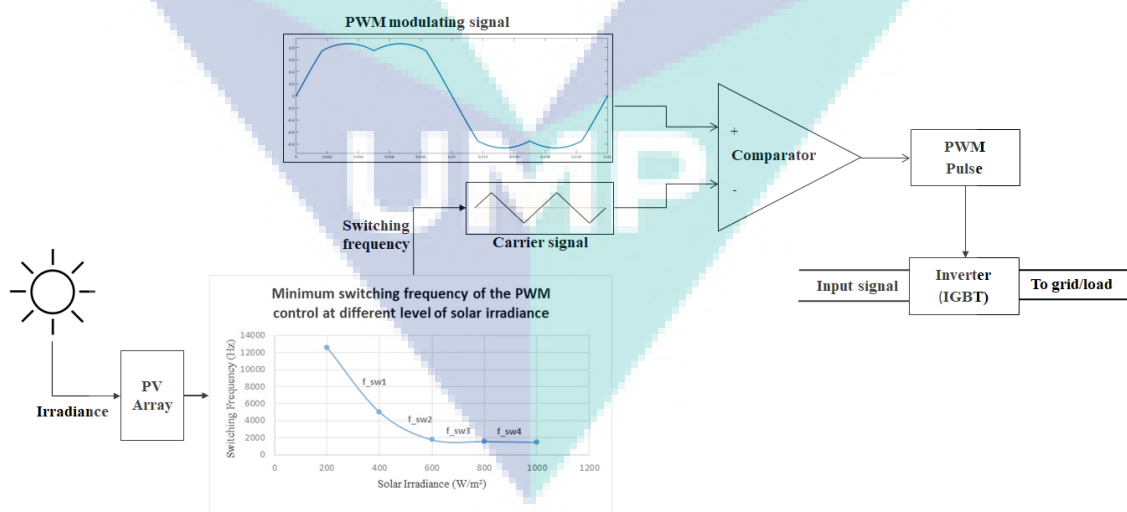


Figure 3.3 PWM switching frequency selection

Table 3.2 Switching frequency selection based on solar irradiance range

Solar Irradiance Range (W/m <sup>2</sup> )	Switching Frequency Value
200 - 400	$f_{sw1}$
401 - 600	$f_{sw2}$
601 - 800	$f_{sw3}$
801 - 1000	$f_{sw4}$

### 3.2.2 PWM Implementation in GCPV System

The designed PWM can be used as the controller in the inverter later in the GCPV system model that used the MATLAB/Simulink environment as simulation. SPWM is very popular and easy to implement in MATLAB/Simulink using comparator. It basically contains a sinusoidal wave generator, high frequency of the triangle wave generator and comparator. The modulating signal or sinusoidal wave can be generated by the Three-Phase Voltage Source block. Three reference signals are required in order to generate three-phase pulses.

The modulation signal of the other PWM types except for SPWM are injected with the third harmonic in the fundamental signal. SPWM can be the base for other PWM and the same goes with the generation of the TTHIPWM and DPWM2 in the MATLAB/Simulink. The modulation signal of TTHIPWM and DPWM2 that were generated in MATLAB/Simulink are shown in Figure 3.4 and Figure 3.5 respectively. The difference between SPWM and other PWM is at the modulation signal generator part where the third harmonic was injected. The injection of the third harmonic was obtained by using the analytical expression shown in equation 2.18 – 2.21 for each type.

The generated fundamental signal were compared in the blocks that has been set according to the analytical equation in order to inject the third harmonic into the signal so that it will bring down the peak magnitude of the resultant modulating waveform and 15.5 % can improve the inverter output voltage compared to PWM that not involve third harmonic injections (Zahim & Erlich, 2012). As the results, the modulating signal of TTHIPWM and DPWM2 were produced. These signals were proceed in the comparison process with the triangle carrier signal and lastly the PWM output signal was produced.

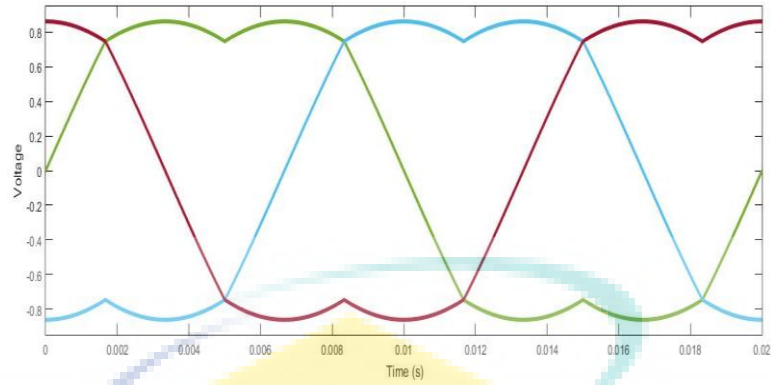


Figure 3.4 TTHIPWM modulating signal

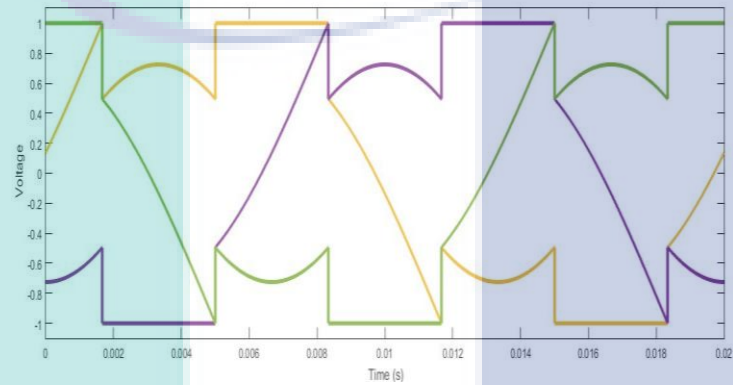


Figure 3.5 DPWM2 modulating signal

Meanwhile, the triangle carrier wave can be generated from the repeating sequence block. The comparator consists of a Hit Crossing block, S-R Flip-Flop block and Data Type Conversion block which can be found in the MATLAB/Simulink library. The pulses were created by comparing the triangle carrier signal and modulation signal in three separate comparators. The modulating signal and the triangle carrier signal that were compared in the comparator are shown in Figure 3.6 and Figure 3.7 below.

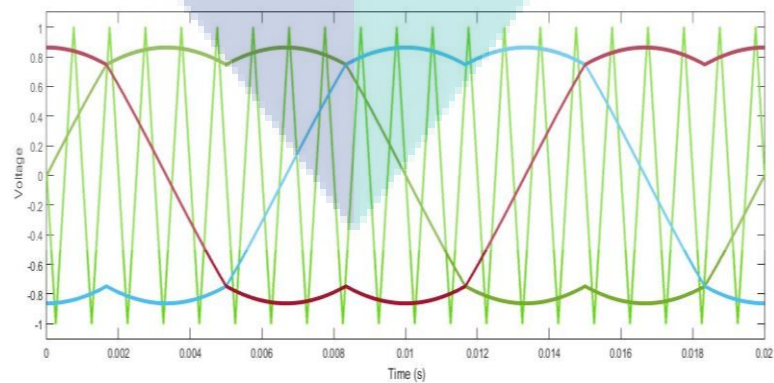


Figure 3.6 Comparison between modulation and carrier signal of TTHIPWM

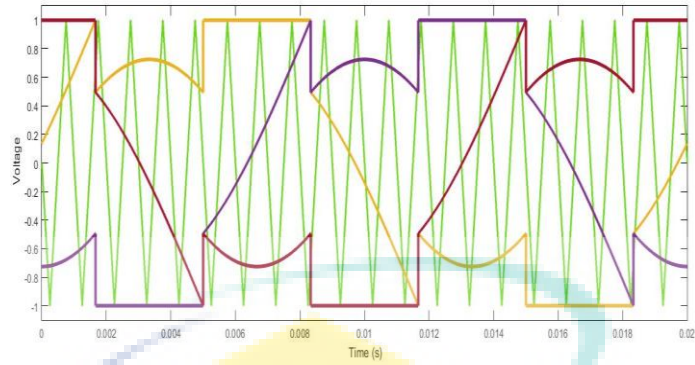


Figure 3.7 Comparison between modulation and carrier signal of DPWM2

Thus three PWM output signals were produced. In this research, three-phase two-level inverter was applied and there are six switches in total, two switches in each leg for each phase. Therefore, three of the PWM pulses that already be produced after compared in the three comparators were reversed by using three separate NOT gates and six of the PWM pulses were produced. The output of the PWM signal can be observed with scope. These PWM output signals then become the control signals for the inverter. Figure 3.8 and Figure 3.9 present one phase output pulses of TTHIPWM and DPWM2.

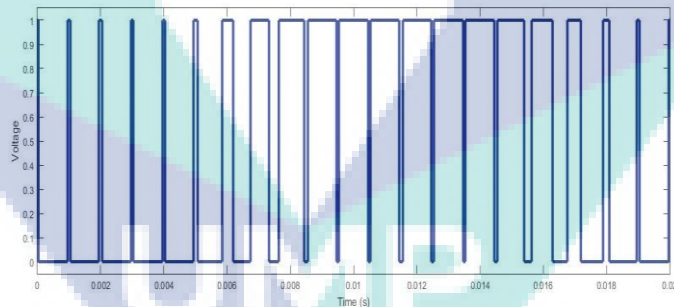


Figure 3.8 TTHIPWM output signal

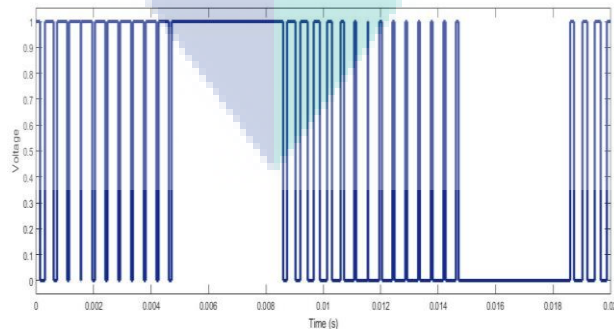


Figure 3.9 DPWM2 output signal

The TTHIPWM and DPWM2 simulations were developed first and MATLAB/Simulink simulation circuit of the PWM can be refer in Appendix F and Appendix G for TTHIPWM and DPWM2 respectively. Then, it was implemented in the inverter control in the GCPV system model by creating the subsystem for both PWM as presented in the next section. After the subsystems were created, a subsystem was added into the MATLAB/Simulink library to replace the existing SPWM in the inverter control of the system model. In this model, a close loop inverter was created where the voltage output was produced from the GCPV system was used as the fundamental pulse of the TTHIPWM and DPWM2. The switching frequency of the TTHIPWM and DPWM2 carrier signal were tuned in the inverter control. In this research, the carrier signal is manipulated by inserting the switching frequency value in the repeating sequence block and change it accordingly until the desired value of switching frequency meet the standard THD requirement and thus, minimize switching losses was found.

### 3.2.3 Control of GCPV System Based on CPWM

In this section, the control of the GCPV system based on CPWM represented by TTHIPWM as the inverter control is discussed. TTHIPWM was implemented in the GCPV system model by inserting the TTHIPWM subsystem shown in Figure 3.10 into the inverter control of the system model to replace the existing SPWM that already available in the inverter control. Different level of solar irradiance were tested in this research along with different switching frequency of the TTHIPWM carrier signal. These two are the variable used to be observed and analysed the THD and switching losses in the system.

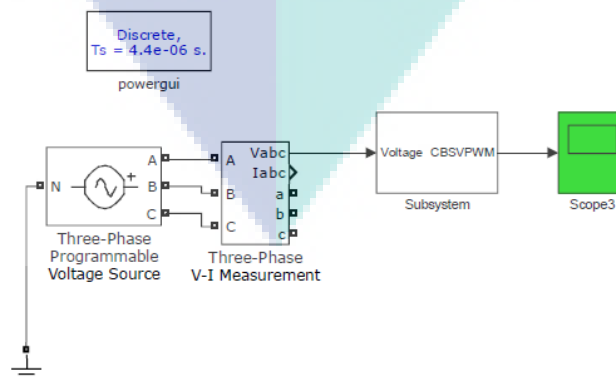


Figure 3.10 CPWM (TTHIPWM) subsystem

The first two steps to be completed before running the system simulation was to set the solar irradiance and switching frequency of TTHIPWM carrier signal in the system model. The initial solar irradiance input was set to 1000 W/m<sup>2</sup> in the Source Block Parameters: Irradiance (W/m<sup>2</sup>) at the amplitude section. According to IGBT Infineon Technologies IRG4PH40UDPbF datasheet, the switching frequency can be minimized for high operating frequencies up to 40 kHz in hard switching. In that case, chosen as the first switching frequency value was set to be 1 kHz in the Source Block Parameters: Repeating Sequence at the time values section. Next, the simulation was run and the logged workspace data were sent to the data inspector with the aim to save the data, for example waveform of the voltage, current and power output and included in this thesis.

After the simulation was 100 % completed, FFT analysis was performed to check the THD level of the system model of 1000 W/m<sup>2</sup> solar irradiance and 1 kHz switching frequency of the TTHIPWM carrier signal. The main objective is to obtain THD less than 5 %. Hence, if the THD was more than 5 % the switching frequency was set to another value but the value of solar irradiance still remain 1000 W/m<sup>2</sup>. The adjusted switching frequencies and results of the THD obtained during the process to find the suitable carrier signal switching frequency with standard THD are tabulated in Appendix A. High switching frequency need to be used to reduce the THD, but the effect according to (Asiminoaei et al., 2008), inverter cannot operate at very high switching frequencies because the switching losses can be increased. In case the THD is in standard THD value, the switching frequency of the TTHIPWM carrier signal was recorded and the optimal result for 1000 W/m<sup>2</sup> solar irradiance level was obtained.

Once the necessary value for 1000 W/m<sup>2</sup> solar irradiance was found, the research was continued with next solar irradiance level. In this research, the simulation and test were conducted for 1000 W/m<sup>2</sup> as the maximum solar irradiance value while 200 W/m<sup>2</sup> is the minimum solar irradiance value. The simulation of the GCPV system model was tested at 200 W/m<sup>2</sup> solar irradiance interval by referring to (Shaari et al., 2010b) as shown in Figure 2.4 which are 800 W/m<sup>2</sup>, 600 W/m<sup>2</sup>, 400 W/m<sup>2</sup> and 200 W/m<sup>2</sup>. Solar irradiance in Malaysia varies daily and also throughout the year plus PV array experience large variations of its output power during bad weather (Yunus, Koingud, Kutty, & Yaakub, 2014). The same process was repeated with each of the



solar irradiance listed until the minimum switching frequency of the TTHIPWM carrier signal is found to be resulted in optimal harmonic's level and switching losses in the system.

### 3.2.4 Control of GCPV System Based on DPWM

This section explains the control of the GCPV system based on DPWM represented by DPWM2 as the inverter control. A DPWM2 subsystem as shown in Figure 3.11 was implemented in the GCPV system model by inserting it in the inverter control of the system model. Different level of solar irradiance was tested in this research as well as different switching frequency of the DPWM2 carrier signal. These two are the variable to be noted and analyse the THD and switching losses in the system.

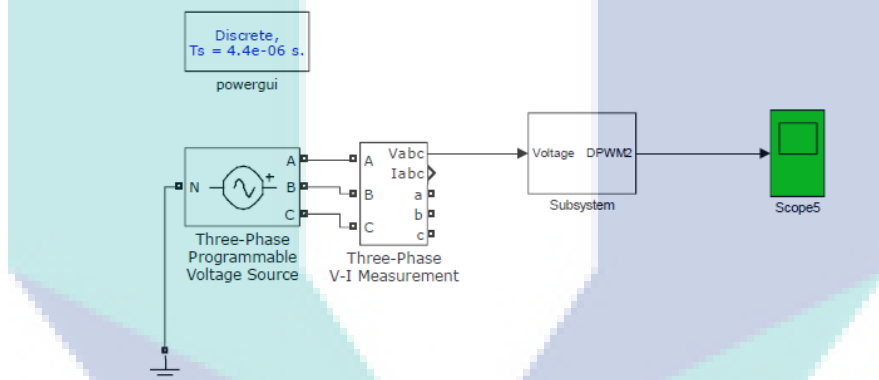


Figure 3.11 DPWM (DPWM2) subsystem

The first two steps to be completed before running the system simulation was to set the solar irradiance and switching frequency of DPWM2 carrier signal. In the first place, the solar irradiance was set to  $1000 \text{ W/m}^2$  in the Source Block Parameters: Irradiance ( $\text{W/m}^2$ ) at the amplitude section. According to IGBT Infineon Technologies IRG4PH40UDPbF datasheet, the switching frequency can be minimized for high operating frequencies up to 40 kHz in hard switching. In that case, chosen as the first switching frequency value was set to be 1 kHz in the Source Block Parameters: Repeating Sequence at the time values section. Next, the simulation was run and the logged workspace data were sent to the data inspector with the aim to save the data, for example waveform of the voltage, current and power output and included in this thesis.

As soon the simulation finished, the harmonic's level of the 1000 W/m<sup>2</sup> solar irradiance and 1 kHz switching frequency of the DPWM2 carrier signal simulation can be analysed. The main objective is to obtain THD less than 5 %. Hence, if the THD was more than 5 % the switching frequency was set to another value but the value of solar irradiance still remain 1000 W/m<sup>2</sup>. The adjusted switching frequencies and results of the THD obtained during the process to find the suitable carrier signal switching frequency with standard THD are tabulated in Appendix B. In case the THD was in standard THD value, the switching frequency of the DPWM2 carrier signal was recorded and the optimal result for 1000 W/m<sup>2</sup> solar irradiance level was acquired.

Once the necessary value for 1000 W/m<sup>2</sup> solar irradiance was found, the research was continued with next solar irradiance level. The simulation of the GCPV system model was tested at 200 W/m<sup>2</sup> solar irradiance interval by referring to (Shaari et al., 2010b) as shown in Figure 2.4 which are 800 W/m<sup>2</sup>, 600 W/m<sup>2</sup>, 400 W/m<sup>2</sup> and 200 W/m<sup>2</sup>. The same process was repeated with each of the solar irradiance listed until the minimum switching frequency of the DPWM2 carrier signal was found to be resulted in optimal harmonic's level and switching losses in the system.

### **3.2.5 FFT Analysis**

Fourier series is a way to represent a function as the sum of simple sine waves. Meanwhile, FFT is an algorithm that computes the discrete Fourier transform of a sequence or its inverse and it widely used in the area of engineering, science and mathematics. A signal from its original domain which are time or space domain, then converts to a representation in the frequency domain or vice versa is known as Fourier analysis. Harmonic analysis is conventionally based on the Fourier transform which a way of expressing a signal as a weighted sum of sine and cosine wave. There is a computer tool call FFT and it is to optimized computational method of doing Fourier analysis on a computer. In MATLAB, the FFT function uses a FFT algorithm to compute the Fourier transform of the data ("Fourier Transforms - MATLAB & Simulink," n.d.).

THD can be measured in MATLAB/Simulink through FFT analysis. Powergui block is a graphical user interface (GUI) for analysis of circuits and systems. Powergui block main menu provides tools to display steady-state voltage and currents, display and

modify initial state values, perform load flows and machine initialization, display impedance and FFT analysis, use linear system analyzer, hysteresis design, RLC line parameter and generate reports of the steady-state calculation. One advance tool available is customizing SPS blocks.

Next, choose FFT Analysis in the Powergui tools. This section displays the Signal, Available Signal Setting, FFT Analysis and FFT Setting. In Available Signal Setting, select scope and then select signal. FFT setting required the user setting the Start Time, Number of Cycles, Fundamental Frequency and Max Frequency and then clicks on the Display button. The percentage of THD is shown at the top of the frequency domain in FFT Analysis section.

The main goal of this research is to obtain THD that is in standard by referring to IEEE Std 519-1992 and TNB standard, THD should be less than 5 % in the rated inverter output of the cable connected to PCC. It is not necessary that for the first time the simulation is run, the THD obtain is in standard. Therefore, the same process to obtain the THD value of the FFT analysis for different switching frequency value is repeated many times after the simulation is 100 % run and completed.

In addition, the waveform of the selected signal can be observed in the Signal section above the FFT Analysis section and the waveform of the signal can be observed either closer to sinusoidal waveform or not to conclude the harmonic distortion in the signal. The closer the wave to sinusoidal, the smallest the THD (Rahimi et al., 2016). An example of the results obtains from the powergui FFT analysis tool in MATLAB is as shown in Figure 3.12.

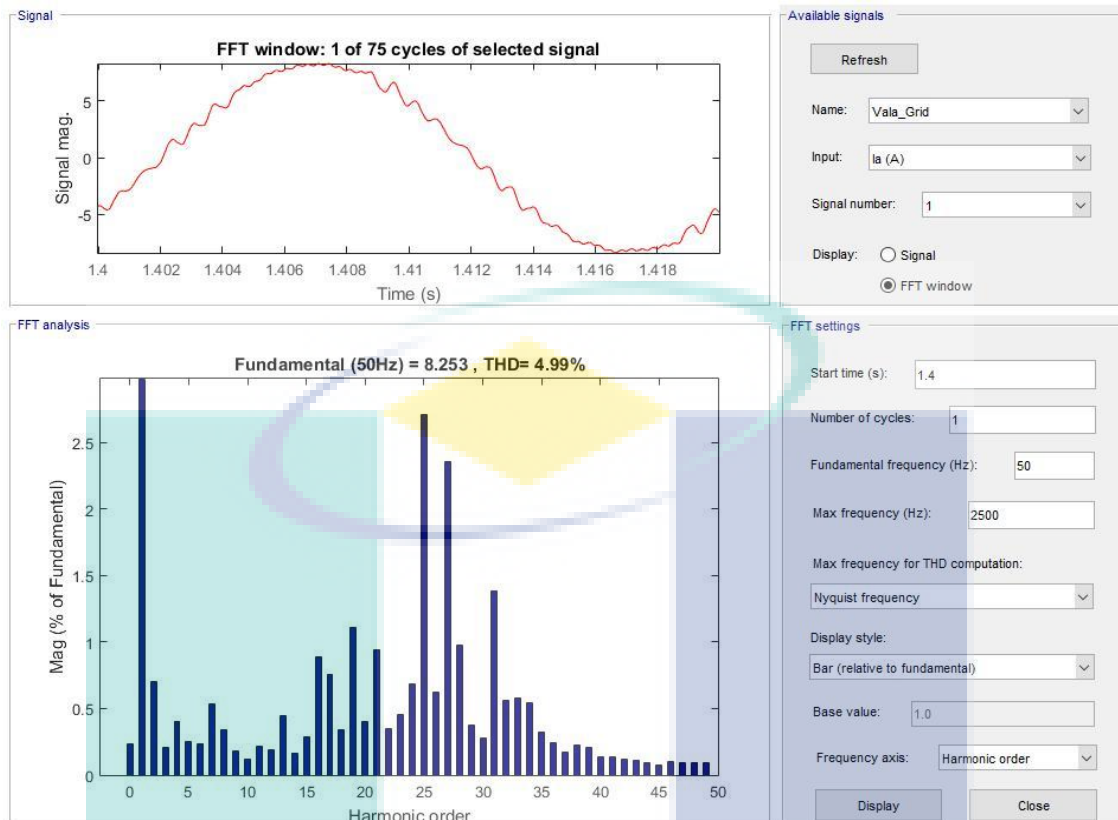


Figure 3.12 Powergui FFT analysis tool

### 3.2.6 Switching Losses Analysis

One of the reasons that can cause system losses is the switching losses in power electronics since the switching losses can occur when there are switched ON or OFF occur. In this case, for switching losses in IGBT, the switching losses occur when there was a turn-on and a turn-off signal at IGBT's gate. The previous research that investigates the switching losses in CPWM and DPWM found that DPWM can reduce more switching losses compared to CPWM. According to (Asiminoaei et al., 2008), it was stated that theoretically DPWM give an average of 33 % reduction in switching losses compared to CPWM or alternatively allows an increase of the switching frequency by 33 %. Therefore, the calculation was performed to observe the switching frequency level when the switching frequency of CPWM increased 33 %, meanwhile switching frequency of DPWM was decreased 33 % and then the results from the calculation is compared to determine which PWM has lower switching losses.

### 3.3 Conclusion

The designed PWM can be used as the controller in the inverter later in the GCPV system model that used MATLAB/Simulink environment as simulation. Then proceeds with FFT analysis to obtain the THD of CPWM and DPWM with different level of irradiance by reason of current and voltage waveforms at the PCC with the power grid contain harmonic distortion that may exceed recommended standard. The switching frequency of the carrier signal is modified until the THD is less than 5 %. According to IGBT Infineon Technologies IRG4PH40UDPbF datasheet, the switching frequency can be optimized for high operating frequencies up to 40 kHz in hard switching.

An overview of three-phase single-stage GCPV modelling scheme designed in this research is illustrated in Figure 3.2. Electrical components and their parameters of the GCPV system are shown in Table 3.1. This scheme includes PV array, dc-link capacitor that connects to the output terminal of the PV array, three-phase two-level IGBT inverter with PWM control and a three-phase transformer is used to connect the inverter to the utility grid. In addition, the harmonics generated by the inverter are filtered by harmonics filter.

The simulation of the GCPV system model is tested at solar irradiance 1000 W/m<sup>2</sup>, 800 W/m<sup>2</sup>, 600 W/m<sup>2</sup>, 400 W/m<sup>2</sup> and 200 W/m<sup>2</sup>. Meanwhile, the temperature is kept constant at 25 °C by the reason of solar cell performance is absorbing sunlight at this peak of the optimum temperature range of the solar panel at a maximum. In order to limit the generated THD below the standard requirement during the variance of solar irradiance, switching frequency selection method is proposed. The switching frequency of the carrier signal is adjusted based on output from the Table 3.2 that depend on the solar irradiance range.

## CHAPTER 4

### RESULTS AND DISCUSSION

#### 4.1 Introduction

In Chapter 4, the results of the GCPV system model for each of the different solar irradiance level for CPWM and DPWM which were implemented in the inverter control are analysed and discussed in details. THD level and switching losses of the simulation for the different level of the solar irradiance is the main focus of this research. The results are taken after the THD level of the simulation is in standard or not more than 5 %. There are two variables that effect the results which are solar irradiance level and switching frequency of the CPWM and DPWM carrier signal. Thus, the two variables are set before running the simulation. The process to get the optimal results happened in a loop. The results are then analysed and compared to choose and suggest which one between CPWM and DPWM have better performance and select the appropriate value of switching frequency. Later, the results are analysed and compare to choose and suggest which one between CPWM and DPWM have the better performance.

#### 4.2 Performance Analysis

The THD level of the GCPV system model when the initial input for the solar irradiance was 1000 W/m<sup>2</sup> and the switching frequency was set at 1 kHz is not necessarily less than 5 %. Hence, the process of setting the switching frequency of the inverter control either CPWM or DPWM need to be repeated until the THD level was found in the standard. Once the THD level was in the acceptable level, the switching frequency of the PWM carrier signal was recorded together with the FFT analysis result and power, voltage and current output of the system. Next, the same steps were applied but with 800 W/m<sup>2</sup>, 600 W/m<sup>2</sup>, 400 W/m<sup>2</sup> and 200 W/m<sup>2</sup> solar irradiance. The results

were then analysed and compared to choose and suggest which one between CPWM and DPWM have better performance and select the appropriate value of switching frequency.

#### 4.2.1 Analysis of Output Power at Different Irradiance

PV effect is a phenomenon where conversion of light energy into electrical energy takes place. The basic reason for producing electrical energy is a solar cell, the basic element of solar panels is an electrical device that utilizes the PV effect to convert the sunlight energy directly into electrical energy. The solar cell is basically a p-n junction diode. It is a photoelectric cell form, vary when exposed to light and it is used as a photo detector (Mohammad Bagher et al., 2015).

Since the output characteristic of the PV system is non-linear and varies due to the dependency on solar irradiance and temperature, thus it is not easy to maintain an optimum output level of the system at different condition (Pradhan et al., 2013). In this research, the GCPV system model was executed with several solar irradiance levels, which is 1000 W/m<sup>2</sup>, 800 W/m<sup>2</sup>, 600 W/m<sup>2</sup>, 400 W/m<sup>2</sup> and 200 W/m<sup>2</sup> and for a constant temperature equal to 25 °C. Changing of the solar irradiance create significant impact of the output current of the PV array but theoretically the output voltage alter slightly.

In this research, the output voltage obtained was 20 kV and does not change even different level of solar irradiance was set during the simulation. Thus, this situation does prove the theory that is an amperage output increase while the voltage does not have a lot of change when the irradiance increase (Ehmidat, 2013) (Phap et al., 2017) and presented in Figure 2.4. Therefore, it can give impact to the working efficiency of the PV system.

Knowing the current and voltage characteristics of the PV array is critical to determine the system's output performance. The output characteristics of the PV system are plotted on an I-V curve. It is preferably that the measurement of the I-V curve is made under the most stable conditions and variations in irradiance. The instability of the solar irradiance is due to the fact that solar irradiance varies throughout the year and it also varies daily depending on the position of the sun and the weather. Given these points, solar irradiance is varying from time to time and results in different output even

though from the same PV modules. In other words, reduction of sunlight results in reduction of the PV array performance in respect of current and power output.

This research was performed with two different inverter control which is CPWM and DPWM. In that case, the results of the average output current and power of the simulation are presented for both control techniques. The outputs between the two inverter controls only have lightly different and thus can be concluded that the PWM does not affect the outputs of the GCPV system as can be observed the results in Table 4.1 below.

Table 4.1 Average output current and power of the GCPV system model based on solar irradiance for CPWM and DPWM

Solar Irradiance (W/m <sup>2</sup> )	Average output Current of the GCPV system model (A)		Average output Power of the GCPV system model (kW)	
	CPWM	DPWM	CPWM	DPWM
1000	8.35	8.20	250.50	252.00
800	6.68	6.70	200.80	200.10
600	5.02	5.10	149.90	151.00
400	3.20	3.40	99.20	99.00
200	1.70	1.70	48.00	48.00

It is obviously that solar irradiance influence the average output current and power of the system. The results are plotted as in Figure 4.1 shows and proven that solar irradiance and output current is a linear relationship. As the solar irradiance level increase, the average output current and power shows an increment. In contrast when the solar irradiance is at 400 W/m<sup>2</sup> and 200 W/m<sup>2</sup> the PV array does not receive much input and thus the average output current and power are lower due to low input of the inverter.

When solar irradiance was at 1000 W/m<sup>2</sup>, the average output current is 8.35 A and 8.20 A for CPWM and DPWM which is the highest compared to the other solar irradiance level. It is in this state, the PV array receives much input thus the inverter input also high. The average output current decrease to 6.68 A and 6.70 A when the solar irradiance decrease to 800 W/m<sup>2</sup>. The decrement of the output current continuous as the solar irradiance values were set to a lower value than the previous. The average output current for 600 W/m<sup>2</sup> and 400 W/m<sup>2</sup> are 5.02 A and 3.20 A respectively when CPWM was used. On the other side, when DPWM was implemented the average output



current are 5.10 A and 3.40 A respectively. The lowest average output current, 1.70 A is obtained at 200 W/m<sup>2</sup> irradiance for both PWM techniques.

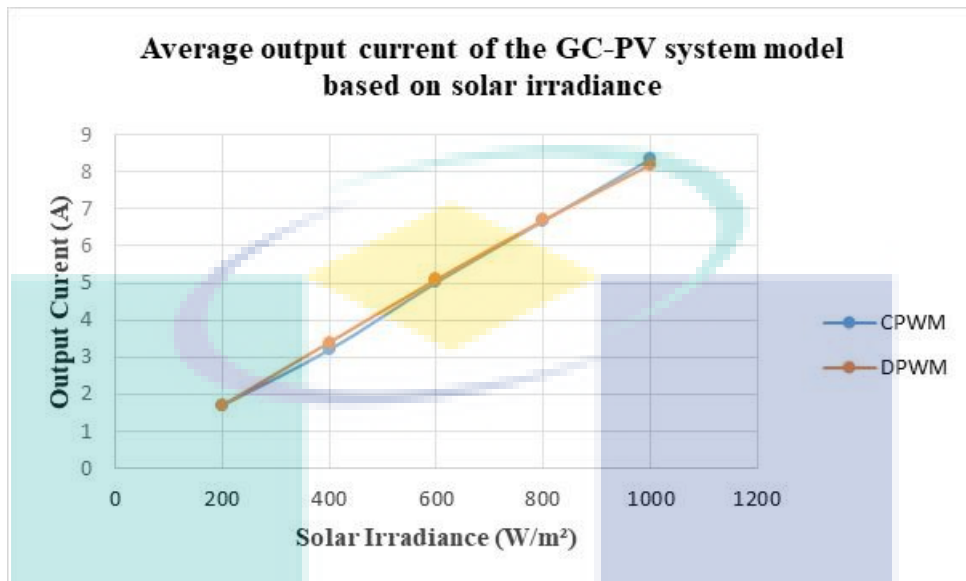


Figure 4.1 Average output current of the GCPV system model based on solar irradiance for CPWM and DPWM control techniques

Besides that, the relation between solar irradiance and output power also presented in Figure 4.2. It is clear that the output power of the system increase as the solar irradiance increase. 250 kW is the value of the nominal power of this GCPV system model and this average output power value is achieved when the solar irradiance was set at 1000 W/m<sup>2</sup>. During 800 W/m<sup>2</sup>, the value of the average output power has reduce by 50 kW. As the solar irradiance values were set to be 600 W/m<sup>2</sup>, 400 W/m<sup>2</sup> and 200 W/m<sup>2</sup>, the average output power produced are reduced and the minimum values obtained is 48.00 kW. Finally, the results of the output current and power between CPWM and DPWM can be compared based on the Figure 4.1 and Figure 4.2 and it proven that the PWM techniques does not influence the outputs of the system.

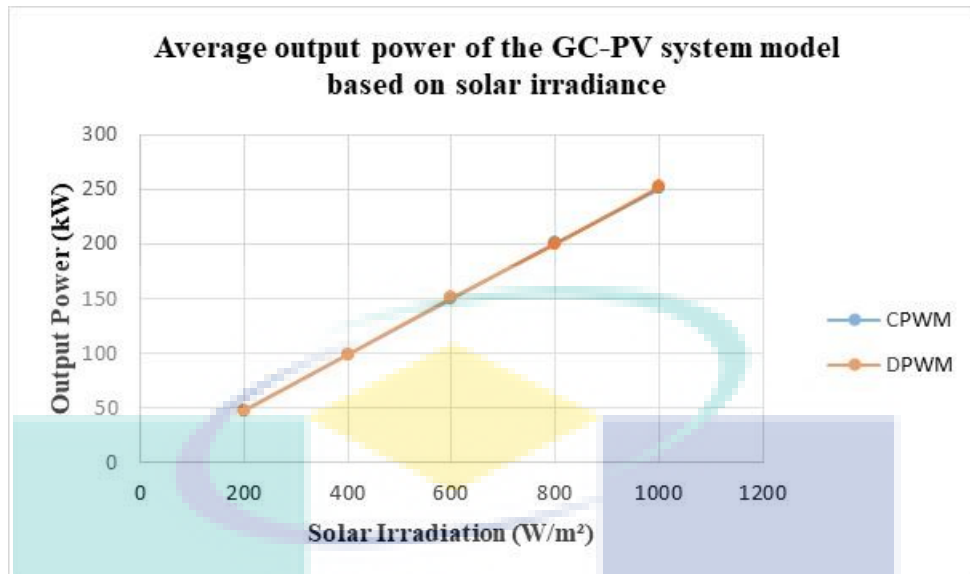


Figure 4.2 Average output power of the GCPV system model based on solar irradiance for CPWM and DPWM control techniques

#### 4.2.2 Analysis THD at Different Irradiance

Harmonic control and performance of PV system analysis based on solar irradiance has been the topic for many previous research and it has been reported that the solar irradiance can bring a big impact to the THD in the PV system. In the event that the solar irradiance is at low level, the output of the inverter has been low since under such conditions the PV array does not receive much input and thus the current and voltage outputs are lower than the rated value. Under those circumstances, the inverter exhibits large non-linearity which the results in more THD in the system.

Solar irradiance and THD are inversely proportional. THD increase when the solar irradiance level decreases. The concept that comes out from (Salim et al., 2013) (Al-Shetwi & Sujod, 2017) and (Hicks et al., 2018) are discussed according to the results obtained from the simulation in this research. For this purpose, the solar irradiance of the GCPV model was set to 1000 W/m<sup>2</sup>, 800 W/m<sup>2</sup>, 600 W/m<sup>2</sup>, 400 W/m<sup>2</sup> and 200 W/m<sup>2</sup> while the switching frequency of the CPWM and DPWM carrier signal were set to be 1 kHz.

In this case, the switching frequency must remain the same because the main variable to be observed here is solar irradiance level and how it effects THD in a system. The outcome from the simulation are current total harmonic distortion ( $THD_i$ ) and voltage total harmonic distortion ( $THD_v$ ) that can be analysed from FFT analysis

available in MATLAB/Simulink. As can be seen in Table 4.2, as solar irradiance level reduced, the value of  $THD_v$  value is almost constant for both CPWM and DPWM which are in the average of 0.954 % and 1.816 % respectively even when the solar irradiance undergo changes. Hence, it can be concluded that  $THD_i$  analysis is more significant for the purpose to observe the pattern for THD effect compared to  $THD_v$  (Hicks et al., 2018). In ascending order of the solar irradiance,  $THD_i$  value obtained are 176.83 %, 74.02 %, 48.29 %, 35.63 % and 28.57 % for CPWM and for DPWM, the  $THD_i$  value obtained are 726.21 %, 194.75 %, 107.26 %, 75.44 % and 64.17 %.

Table 4.2 THD level for CPWM and DPWM based on different solar irradiance level at 1 kHz switching frequency

Solar Irradiance (W/m <sup>2</sup> )	CPWM		DPWM	
	$THD_v$ (%)	$THD_i$ (%)	$THD_v$ (%)	$THD_i$ (%)
1000	0.96	28.57	1.83	64.17
800	0.96	35.63	1.85	75.44
600	0.95	48.29	1.80	107.26
400	0.95	74.02	1.80	194.75
200	0.95	176.83	1.80	726.21

One of the objectives in this research is to implement CPWM and DPWM in a GCPV system model to investigate the THD and switching losses performance in different level of irradiance. This objective is achieved and the results from the GCPV model system simulation is shown in Table 4.2. The relation between solar irradiance and THD level for each of the PWM can be analysed from the curve presented in Figure 4.3 to show the statement from the previous research is true and only  $THD_i$  was considered.

According to the graph of  $THD_i$  level based on different solar irradiance level, evidently there is a huge difference of  $THD_i$  level between CPWM and DPWM when the solar irradiance below 400 W/m<sup>2</sup>.  $THD_i$  level starting from 400 W/m<sup>2</sup> and huge difference is achieve when solar irradiance level is at 200 W/m<sup>2</sup>. Thus, once the solar irradiance value less than 400 W/m<sup>2</sup>, the value of THD is increasing extremely which create unstable situation. Generally, the graph above obviously show that CPWM produce less  $THD_i$  compared to DPWM.

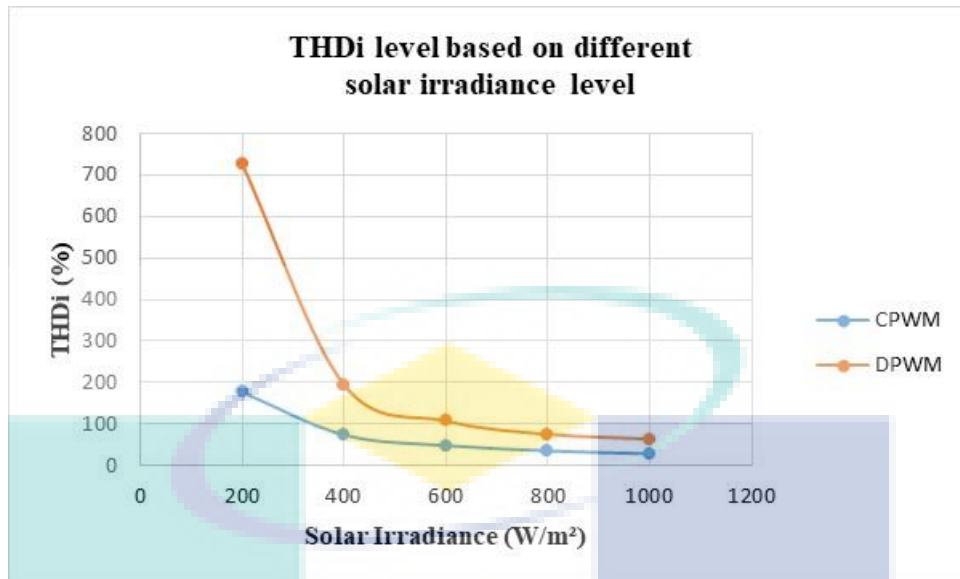
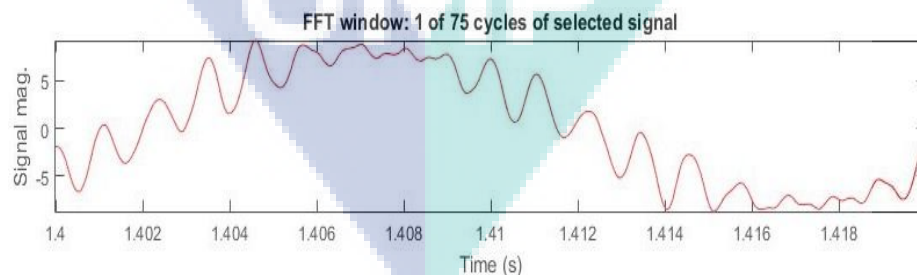


Figure 4.3  $THD_i$  level for CPWM and DPWM based on different solar irradiance level at 1 kHz switching frequency

Moreover, the quality of the AC current is measured by  $THD_i$  and the closer the wave to sinusoidal, the smallest the  $THD_i$  (Kharjule, 2015). Figure 4.4 are one cycle output current waveform with the starting time is 1.4 seconds for each solar irradiance obtain from the simulation with CPWM as the inverter control. What can be observed from the waveform is the quality of the current produce for different solar irradiance level and how close the waveform to sinusoidal. As can be seen, the waveform becomes more non-sinusoidal when the solar irradiance level reduces. Take note that in this section analysis the  $THD_i$  still not in the standard and the switching frequency for both PWM carrier signal are 1 kHz.



(a) 1000 W/m<sup>2</sup>

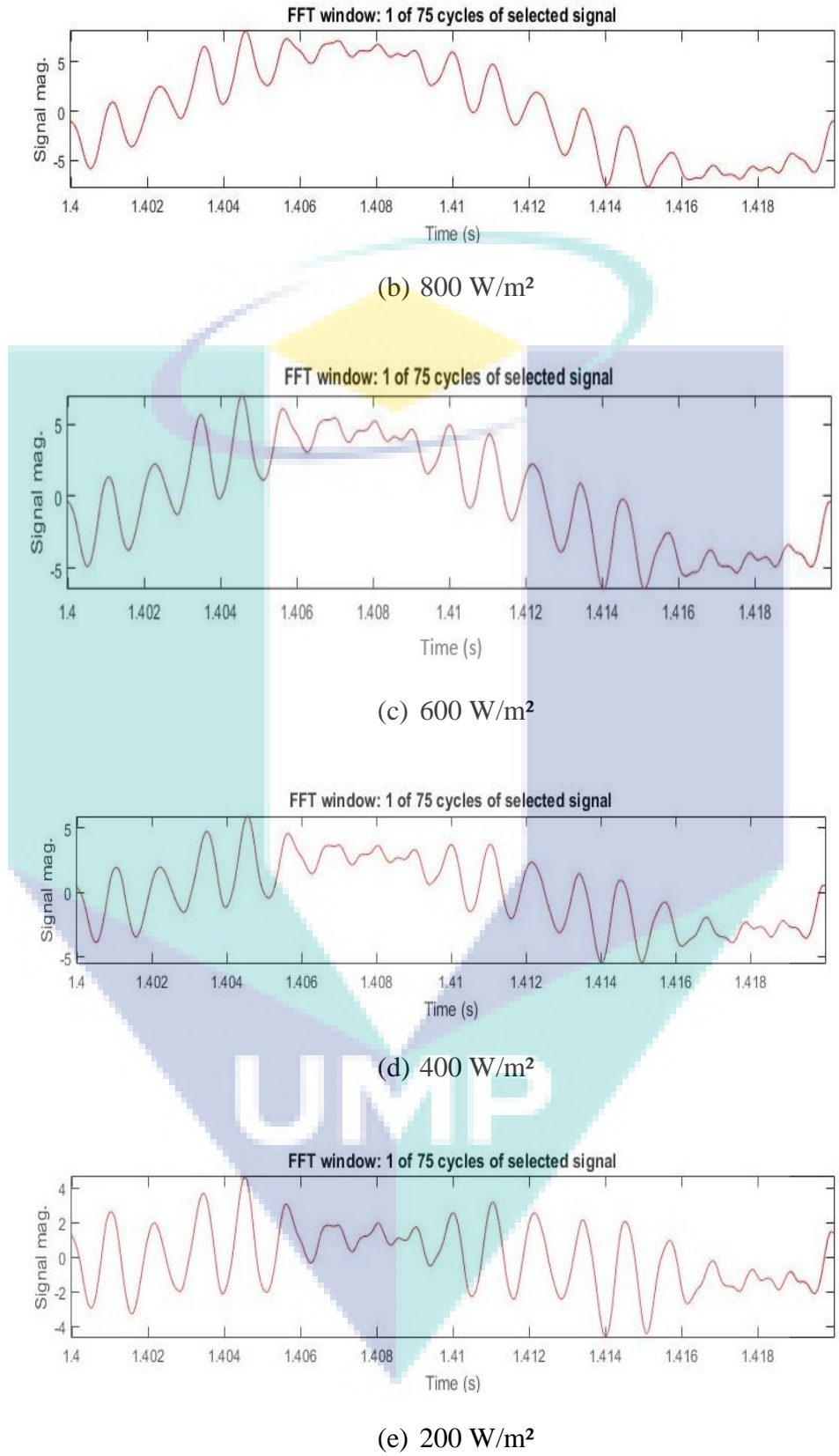
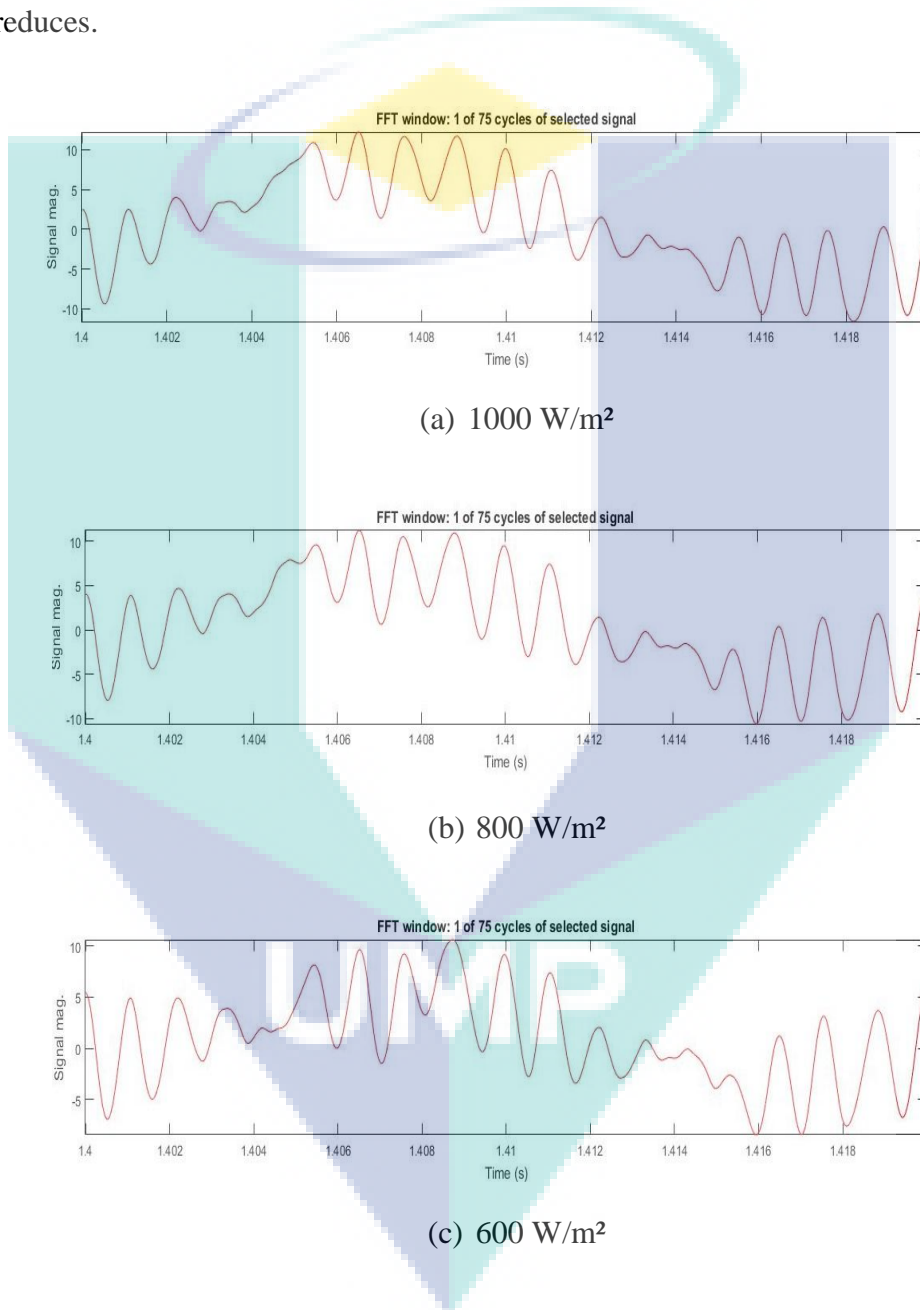
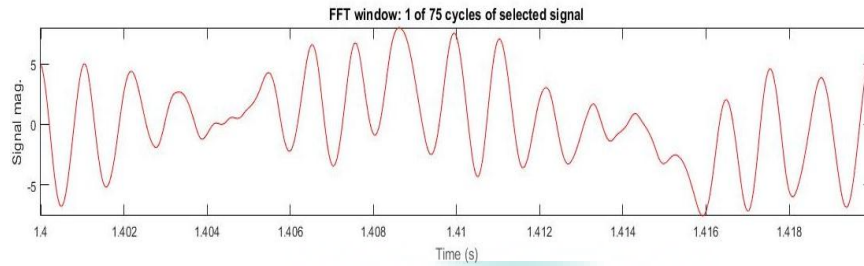


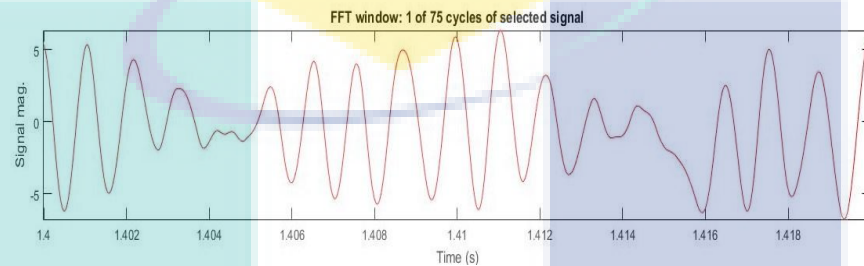
Figure 4.4 One cycle output current waveform for CPWM control technique

Figure 4.5 below are one cycle output current waveform and the starting time is 1.4 seconds for each solar irradiance obtain from the simulation with DPWM as the inverter control. What can be observed from the waveform is the quality of the current produce for different solar irradiance level and how close the waveform to sinusoidal. As can be seen, the waveform becomes more non-sinusoidal when the solar irradiance level reduces.





(d) 400 W/m<sup>2</sup>



(e) 200 W/m<sup>2</sup>

Figure 4.5 One cycle output current waveform for DPWM control technique

To summarize, the analysis result in this section gives an idea of selecting which PWM control technique to be applied. In short, two factors are considered to choose the best PWM that can produce less  $THD_i$ . The first factor is the  $THD_i$  value and second factor is how close to sinusoidal the waveform of the output current. By considering these two factors, it is clearly that CPWM give the best result compared to DPWM. For instance, CPWM only produce 176.83 %  $THD_i$ , meanwhile DPWM produce 726.21 %  $THD_i$  when solar irradiance level is dropped until 200 W/m<sup>2</sup>. Obviously, DPWM produces too much  $THD_i$  compared to CPWM which can be concluded that CPWM is the best PWM control to be implemented in a system.

In addition, in Figure 4.4 from 1000 W/m<sup>2</sup> until 600 W/m<sup>2</sup>, the waveform observed still have sinusoidal pattern. Non-sinusoidal pattern starts to form when the solar irradiance is at 400 W/m<sup>2</sup> where the solar irradiance low. Unlike DPWM case, non-sinusoidal output current waveform is generated even when the solar irradiance is at 1000 W/m<sup>2</sup>. Henceforth, this show that CPWM has more potential to produce better output current since quality waveform of CPWM is more preferable than DPWM output waveform.

### 4.2.3 Analysis of Switching Frequency of PWM at Different Irradiance

The main aim of the research reported in this thesis is to investigate the performance of the PWM at different level of solar irradiance and adjusted the switching frequency of the PWM carrier signal in order to fulfil the standard of the grid owing to the fact that the current and voltage at the point of PCC with grid contain harmonic distortion. This is the effect of non-linear load used in the system which is the inverter. In a PV system that connected to the grid, it is mandatory to implement the inverter to connect the PCC and the grid. The output current of the system must be in phase with the grid electrical parameters and sinusoidal in nature. For this purpose, the inverter control unit is implemented to regulate the output current (Khatri & Kumar, 2017).

The results in this section suggest the appropriate selection of switching frequency of the PWM carrier signal associated with the suitable PWM type either CPWM or DPWM. The main idea behind the PWM control is that it improves and produce a sinusoidal-like output signal by comparing a modulating signal with a triangular carrier signal. The frequency of the carrier signal waveform defines the switching frequency. The higher switching frequency has more tendency to produce higher switching losses. In this research, the IGBT chosen as the reference. The switching frequency can be minimized for high operating frequencies up to 40 kHz in hard switching.

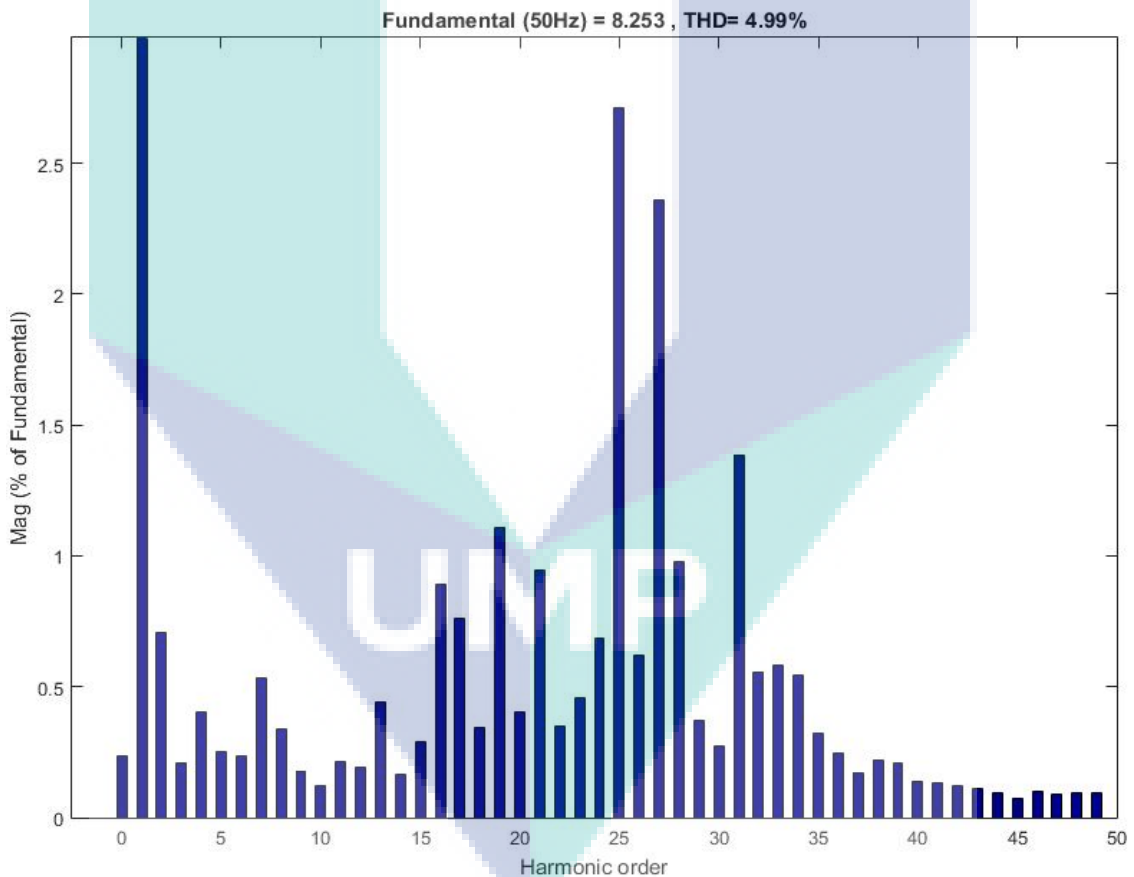
The minimum switching frequencies for both PWM were recorded after the simulation. FFT analysis results show the  $THD_i$  of the simulation is less than 5 % for the first time in the simulation after a few trials with different switching frequency set in the PWM. The THD standard in this research is referring to the standard stated by IEEE Std 929-2000 and TNB standard. The simulation was conducted with different level of solar irradiance which were 1000 W/m<sup>2</sup>, 800 W/m<sup>2</sup>, 600 W/m<sup>2</sup>, 400 W/m<sup>2</sup> and 200 W/m<sup>2</sup>.

The harmonic spectrum of the current at PCC from FFT analysis that contains the  $THD_i$  value obtain from MATLAB/Simulink GCPV system simulations according to each of the solar irradiance stated above using CPWM control are presented in Figure 4.6 and the results for DPWM control are presented in Figure 4.7. The results shown in

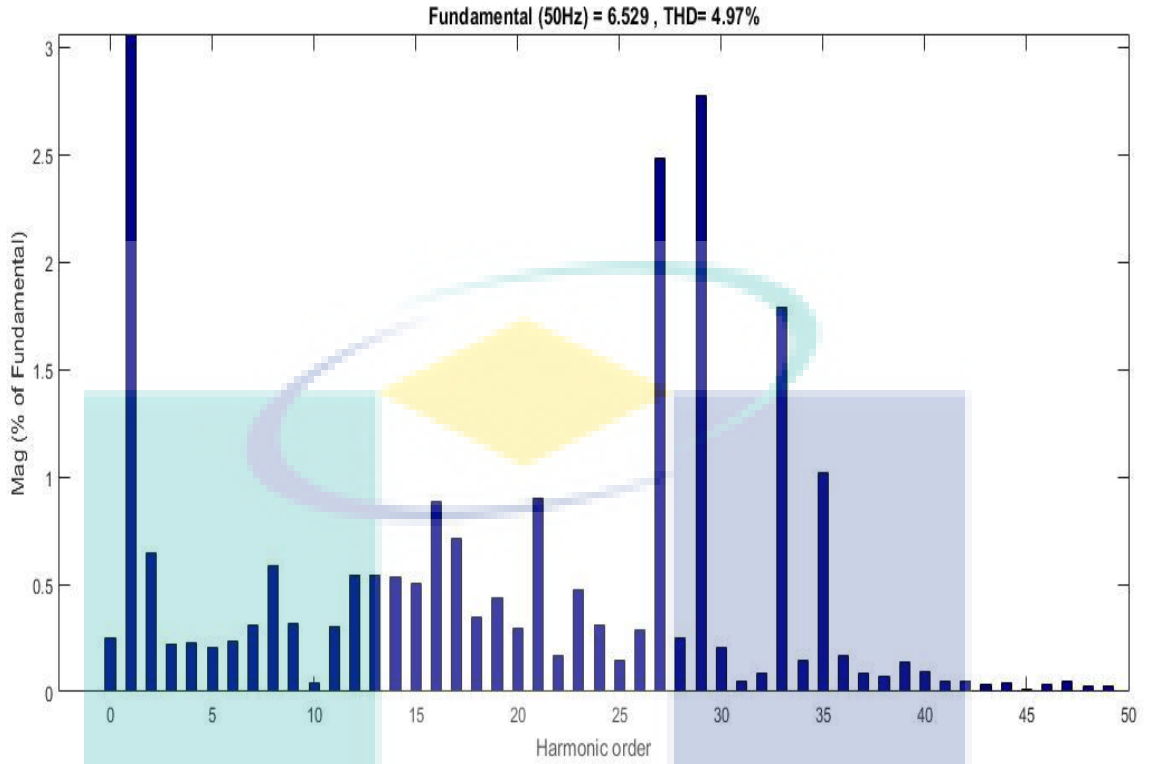


figures below include the first 50 harmonics. The THD for each solar irradiance is below than 5 % but the harmonic spectrum for CPWM and DPWM can be observed and compared based on the harmonic spectrum produce from FFT analysis.

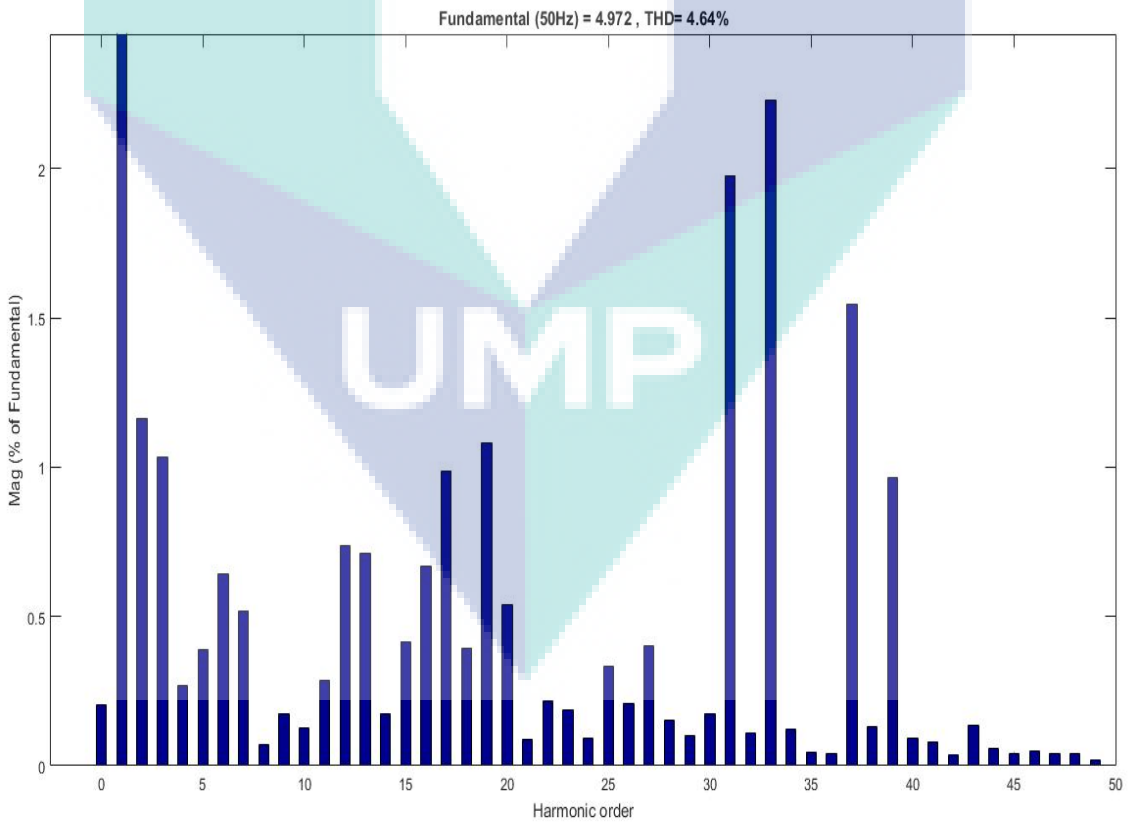
Referring to the harmonic spectrum of CPWM at 1000 W/m<sup>2</sup>, the 25<sup>th</sup>, 27<sup>th</sup> and 31<sup>st</sup> harmonic are very high. 27<sup>th</sup>, 29<sup>th</sup>, 33<sup>rd</sup> and 25<sup>th</sup> harmonic and 31<sup>st</sup>, 33<sup>rd</sup>, 37<sup>th</sup> and 39<sup>th</sup> harmonic are the highest for 800 W/m<sup>2</sup> and 600 W/m<sup>2</sup> respectively. Different case for 400 W/m<sup>2</sup>, the harmonic produce is lower compared to the other solar irradiance while for 200 W/m<sup>2</sup> the harmonic is high from 10<sup>th</sup> until the 20<sup>th</sup> harmonic. DPWM has higher harmonic compared to CPWM. Thus, the harmonic spectrum shown in Figure 4.7 prove the statement stated by (Oh & Sunwoo, 2008). Generally, the harmonic of DPWM is higher starting from 2<sup>nd</sup> harmonic until the 20<sup>th</sup> harmonic.



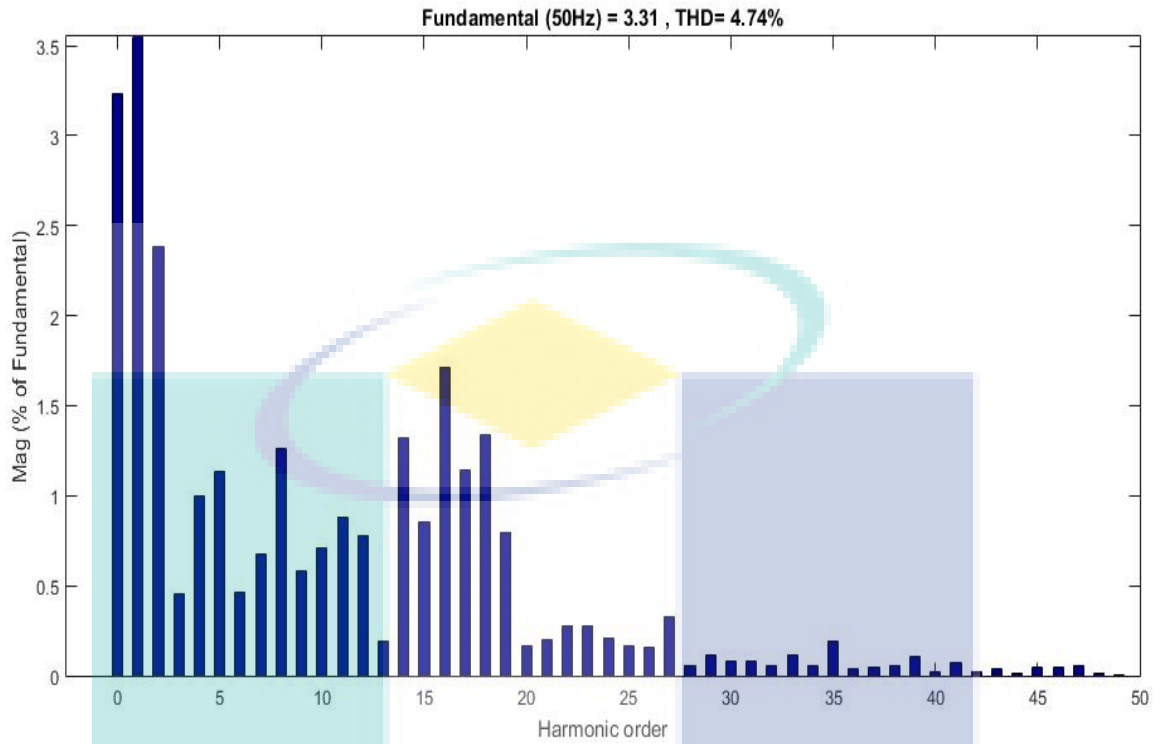
(a) 1000 W/m<sup>2</sup>, 1462.0 Hz



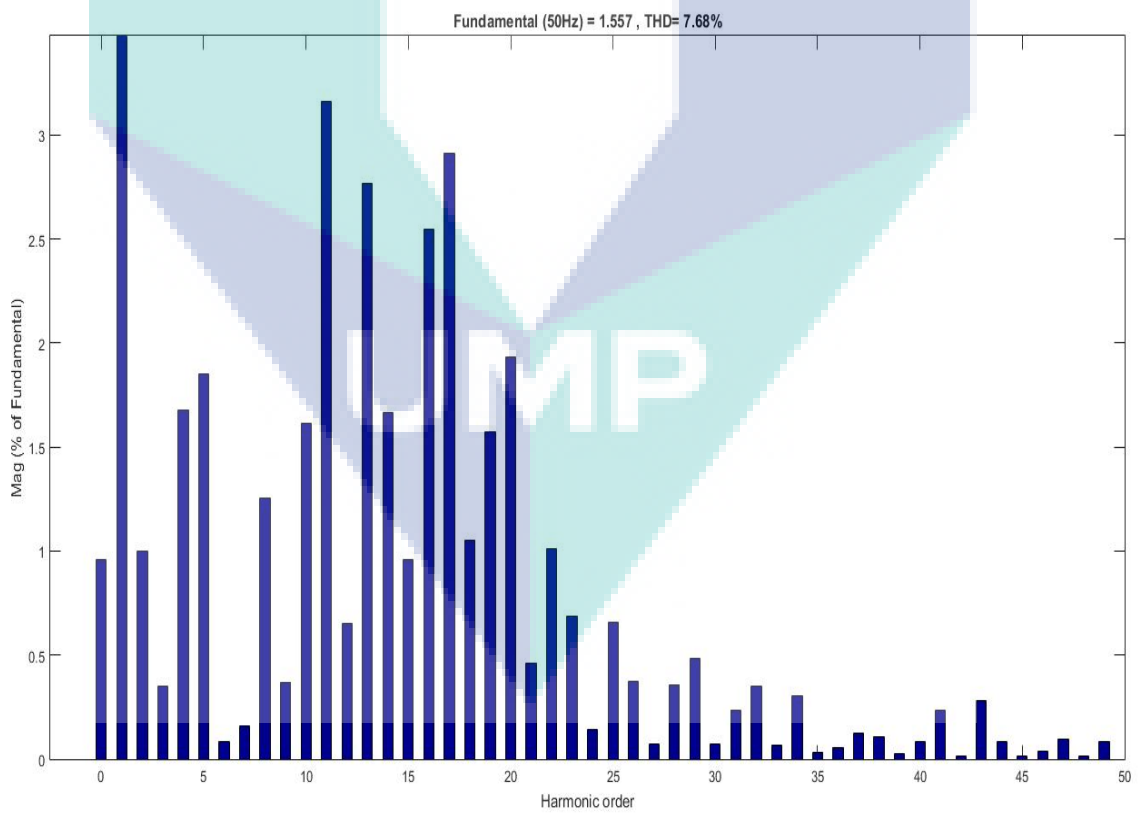
(b) 800 W/m<sup>2</sup>, 1545.5 Hz



(c) 600 W/m<sup>2</sup>, 1746.0 Hz

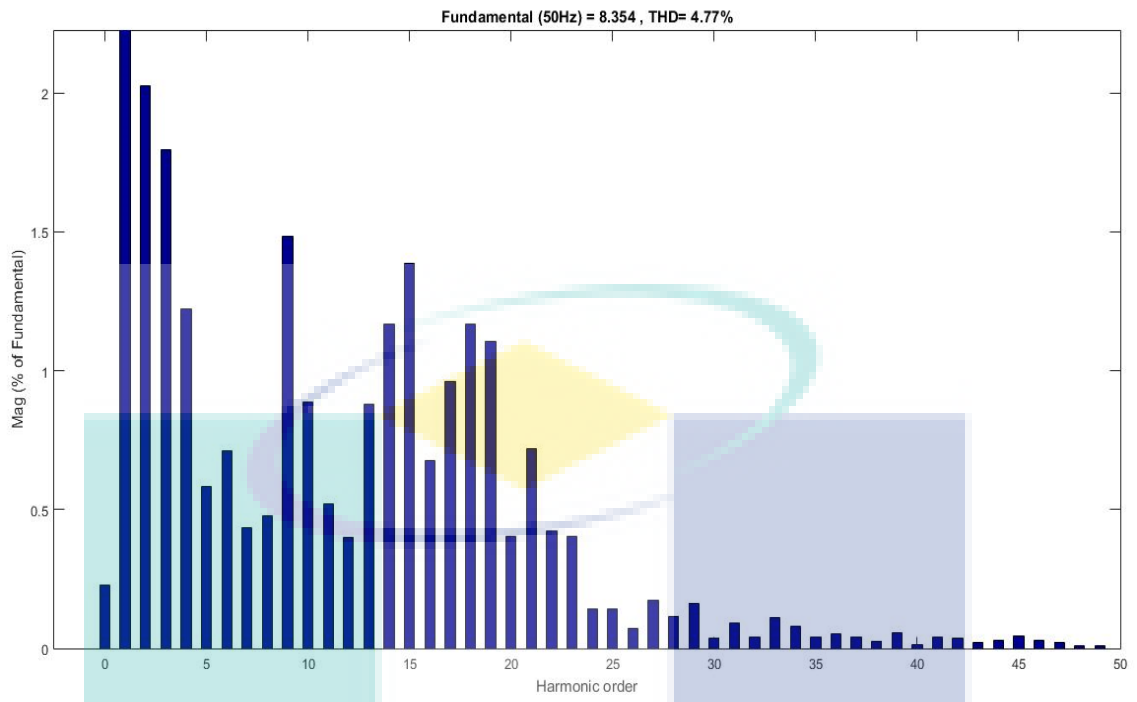


(d) 400 W/m<sup>2</sup>, 5000.0 Hz

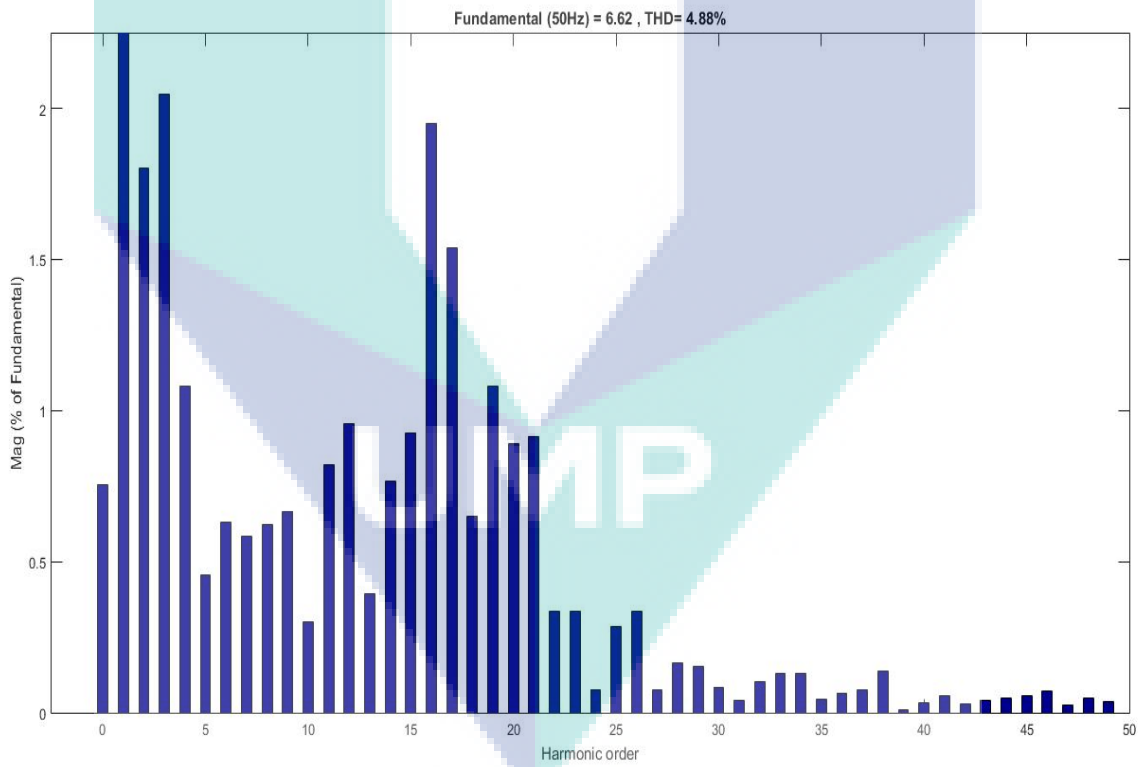


(e) 200 W/m<sup>2</sup>, 12600.00 Hz

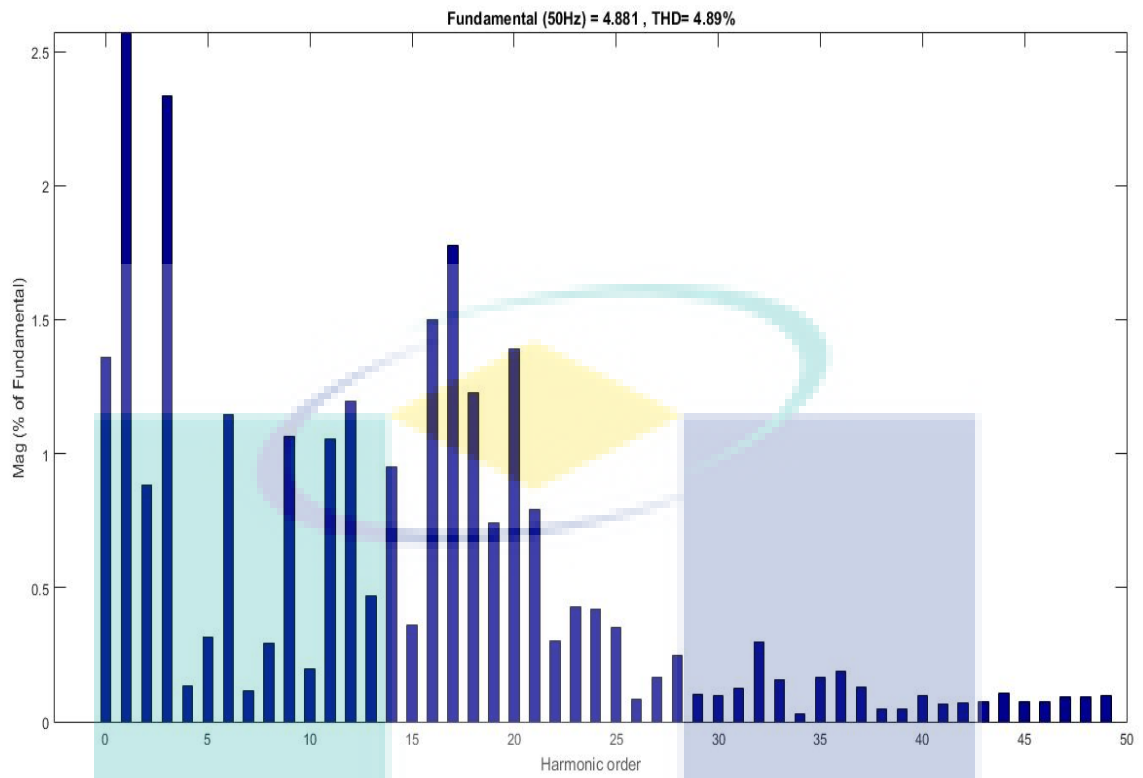
Figure 4.6 Harmonic spectrum of the current at PCC using CPWM control at different solar irradiance level



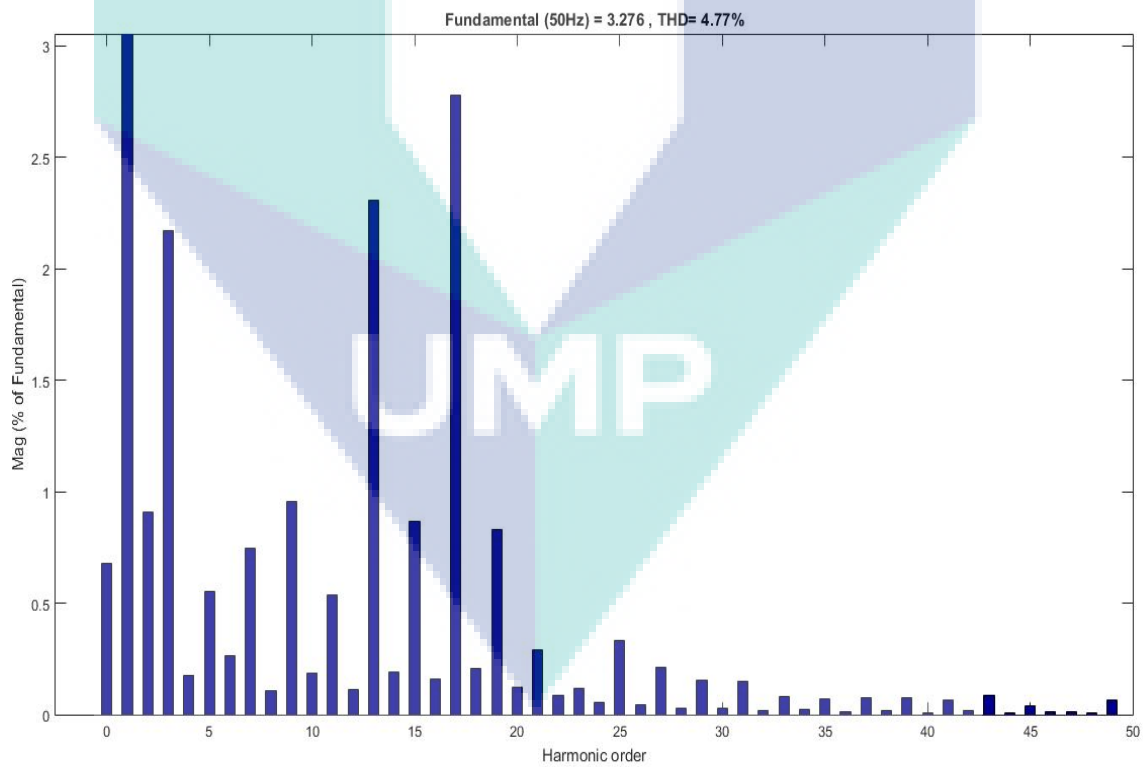
(a) 1000 W/m<sup>2</sup>, 5600 Hz



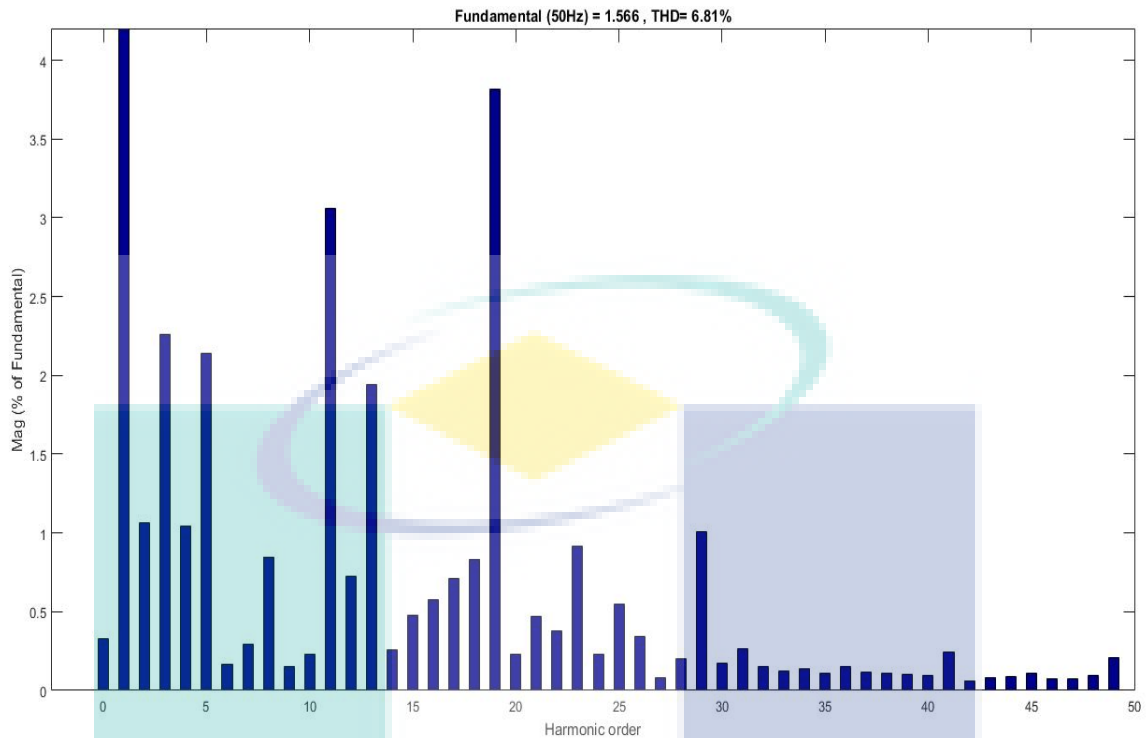
(b) 800 W/m<sup>2</sup>, 6500 Hz



(c) 600 W/m<sup>2</sup>, 7650 Hz



(d) 400 W/m<sup>2</sup>, 9000 Hz



(e) 200 W/m<sup>2</sup>, 23550 Hz

Figure 4.7 Harmonic spectrum of the current at PCC using DPWM control at different solar irradiance level

The findings are tabulated in Table 4.3. The reason why the minimum switching frequency is selected to be analysed in this research is because the switching losses may increase when switching frequency increase. It is known that the THD can be reduced when the switching frequency is increased but the unwanted consequence when the switching frequency too high is switching losses occur in the system and might downgrade the quality of the power grid and affect the reliability.

Table 4.3 Minimum switching frequency of the PWM and THD at different level of solar irradiance

Solar Irradiance (W/m <sup>2</sup> )	CPWM		DPWM	
	<i>THD<sub>i</sub></i> (%)	Minimum Switching Frequency (Hz)	<i>THD<sub>i</sub></i> (%)	Minimum Switching Frequency (Hz)
1000	4.89	1462.0	4.26	5600
800	4.97	1545.5	4.82	6500
600	4.44	1746.0	3.36	7650
400	4.84	5000.0	4.02	9000
200	7.68	12600.0	6.81	23550

The results of the findings support the hypothesis of the previous research. The theory can be abstract from the previous research is that the PWM control can help to

improve the quality of the system by reducing the THD. Compared to the PWM type's characteristics, it is found that CPWM has more benefit in order to reduce THD level as stated by (Oh & Sunwoo, 2008) and (A. M. Hava et al., 1998). In addition, the results from this research can validate that CPWM which is represented with TTHIPWM can reduce the  $THD_i$  level with lower switching frequency than DPWM.

The switching frequency of the PWM carrier signal needed for CPWM and DPWM to reach the optimum level of  $THD_i$  is displayed in Figure 4.8. Clearly can be seen that the switching frequency required for CPWM in order to meet the standard  $THD_i$  always lower than that of DPWM. As a result less switching losses produced. According to the previous research, the THD level is reduced when the solar irradiance increase (Hicks et al., 2018).

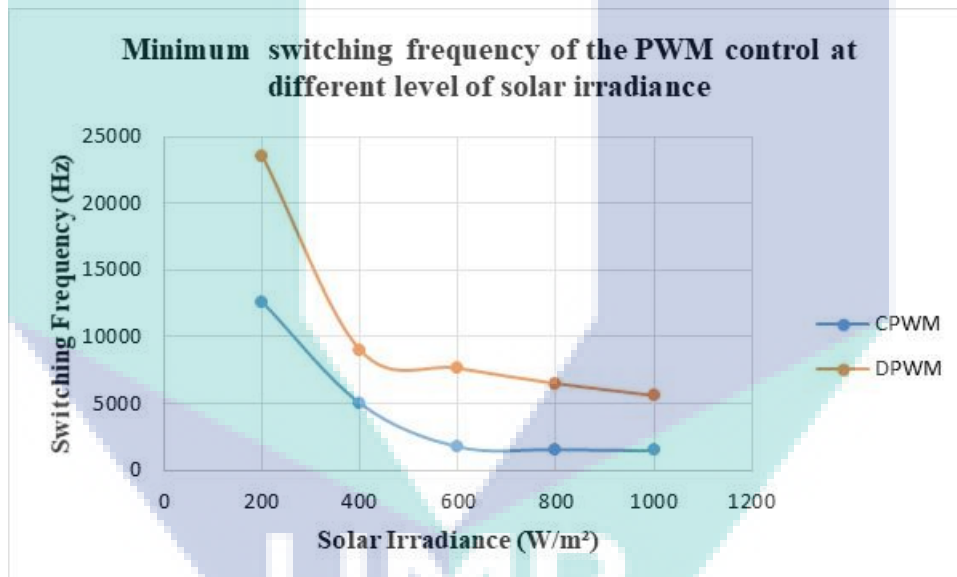


Figure 4.8 Minimum switching frequency of CPWM and DPWM carrier signal to obtain in standard  $THD_i$  at different level of solar irradiance

The results from this research showed that the switching frequency needed for CPWM and DPWM to fulfil the  $THD_i$  standard at 1000 W/m<sup>2</sup> is 1462 Hz and 5600 Hz respectively. Moreover, it can be concluded that at 1000 W/m<sup>2</sup> CPWM only required 1462 Hz to produce 4.89 %  $THD_i$  value and this means that CPWM is way better than DPWM. Thus less switching frequency should be applied to PWM to achieve the standard of the  $THD_i$ .

Another important finding from Table 4.3 is at 800 W/m<sup>2</sup> and 600 W/m<sup>2</sup> solar irradiance level for CPWM required only 5.71 % and 12.97 % of the switching

frequency increment needed to obtain less than 5 %  $THD_i$  respectively. In contrast, for DPWM there is a huge difference of the switching frequency required to obtain in standard  $THD_i$ . From 1000 W/m<sup>2</sup> to 800 W/m<sup>2</sup>, the switching frequency increase at 16.07 % and from 800 W/m<sup>2</sup> to 600 W/m<sup>2</sup>, the value of the switching frequency raise is 17.69 %. Thus, comparing both techniques, CPWM shows better performance in order to meet the standard  $THD_i$  since the switching frequency needed is lower than DPWM did. Also the switching frequency increments between different solar irradiance levels are lesser.

Above all, the switching frequency for both PWMs become greater when the solar irradiance reaching 400 W/m<sup>2</sup>. Poor  $THD_i$  can be expected when the solar irradiance is lower and unstable. According to IEC 61829:2015, on-site measurement of I-V characteristics recommends that the total in-plane irradiance shall be at least 700 W/m<sup>2</sup>. After multiple trials with 200 W/m<sup>2</sup> solar irradiance, it is observed that  $THD_i$  that less than 5 % was not found. However, the smallest value of  $THD_i$  for CPWM and DPWM is 7.68 % and 6.81 % accordingly. Thus, the switching frequency of those  $THD_i$  values are considered in this research.

#### **4.2.4 Analysis of Switching Losses between PWM Techniques at Different Irradiance**

In this research, the switching losses of the CPWM and DPWM were roughly analysed by applying to the consideration of DPWM allows an increase of the switching frequency by 33 % (Asiminoaei et al., 2008). Besides that, the results of investigating THD levels of the PWM that meet the standard level are found that different switching frequency for different level of irradiances. Thus, it cannot be concluded that DPWM has less switching losses at different switching frequency. Therefore, the calculation was done to observe the switching frequency level when the switching frequency of CPWM increased 33 %, meanwhile switching frequency of DPWM was decreased 33 %.

The results of the calculation are to observe whether or not the CPWM switching frequency is more than the DPWM switching frequency and thus can be assumed that CPWM has a higher switching losses as stated by (Asiminoaei et al., 2008) and (Oh & Sunwoo, 2008). If CPWM has higher switching frequency even after



decreasing 33 % of the DPWM switching frequency, then it can be assumed that CPWM has a higher switching losses. The results of the calculations are presented in Table 4.4. The minimum switching frequency values of the CPWM and DPWM are obtained from Table 4.3.

Table 4.4 Results of increasing 33 % of CPWM and decreased 33 % of DPWM switching frequency to analyse switching losses

Solar Irradiance (W/m <sup>2</sup> )	CPWM		DPWM	
	Minimum Switching Frequency (Hz)	Switching Frequency Increased 33 % (Hz)	Minimum Switching Frequency (Hz)	Switching Frequency Decreased 33 % (Hz)
1000	1462.0	1944.5	5600	3752.0
800	1545.5	2055.5	6500	4355.0
600	1746.0	2322.2	7650	5125.5
400	5000.0	6650.0	9000	6030.0
200	12600.0	16758.0	23550	15778.5

Referring the results in the table above, it turns out that CPWM can be assume has lower switching losses as compared to DPWM. This is due to the switching frequency of the CPWM appear to be lower even after increased 33 % than the minimum switching frequency of DPWM when the switching frequency decreased 33 %. A conclusion can be made from these results is that the switching frequency of CPWM is lower than DPWM even before the 33 % increment or decrement are taken into account. These result can support the decision to choose which PWM technique has better performance. After the increment and decrement were calculated, the switching frequency of DPWM doubled and even more from CPWM switching frequency. Additionally, switching losses increased when the inverter operates at very high switching frequencies (Dawidowski et al., 2014).

### 4.3 Discussion

This research concentrates on a GCPV system model and use MATLAB/Simulink environment as simulation. This idea occurs because Malaysia has wide-ranging solar irradiance throughout the year. PWM was used as the solution to reduce the THD level. CPWM and DPWM were chosen as the PWM techniques to be implemented in the inverter control of the GCPV system model. The techniques were compared and CPWM was suggested as the recommended solution. It is found that CPWM has more benefit in order to reduce THD level. In addition, the results from this

research validates that CPWM can reduce the  $THD_i$  level with lower switching frequency than DPWM. The results from this research showed that the switching frequency needed for CPWM and DPWM to fulfil the  $THD_i$  standard at 1000 W/m<sup>2</sup> is 1462 Hz and 5600 Hz respectively and this means that CPWM is better than DPWM since at a maximum solar irradiance supposedly the  $THD_i$  is already at low levels.

Besides that, the current and power output of the system was linear with the solar irradiance level regardless the PWM techniques applied. The voltage output remains constant even the solar irradiance changes. Next, the analysis of the  $THD_i$  based on the PWM used shows that the  $THD_i$  increased when the solar irradiance decreased and it becomes worse when the solar irradiance is approaching 400 W/m<sup>2</sup> where the solar irradiance exhibits unstable condition. Additionally,  $THD_i$  using DPWM was higher compared to CPWM at all solar irradiance levels. Thus, the switching frequency selection under different solar irradiance range was proposed and showed in the section 4.2.3. Power system operating with less power quality issue may guarantee the safety and reliability of the electrical equipment.

#### **4.4 Conclusion**

To sum up, all the research objectives are achieved. As can be seen, CPWM and DPWM were used as the PWM techniques implemented in the inverter control of the GCPV system model. The techniques were compared and CPWM was suggested as the recommended solution. This was based on the results of the  $THD_i$  value at different level of solar irradiance and the switching frequency of the PWM carrier signal. Besides that, the current and power output of the system was linear with the solar irradiance level but not depends on the PWM techniques applied. The voltage output remains the same even the solar irradiance changes. Next, the analysis of the  $THD_i$  based on the PWM used to show that the  $THD_i$  increased when the solar irradiance decreased and it becomes worse when the solar irradiance is approaching 400 W/m<sup>2</sup>. Additionally,  $THD_i$  for DPWM was higher compared to CPWM at all solar irradiance levels.

## CHAPTER 5

### CONCLUSION

The research reported in this thesis is based on renewable energy field studies which is harmonic distortion and switching losses in a GCPV system. The present of THD in the system leave a question on how to reduce the power quality issue and how this research may give a solution for that problem. Lack of knowledge in PWM techniques leads this research to understand more about PWM techniques that can be the solution to the problem. Consequently, the decision was made to concentrate on a GCPV system model and use MATLAB/Simulink environment as simulation. This is based on the literature review related to PV system technology research that apply MATLAB/Simulink environment and in addition the available inbuilt model as the reference.

The experiment was conducted using PWM switching frequency selection. The switching frequency value that produce THD in standard were recorded and analysis was performed based on output power, THD value, switching frequency and switching losses of the PWM at different irradiance level. Lastly, a control method which is CPWM and the results of the switching frequency value that is acceptable in order to maintain THD within the standard requirement during various irradiance was proposed in this thesis.

In this research, PWM was used as the solution to reduce the THD level and switching losses. TTHIPWM and DPWM2 from CPWM and DPWM types respectively were chosen as the PWM techniques implemented in the inverter control since both give best performance as stated in the literature review in Chapter 2. The techniques were compared and CPWM was suggested as the recommended solution. This was based on the results of the  $THD_i$  value at different level of solar irradiance and switching losses

of the PWM. To investigate the switching frequency effects on  $THD_i$  in the system model's PCC at different solar irradiance level, the switching frequency of the PWM carrier signal was set to a value, run the simulation and lastly performs the FFT analysis tool to record the  $THD_i$  and the output values. Details of the method explained in Chapter 3 under section 3.2.

The steps were continued by adjusting the switching frequency until the value of the switching frequency inserted in the PWM carrier signal able to meet the standard THD. The minimum switching frequency selection based on the solar irradiance range was proposed and showed in Chapter 4 under section 4.3. It is observe that, the current and power output of the system is linear with the solar irradiance level regardless on the PWM techniques applied. The voltage output remains the same even the solar irradiance changes. Next, the analysis of the  $THD_i$  based on the PWM used showed that the  $THD_i$  increased when the solar irradiance decreased and it becomes worse when the solar irradiance is approaching 400 W/m<sup>2</sup> where the solar irradiance unstable. Additionally,  $THD_i$  for DPWM was higher compared to CPWM at all solar irradiance levels.

The investigation was also carried out on the switching frequency of the PWM carrier signal analysis as written in Chapter 4, section 4.2.3. It is found that the switching frequency needed in order to obtain  $THD_i$  that less than 5 % for CPWM is lower than the switching frequency needed for DPWM carrier signal. It is found that the DPWM control required higher switching frequency of the carrier signal to reduce the  $THD_i$  in the system. Switching losses analysis of the PWM was roughly analyse by referring to the fact that DPWM allows 33 % increase switching frequency or give 33 % reduction in switching losses compared to CPWM.

It is found the switching frequency of DPWM is double than CPWM and thus CPWM has less switching losses. The important finding in this investigation is the appropriate selection of switching frequency of the PWM may decrease the THD content of the current output waveform at different solar irradiance level. Based on the results obtain it can be concluded that harmonic distortion at PCC can be reduced and the system can meet the standard with the correct techniques used in the system.

Finally, all the objectives of this research are achieved. The main objective is to carry out research to minimize harmonics and switching losses in the GCPV system.

PWM techniques were implemented in the inverter control of a GCPV system model using MATLAB/Simulink environment by creating the subsystem of the CPWM and DPWM and replace the existing SPWM in the system model with the designed PWM. The effect of switching frequency on THD and switching losses performance at different solar irradiance was investigated by executed the simulation on the GCPV system model with PWM techniques as the inverter control.

### 5.1 Recommended Solution

Based on all analysis the CPWM is proposed as the recommended solution. The proposed block diagram of the recommended solution is shown in Figure 5.1. Table 5.1 consists of recommended switching frequency for difference solar irradiance. The switching frequency values are collected from Table 4.3. The block diagram presents the proposed switching frequency control method to meet the THD standard and minimize switching losses problem in a GCPV system. The main focused in this block diagram is the sunlight strike the PV array with different solar irradiance level throughout the day. Then, the carrier signal was generated based on the minimum switching frequency proposed in Table 5.1. The comparator functions as to compare the CPWM modulating signal and the carrier signal and thus the CPWM pulse was produced. The CPWM pulse produced act as the logic gate signal of the inverter.

Table 5.1 Recommended switching frequency selection based on solar irradiance range

Solar Irradiance (W/m <sup>2</sup> )	Switching Frequency Range	Switching Frequency Value (Hz)
200 - 400	$f_{sw1}$	12600.00 Hz
401 - 600	$f_{sw2}$	5000.00 Hz
601 - 800	$f_{sw3}$	1746.00 Hz
801 - 1000	$f_{sw4}$	1545.50 Hz

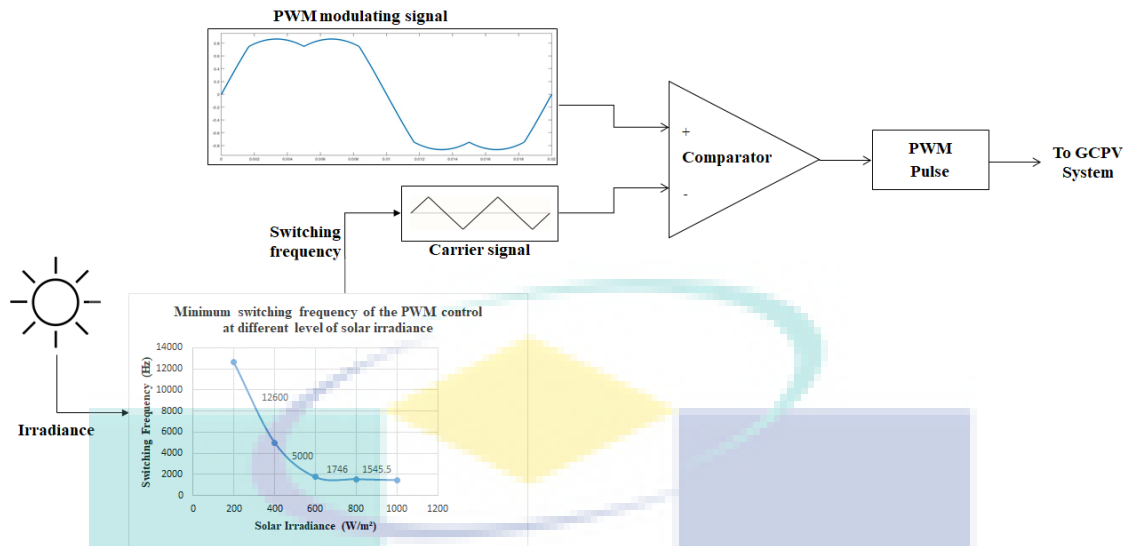


Figure 5.1 Block diagram of proposed CPWM as the recommended solution to meet the standard THD and minimize switching losses in a GCPV system

## 5.2 Suggestion for Future Work

The research carried out in this thesis represents a starting point and additional work in the future is to propose minimum switching frequency recommends as the switching frequency for the PWM used in the GCPV system.

In this research, a step by steps need to be taken to make sure the GCPV system meets the standard THD requirement when the solar irradiance changing. The solar irradiance keep changing throughout the day and it is recommended to develop a suitable mitigation method where the switching frequency of the PWM carrier signal can be automatically regulated to the appropriate value when the solar irradiance change in order to alleviate the THD problem.

## REFERENCES

- Aamri, F. E., Maker, H., Mouhsen, A., & Harmouchi, M. (2015). A new strategy to control the active and reactive power for single phase grid-connected PV inverter. *2015 3rd International Renewable and Sustainable Energy Conference (IRSEC)*, 1–6. <https://doi.org/10.1109/IRSEC.2015.7455080>
- Abd Halim, H. (2013). *Three Phase Inverter Development Using Common Mode Voltage Pulse Width Modulation (PWM) Method* (Thesis, Universiti Tun Hussein Onn). Retrieved from [http://eprints.uthm.edu.my/4693/1/HASMIZAR\\_BINTI\\_ABD\\_HALIM.pdf](http://eprints.uthm.edu.my/4693/1/HASMIZAR_BINTI_ABD_HALIM.pdf)
- Abdool, A., & Alwannan, K. (2014). Current harmonic generation of a modeled and simulated single phase grid connected PWM current controlled photovoltaic inverter. *2014 First International Conference on Green Energy ICGE 2014*, 89–95. <https://doi.org/10.1109/ICGE.2014.6835403>
- Al-Shetwi, A. Q., & Sujod, M. Z. (2017, October). *Harmonic Distortion and Voltage Imbalance Study of Photovoltaic Power Plant Connected to the Malaysian Grid*. Presented at the 4th International Conference on Electrical, Control & Computer Engineering (InECCE), Langkawi, Malaysia.
- Asiminoaei, L., Rodriguez, P., & Blaabjerg, F. (2008). Application of Discontinuous PWM Modulation in Active Power Filters. *IEEE Transactions on Power Electronics*, 23(4), 1692–1706. <https://doi.org/10.1109/TPEL.2008.924599>
- Ayub, M., Gan, C. K., & Kadir, A. F. A. (2014). The impact of grid-connected PV systems on Harmonic Distortion. *2014 IEEE Innovative Smart Grid Technologies - Asia (ISGT ASIA)*, 669–674. <https://doi.org/10.1109/ISGT-Asia.2014.6873872>
- Badi, L. W. A., Zakaria, Z., Nordin, A. H. M., & Mustapa, R. F. (2014). Unbalanced faults analysis in grid - Connected PV system. *2014 IEEE International Conference on Power and Energy (PECon)*, 360–365. <https://doi.org/10.1109/PECON.2014.7062471>
- Cai, W., Ren, H., Jiao, Y., Cai, M., & Cheng, X. (2011). Analysis and simulation for grid-connected photovoltaic system based on MATLAB. *2011 International Conference on Electrical and Control Engineering (ICECE)*, 63–66. <https://doi.org/10.1109/ICECENG.2011.6056813>
- Cheng, H., Cao, W. s., & Ge, P. j. (2012). Forecasting Research of Long-Term Solar Irradiance and Output Power for Photovoltaic Generation System. *2012 Fourth International Conference on Computational and Information Sciences*, 1224–1227. <https://doi.org/10.1109/ICCIS.2012.157>

- Dawidowski, P., Stosur, M., Szewczyk, M., & Balcerek, P. (2014). Reduction of THD by switching frequency optimization in three-level NPC inverter. *Research Gate*. <https://doi.org/10.12915/pe.2014.08.04>
- Dugan, R. C., McGranaghan, M. F., Santoso, S., & Beaty, H. W. (2004). *Electrical Power System Quality* (Second). Retrieved from [http://www.gcebargur.ac.in/sites/gcebargur.ac.in/files/lectures\\_desk/electrical\\_power\\_systems\\_quality.pdf](http://www.gcebargur.ac.in/sites/gcebargur.ac.in/files/lectures_desk/electrical_power_systems_quality.pdf)
- Ehmidat, M. M. (2013). *The Possible Contribution of Photovoltaic Systems to the Electricity Supply in some Districts in Palestine*. 107.
- Fang, X. P., Cui, J. M., Liu, J., & Cao, M. Y. (2011). Detail research on the traditional inverter and Z-source inverter. *2011 International Conference on Applied Superconductivity and Electromagnetic Devices*, 318–321. <https://doi.org/10.1109/ASEMD.2011.6145133>
- Fezzani, A., Mahammed, I. H., Drid, S., & Chrifi-alaoui, L. (2015). Modeling and analysis of the photovoltaic array faults. *2015 3rd International Conference on Control, Engineering Information Technology (CEIT)*, 1–9. <https://doi.org/10.1109/CEIT.2015.7232983>
- Fourier Transforms - MATLAB & Simulink. (n.d.). Retrieved February 27, 2019, from <https://www.mathworks.com/help/matlab/math/fourier-transforms.html>
- Grigoletto, F. B., Stefanello, M., Silva, G. S. da, & Pinheiro, H. (2016). Space vector pulse width modulation for Modular Multilevel Converters. *IECON 2016 - 42nd Annual Conference of the IEEE Industrial Electronics Society*, 2575–2581. <https://doi.org/10.1109/IECON.2016.7793921>
- Hava, A. M., Kerkman, R. J., & Lipo, T. A. (1998). A high-performance generalized discontinuous PWM algorithm. *IEEE Transactions on Industry Applications*, 34(5), 1059–1071. <https://doi.org/10.1109/28.720446>
- Hava, Ahmet M. (1998). *Carrier Based PWM-VSI Drives in the Overmodulation Region*. University of Wisconsin, Madison.
- Hicks, C., Baghzouz, Y., & Haddad, S. (2018). Power quality of residential PV system under low solar irradiance and off-grid operation. *2018 18th International Conference on Harmonics and Quality of Power (ICHQP)*, 1–5. <https://doi.org/10.1109/ICHQP.2018.8378937>
- IGBT Structure and Circuit Working with Applications. (2015, June 3). Retrieved December 6, 2016, from Edgefxkits International website: <http://efxkits.com/blog/igbt-circuit-working-with-applications/>



- Infineon Technologies AG. (2006). *Different PWM Waveforms Generation for 3-Phase AC Induction Motor with XC164CS*. München.
- Insulated Gate Bipolar Transistor or IGBT Transistor. (2013, August 26). Retrieved October 5, 2017, from Basic Electronics Tutorials website: <http://www.electronics-tutorials.ws/power/insulated-gate-bipolar-transistor.html>
- Jäger-Waldau, A. (2018). *PV Status Report 2018*.
- Jayanth, K. G., Boddapati, V., & Geetha, R. S. (2018). Comparative study between three-leg and four-leg current-source inverter for solar PV application. *2018 International Conference on Power, Instrumentation, Control and Computing (PICC)*, 1–6. <https://doi.org/10.1109/PICC.2018.8384793>
- Jianhui Wong, Y. S. L. (2014). Grid-connected photovoltaic system in Malaysia: A review on voltage issues. *Renewable and Sustainable Energy Reviews*, 29, 535–545. <https://doi.org/10.1016/j.rser.2013.08.087>
- Kamal EL-Sayed, S. (2017). Impact of Photovoltaic Tied to Electrical Grid System On Power Quality. *Journal of Electrical and Electronic Engineering*, 5(2), 23. <https://doi.org/10.11648/j.jeee.20170502.11>
- Khan, N., Siraj, A., Khan, J., Mahboob, F., & Haque, A. (2017). A simple and effective control of single phase solar inverter. *2017 International Conference on Power and Embedded Drive Control (ICPEDC)*, 190–195. <https://doi.org/10.1109/ICPEDC.2017.8081085>
- Khanfara, M., Bachtiri, R. E., Hammoumi, K. E., & Boussetta, M. (2016). A comparison between two filters for PV inverter controlled to eliminate first harmonics. *2016 International Conference on Information Technology for Organizations Development (IT4OD)*, 1–6. <https://doi.org/10.1109/IT4OD.2016.7479323>
- Kharjule, S. (2015). Voltage source inverter. *2015 International Conference on Energy Systems and Applications*, 537–542. <https://doi.org/10.1109/ICESA.2015.7503407>
- Khatib, T., Mohamed, A., & Sopian, K. (2012). A Software Tool for Optimal Sizing of PV Systems in Malaysia. *Hindawi Publishing Corporation, 2012*(Article ID 969248), 11. <https://doi.org/10.1155/2012/969248>
- Khatri, M., & Kumar, A. (2017). Experimental Investigation of Harmonics in a Grid-Tied Solar Photovoltaic System. *INTERNATIONAL JOURNAL of RENEWABLE ENERGY RESEARCH*, Vol.7(No.2), 901–907.

- Kumar, N., Saha, T. K., Dey, J., & Barman, J. C. (2015). Modelling, control, and performance study of cascaded inverter based grid connected PV system. *IREC2015 The Sixth International Renewable Energy Congress*, 1–6. <https://doi.org/10.1109/IREC.2015.7110884>
- Lacanette, K. (1991, April). *A Basic Introduction to Filters-Active, Passive, and Switched-Capacitor*. Retrieved from [www.swarthmore.edu/NatSci/echeeve1/Ref/DataSheet/IntroToFilters.pdf](http://www.swarthmore.edu/NatSci/echeeve1/Ref/DataSheet/IntroToFilters.pdf)
- Mahyudin, B., & Abdul Malek, B. (2012). *National Survey Report of PV Power Applications in Malaysia 2011* (p. 26). Retrieved from [file:///C:/Users/me/Downloads/nsr\\_2011\\_MYS.pdf](file:///C:/Users/me/Downloads/nsr_2011_MYS.pdf)
- Mohammad Bagher, A., Abadi Vahid, M. M., & Mohsen, M. (2015). Types of Solar Cells and Application. *American Journal of Optics and Photonics*, 3, 94–113. <https://doi.org/10.11648/j.ajop.20150305.17>
- Mohanty, P., & Sahoo, S. (2010). *Analysis of Two-level and Three-level Inverters* (National Institute of Technology). Retrieved from <http://ethesis.nitrkl.ac.in/1873/1/piyush.pdf>
- Nguyen, N. V., Nguyen, B. X., & Lee, H. H. (2011). An Optimized Discontinuous PWM Method to Minimize Switching Loss for Multilevel Inverters. *IEEE Transactions on Industrial Electronics*, 58(9), 3958–3966. <https://doi.org/10.1109/TIE.2010.2102312>
- Nordin, N. D., & Rahman, H. A. (2015). Pre-installation Design Simulation Tool for Grid-connected Photovoltaic System Using Iterative Methods. *Energy Procedia*, 68, 68–76. <https://doi.org/10.1016/j.egypro.2015.03.234>
- Nozadian, M. H. B., Ebrahimzadeh, F., Babaei, E., & Asl, E. S. (2017). Current-fed switched Z-source inverters. *2017 14th International Conference on Electrical Engineering/Electronics, Computer, Telecommunications and Information Technology (ECTI-CON)*, 769–772. <https://doi.org/10.1109/ECTICon.2017.8096352>
- Oh, S., & Sunwoo, M. (2008). Variable structure PWM controller for high efficient PV inverters. *2008 IEEE International Conference on Sustainable Energy Technologies*, 933–938. <https://doi.org/10.1109/ICSET.2008.4747141>
- Padure, P., Haraguta, C. I., Vintea, A., & Ghita, O. M. (2014). Evaluation method for harmonic distortion and power losses of photovoltaic systems using LabVIEW software. *2014 49th International Universities Power Engineering Conference (UPEC)*, 1–6. <https://doi.org/10.1109/UPEC.2014.6934827>

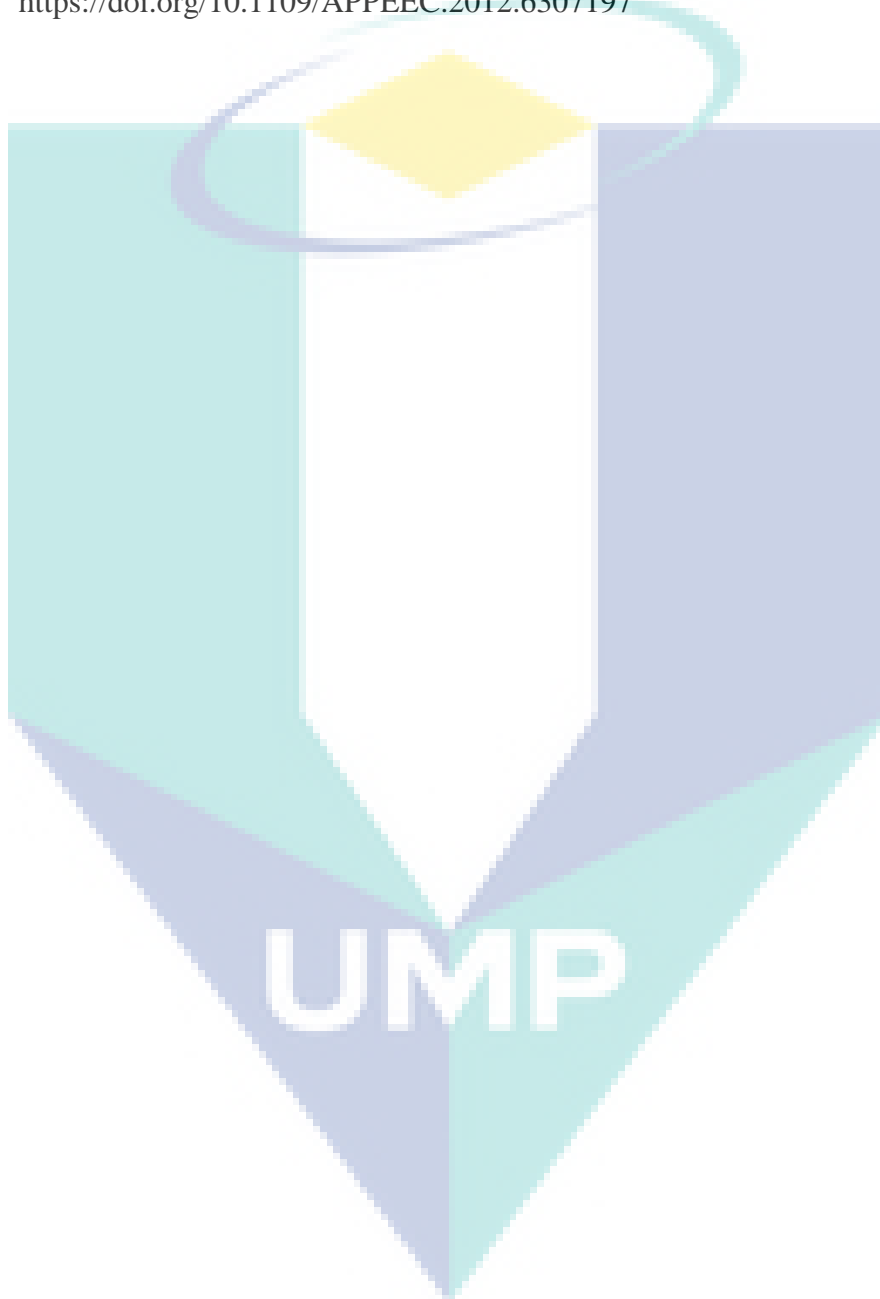
- Parikh, P. R. (2017, July 9). *Operation Overview of Three Phase Inverter With 120°, 150° and 180° Conduction Mode*. 4. Retrieved from [http://sdtechnocrates.com/IIIETEBMS2017/html/papers/III-ETEBMS-2017\\_ENG-EE8.pdf](http://sdtechnocrates.com/IIIETEBMS2017/html/papers/III-ETEBMS-2017_ENG-EE8.pdf)
- Peng, F. Z. (2003). Z-source inverter. *IEEE Transactions on Industry Applications*, 39(2), 504–510. <https://doi.org/10.1109/TIA.2003.808920>
- Penkey, P., Alhajeri, F., & Johnson, B. K. (2016). Modeling, analysis and detection of faults in grid-connected PV systems. *2016 10th International Conference on Intelligent Systems and Control (ISCO)*, 1–5. <https://doi.org/10.1109/ISCO.2016.7727038>
- Phap, V. M., Yamamura, N., Ishida, M., & Nga, N. T. (2017). Impact of solar irradiation on PV cell emulating system in series connection mode. *2017 International Conference on High Voltage Engineering and Power Systems (ICHVEPS)*, 268–271. <https://doi.org/10.1109/ICHVEPS.2017.8225955>
- Portal, E.-E. E. (2014, October 20). 9 Most Common Power Quality Problems | EEP. Retrieved April 4, 2017, from EEP - Electrical Engineering Portal website: <http://electrical-engineering-portal.com/9-most-common-power-quality-problems>
- Pradhan, A., Ali, S. M., & Jena, C. (2013). Analysis of Solar PV cell Performance with Changing Irradiance and Temperature. *International Journal Of Engineering And Computer Science*, 2(1), 214–220.
- Prajapati, D., Ravindran, V., Sutaria, J., & Patel, P. (2014). A Comparative Study of Three Phase 2-Level VSI with 3-Level and 5-Level Diode Clamped Multilevel Inverter. *International Journal of Emerging Technology and Advanced Engineering*, 4(4), 6.
- Rahimi, K., Mohajeryami, S., & Majzoobi, A. (2016). Effects of photovoltaic systems on power quality. *2016 North American Power Symposium (NAPS)*, 1–6. <https://doi.org/10.1109/NAPS.2016.7747955>
- Rajasekaran, R., Thulasi, J. A., & Glenn, J. A. (2016). Three phase solar uninterrupted power supply. *2016 International Conference on Electrical, Electronics, and Optimization Techniques (ICEEOT)*, 4744–4747. <https://doi.org/10.1109/ICEEOT.2016.7755620>
- Renu, V., & Surasmi, N. L. (2014). Optimal control of selective harmonic elimination in a grid-connected single-phase PV inverter. *2014 International Conference on Advances in Green Energy (ICAGE)*, 265–271. <https://doi.org/10.1109/ICAGE.2014.7050175>

- Ruban, A. A. M., Hemavathi, N., & Rajeswari, N. (2012). Real time Harmonic Elimination PWM control for Voltage Source Inverters. *IEEE-International Conference On Advances In Engineering, Science And Management (ICAESM - 2012)*, 479–484.
- Salim, M. S., Mohammed Najim, J., & Mohammed Salih, S. (2013). Practical Evaluation of Solar Irradiance Effect on PV Performance. *Energy Science and Technology*, 6, 36–40. <https://doi.org/10.3968/j.est.1923847920130602.2671>
- Sathishkumar, H., & Parthasarathy, S. S. (2016). Space vector pulse width modulation for DC-AC converter. *2016 Second International Conference on Science Technology Engineering and Management (ICONSTEM)*, 310–314. <https://doi.org/10.1109/ICONSTEM.2016.7560968>
- Selvam, S. G. (2014). *Pre-Installed Economic Analysis Tool In Decision Making For Photovoltaic (PV) Systems Installation* (Universiti Teknologi Malaysia). Retrieved [http://portal.fke.utm.my/fklibrary/files/sriganeshselvam/2014/941\\_SRIGANESHALSELVAM2014.pdf](http://portal.fke.utm.my/fklibrary/files/sriganeshselvam/2014/941_SRIGANESHALSELVAM2014.pdf)
- Shaari, S., Omar, A. M., Haris, A. H., & Sulaiman, S. I. (2010a). *Solar Photovoltaic Power: Designing Grid-Connected Systems*.
- Shaari, S., Omar, A. M., Haris, A. H., & Sulaiman, S. I. (2010b). *Solar Photovoltaic Power: Fundamental*.
- Shah, N. (2013, May). *Harmonic in Power System - Causes, Effect and Control*. SIEMENS.
- Singh, S. K., Kumar, H., Singh, K., & Patel, A. (2014). A Survey and Study of Different Types of PWM Techniques Used in Induction Motor Drive. *International Journal of Engineering Science & Advanced Technology*, 4(1), 5.
- SolarPower Europe, & Schmela, M. (2018). *Global Market Outlook For Solar Power / 2018 - 2022*. Retrieved from [www.solarpowereurope.org](http://www.solarpowereurope.org)
- Sopian, K., Shaari, S., Amin, N., Zulkifli, R., Nizam, M., & Rahman, A. (2007). Performance of a grid-connected photovoltaic system in Malaysia. *ResearchGate*, 4(1), 57–65.
- Subsingha, W. (2016). A Comparative Study of Sinusoidal PWM and Third Harmonic Injected PWM Reference Signal on Five Level Diode Clamp Inverter. *Energy Procedia*, 89, 137–148. <https://doi.org/10.1016/j.egypro.2016.05.020>

- Sujod, M. Z. (2014). *Advanced Converter Control Techniques for Improving the Performance of DFIG based Wind Turbines* (Universität Duisburg-Essen). Retrieved from [https://duepublico.uni-duisburg-essen.de/servlets/DerivateServlet/Derivate-36279/Sujod\\_Zahim\\_Diss.pdf](https://duepublico.uni-duisburg-essen.de/servlets/DerivateServlet/Derivate-36279/Sujod_Zahim_Diss.pdf)
- Sulaiman, Shahril Irwan, Rahman, T. K. A., Musirin, I., Shaari, S., & Sopian, K. (2012). An intelligent method for sizing optimization in grid-connected photovoltaic system. *Solar Energy*, 86(7), 2067–2082. <https://doi.org/10.1016/j.solener.2012.04.009>
- Sulaiman, S.I., Rahman, T. K. A., & Musirin, I. (2010). Design of grid-connected photovoltaic system using evolutionary programming. *2010 IEEE International Conference on Power and Energy (PECon)*, 947–952. <https://doi.org/10.1109/PECON.2010.5697715>
- Sulaiman, S.I., Rahman, T. K. A., & Musirin, I. (2011). Artificial immune system for sizing grid-connected photovoltaic system. *Power Engineering and Optimization Conference (PEOCO), 2011 5th International*, 398–403. <https://doi.org/10.1109/PEOCO.2011.5970448>
- Sulaiman, S.I., Rahman, T. K. A., Musirin, I., & Shaari, S. (2011). Sizing grid-connected photovoltaic system using genetic algorithm. *2011 IEEE Symposium on Industrial Electronics and Applications (ISIEA)*, 505–509. <https://doi.org/10.1109/ISIEA.2011.6108763>
- Sunny, R., & Anto, R. (2013). Harmonics control and performance analysis of a grid connected photovoltaic system. *2013 International Conference on Advanced Computing and Communication Systems*, 1–6. <https://doi.org/10.1109/ICACCS.2013.6938706>
- Winder, S. (2002). *Analog and Digital Filter Design* (Second Edition). United States of America: Elsevier Science.
- Wu, Y., Shafi, M. A., Knight, A. M., & McMahon, R. A. (2011). Comparison of the Effects of Continuous and Discontinuous PWM Schemes on Power Losses of Voltage-Sourced Inverters for Induction Motor Drives. *IEEE Transactions on Power Electronics*, 26(1), 182–191. <https://doi.org/10.1109/TPEL.2010.2054837>
- Xplanator. (2017). *Three Phase Inverter under 180 degree operation and the associated waveforms*. Retrieved from <https://www.youtube.com/watch?v=Jl8PHbv4KQs>
- Zahim, S. M., & Erlich, I. (2012). Control of DFIG based Wind Turbine Converter using Continuous and Discontinuous PWM: A Comparative Study. *IFAC Proceedings Volumes*, 45(21), 542–547. <https://doi.org/10.3182/20120902-4-FR-2032.00095>

Zambri, M. K. M., Aras, M. S. M., Khamis, A., & Hairi, mohd H. (2016). Investigating the Impact of Photovoltaic Connection to the Malaysian Distribution System. *Journal of Telecommunication, Electronic and Computer Engineering (JTEC)*, 8(7), 23–28.

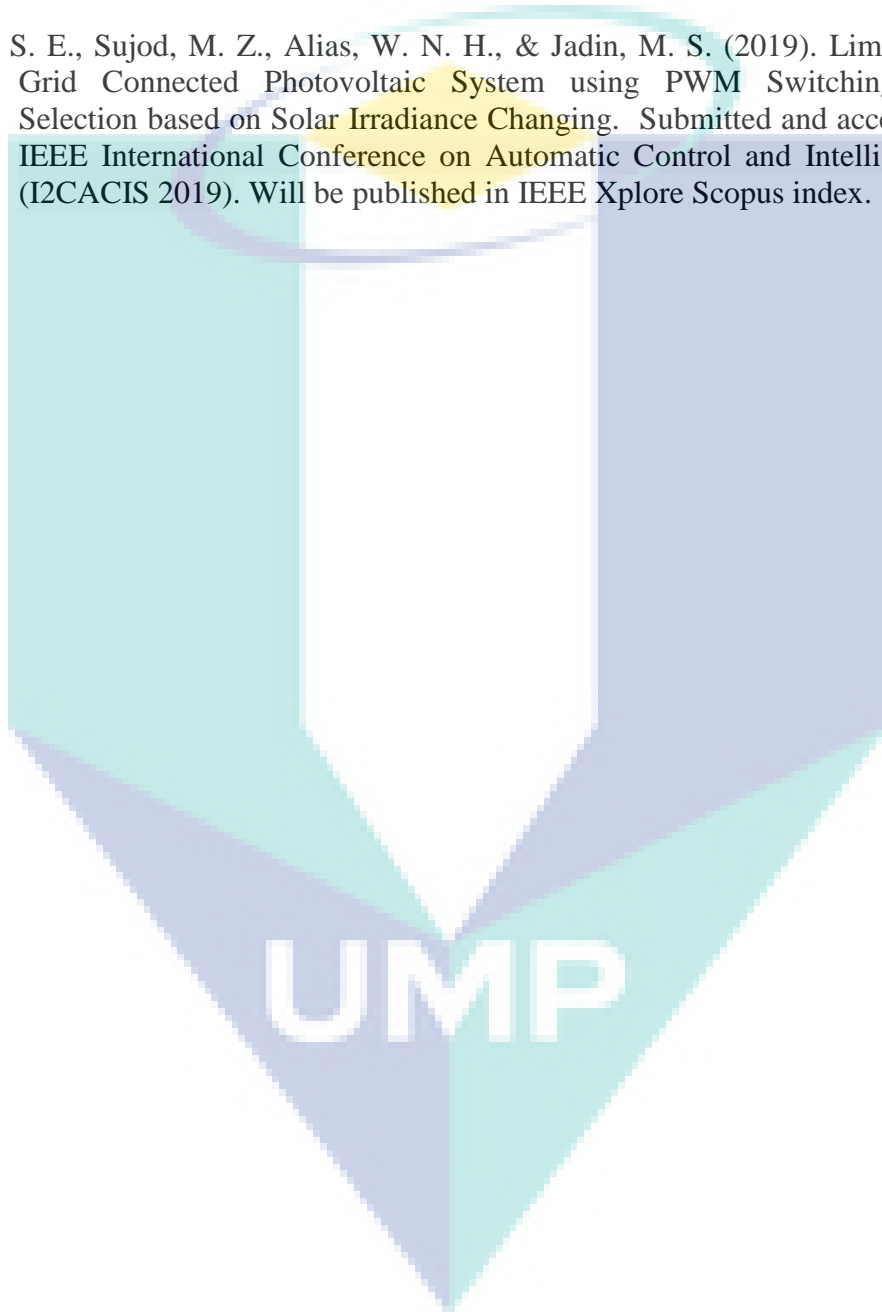
Zhao, X., & Liu, S. (2012). A Research of Harmonics for Multiple PV Inverters in Grid-Connected. *2012 Asia-Pacific Power and Energy Engineering Conference*, 1–4. <https://doi.org/10.1109/APPEEC.2012.6307197>



## PUBLICATIONS

Sabri, S. E., Sujod, M. Z., & Jadin, M. S. (2018). Comparative Study on the Performance of PV System with Various Combinations of Converter Topologies and PWM Types. *Journal of Telemcommunication, Electronic and Computer Engineering (JTEC)*, 10 (1-2), 25-29—29.

Sabri, S. E., Sujod, M. Z., Alias, W. N. H., & Jadin, M. S. (2019). Limiting THD of Grid Connected Photovoltaic System using PWM Switching Frequency Selection based on Solar Irradiance Changing. Submitted and accepted in 2019 IEEE International Conference on Automatic Control and Intelligent Systems (I2CACIS 2019). Will be published in IEEE Xplore Scopus index.



**APPENDIX A**  
**LIST OF CPWM CARRIER SIGNAL TRIAL TO FIND STANDARD THD**

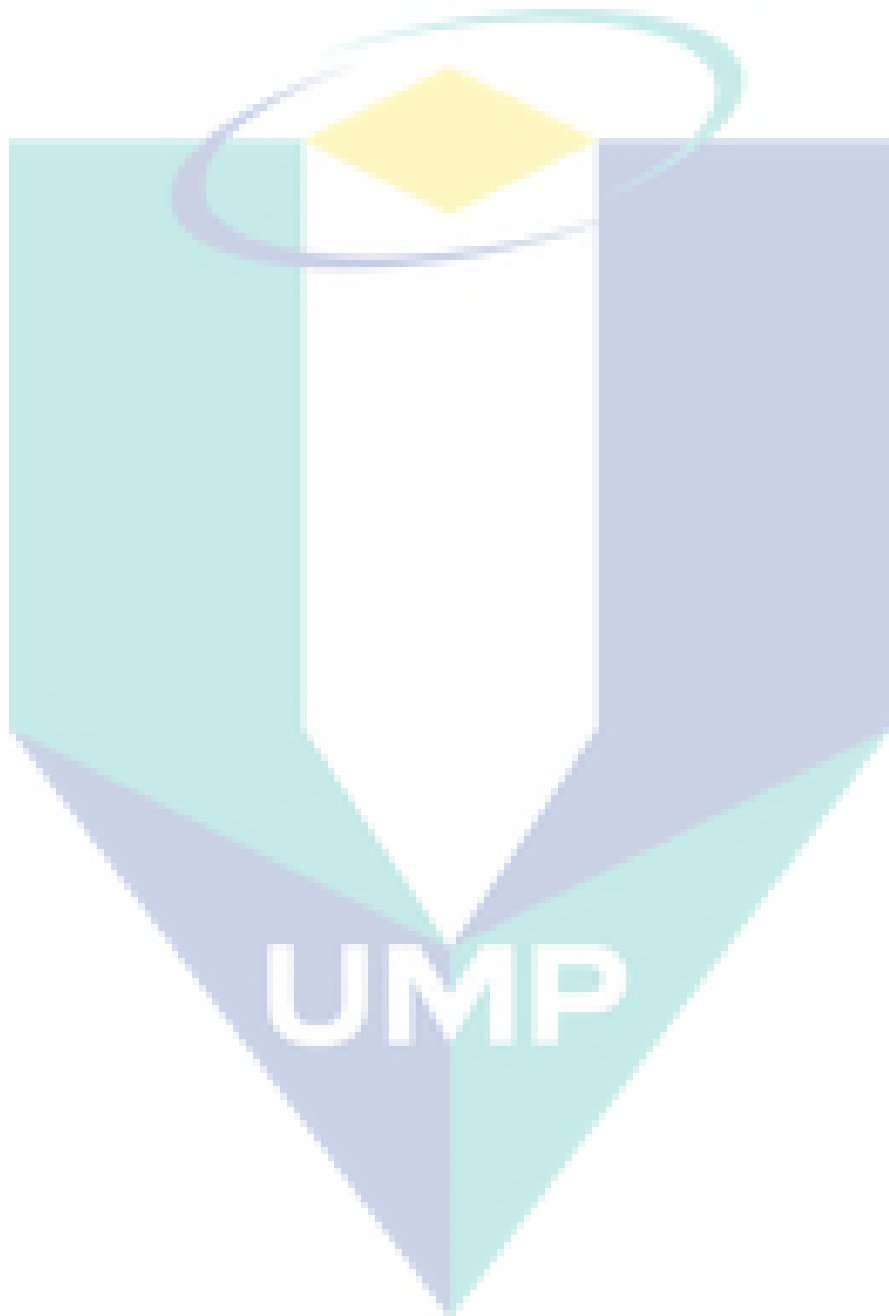
<b>Irradiance (W/m<sup>2</sup>)</b>	<b>Carrier Signal (Hz)</b>	<b>THDi (%)</b>	<b>Power, W (×10<sup>4</sup> )</b>	<b>Current (A)</b>
1000	1000	28.57	24.36	8.50
1000	1100	22.73	24.52	8.60
1000	1200	13.48	24.80	8.40
1000	1300	8.65	24.95	8.36
1000	1400	6.06	25.00	8.35
1000	1410	5.80	25.03	8.30
1000	1420	5.71	25.05	8.35
1000	1430	5.58	25.04	8.34
1000	1440	5.49	25.05	8.35
1000	1450	5.14	25.05	8.35
1000	1460	5.05	25.05	8.30
1000	1461	5.07	25.05	8.35
1000	1462	4.89	25.05	8.35
1000	1470	4.78	25.05	8.35
1000	1480	4.71	25.05	8.35
<b>Irradiance (W/m<sup>2</sup>)</b>	<b>Carrier Signal (Hz)</b>	<b>THDi (%)</b>	<b>Power, W (×10<sup>4</sup> )</b>	<b>Current (A)</b>
800	1000	35.63	19.35	7.50
800	1100	27.73	19.48	7.10
800	1200	16.48	19.76	6.95
800	1300	10.77	19.90	6.75
800	1400	7.51	19.98	6.70
800	1500	5.71	20.02	6.75
800	1510	5.59	20.00	6.65
800	1520	5.26	20.03	6.68
800	1530	5.33	20.04	6.70
800	1540	5.10	20.05	6.65
800	1545	5.09	20.05	6.60
800	1545.5	4.97	20.08	6.68
800	1550	4.79	20.03	6.60
800	1600	4.61	20.05	6.65



<b>Irradiance (W/m<sup>2</sup>)</b>	<b>Carrier Signal (Hz)</b>	<b>THDi (%)</b>	<b>Power, W (×10<sup>4</sup> )</b>	<b>Current (A)</b>
600	1000	48.29	14.25	6.50
600	1300	14.17	14.85	5.05
600	1500	7.35	14.95	5.02
600	1600	6.01	14.95	5.00
600	1700	5.50	14.98	5.06
600	1730	5.09	15.00	5.00
600	1740	5.26	14.98	5.00
600	1745	5.07	15.00	5.05
600	1746	4.44	14.98	5.00
600	1747	4.64	14.99	5.02
600	1748	4.32	15.00	5.03
<b>Irradiance (W/m<sup>2</sup>)</b>	<b>Carrier Signal (Hz)</b>	<b>THDi (%)</b>	<b>Power, W (×10<sup>4</sup> )</b>	<b>Current (A)</b>
400	1000	74.02	9.12	5.50
400	2000	6.35	9.88	3.38
400	3000	4.31	9.90	3.40
400	4000	6.21	9.92	3.25
400	4500	5.34	9.92	3.40
400	4700	5.09	9.92	3.60
400	4800	5.23	9.94	3.35
400	4850	5.63	9.93	3.20
400	4855	6.49	9.94	3.30
400	4955	7.40	9.99	3.50
400	5000	4.74	9.92	3.20
<b>Irradiance (W/m<sup>2</sup>)</b>	<b>Carrier Signal (Hz)</b>	<b>THDi (%)</b>	<b>Power, W (×10<sup>4</sup> )</b>	<b>Current (A)</b>
200	1000	176.83	4.03	4.65
200	2000	13.39	4.75	1.65
200	3000	8.98	4.79	1.70
200	4000	8.45	4.80	1.65
200	5000	11.15	4.85	1.70
200	6000	16.41	4.80	1.70
200	7000	12.46	4.80	1.60
200	8000	13.10	4.80	1.60
200	9000	17.60	4.80	2.00
200	10000	18.76	4.87	1.75
200	11000	19.85	4.80	1.90
200	12000	9.16	4.80	1.70

200	12010	10.82	4.80	1.65
200	12020	9.98	4.80	1.80
200	12030	9.87	4.80	1.70
200	12040	11.63	4.80	1.70
200	12050	9.15	4.80	1.70
200	12060	9.45	4.80	1.70
200	12070	12.41	4.80	1.70
200	12080	9.74	4.80	1.75
200	12090	12.75	4.80	1.65
200	12100	14.75	4.80	1.70
200	12200	10.69	4.80	1.70
200	12300	24.26	4.78	1.90
200	12400	30.28	4.80	2.40
200	12500	13.47	4.80	1.70
200	12550	9.40	4.80	1.70
200	12560	8.61	4.80	1.70
200	12570	8.19	4.80	1.65
200	12580	10.32	4.80	1.70
200	12585	12.66	4.80	1.65
200	12595	11.60	4.80	1.70
200	12600	7.68	4.80	1.70
200	12610	8.15	4.80	1.65
200	12650	10.92	4.80	1.70
200	12700	9.21	4.80	1.70
200	12800	11.51	4.80	1.70
200	12900	11.36	4.80	1.75
200	13000	10.72	4.80	1.65
200	14000	16.41	4.78	1.65
200	15000	10.91	4.77	1.75
200	16000	12.55	4.78	1.65
200	17000	12.54	4.80	1.70
200	18000	40.32	4.80	2.25
200	19000	10.01	4.80	1.65
200	20000	13.71	4.80	1.65
200	21000	13.63	4.80	1.70
200	22000	77.71	4.80	3.25
200	23000	10.92	4.80	1.65
200	24000	15.57	4.80	1.75
200	25000	11.64	4.80	1.70
200	26000	8.83	4.80	1.62
200	27000	23.75	4.80	2.25

200	28000	8.65	4.80	1.65
200	29000	11.04	4.80	1.65
200	30000	16.56	4.80	1.70



**APPENDIX B**  
**LIST OF DPWM CARRIER SIGNAL TRIAL TO FIND STANDARD THD**

<b>Irradiance (W/m<sup>2</sup>)</b>	<b>Carrier Signal (Hz)</b>	<b>THDi (%)</b>	<b>Power (×10<sup>4</sup>)</b>	<b>Current (A)</b>
1000	1000	64.17	22.50	12.00
1000	2000	15.72	24.90	7.95
1000	3000	5.28	25.10	8.40
1000	3500	7.51	25.10	8.20
1000	4000	7.58	25.15	7.95
1000	5000	6.49	25.18	8.10
1000	5500	5.17	25.20	8.00
1000	5600	4.26	25.18	8.20
1000	5700	5.50	25.20	8.30
1000	5800	3.74	25.20	8.40
<b>Irradiance (W/m<sup>2</sup>)</b>	<b>Carrier Signal (Hz)</b>	<b>THDi (%)</b>	<b>Power (×10<sup>4</sup>)</b>	<b>Current (A)</b>
800	1000	75.44	17.40	10.00
800	2000	17.88	19.90	7.50
800	3000	9.55	20.05	7.30
800	4000	6.89	20.10	6.50
800	4100	8.37	20.10	6.75
800	4200	3.64	20.10	7.00
800	4300	6.02	20.10	6.60
800	4400	8.54	20.10	6.50
800	4450	9.62	20.10	6.50
800	4455	8.89	20.10	6.70
800	4460	7.74	20.10	6.75
800	4465	7.46	20.10	6.75
800	4470	8.32	20.10	6.60
800	4475	7.36	20.10	6.70
800	4480	6.35	20.10	6.70
800	4485	8.73	20.10	6.70
800	5700	7.17	20.10	6.80
800	5745	6.85	20.10	6.75
800	6000	7.75	20.10	6.50
800	6500	4.82	20.10	6.60

<b>Irradiance (W/m<sup>2</sup>)</b>	<b>Carrier Signal (Hz)</b>	<b>THDi (%)</b>	<b>Power (×10<sup>4</sup>)</b>	<b>Current (A)</b>
600	1000	107.26	12.30	8.60
600	2000	21.28	14.80	5.50
600	3000	15.88	15.00	5.80
600	4000	11.70	15.00	5.00
600	4490	9.83	15.00	5.25
600	5000	7.69	15.03	5.35
600	5500	7.21	15.04	5.00
600	6000	6.56	15.10	5.10
600	6500	5.47	15.05	5.00
600	7000	5.57	15.10	5.10
600	7100	5.64	15.10	5.00
600	7200	8.89	15.06	5.00
600	7300	7.70	15.10	5.20
600	7400	6.43	15.00	5.10
600	7500	10.20	15.05	5.00
600	7600	5.99	15.00	5.00
600	7650	3.36	15.05	5.20
600	7700	4.89	15.10	5.10
600	7800	4.21	15.10	5.20
<b>Irradiance (W/m<sup>2</sup>)</b>	<b>Carrier Signal (Hz)</b>	<b>THDi (%)</b>	<b>Power (×10<sup>4</sup>)</b>	<b>Current (A)</b>
400	1000	194.75	7.30	6.85
400	2000	39.58	9.68	3.15
400	3000	8.15	9.90	3.50
400	4000	17.62	9.90	3.00
400	5000	14.81	9.90	3.50
400	6000	19.59	9.90	3.80
400	7000	11.39	9.90	3.50
400	7700	10.78	9.90	3.30
400	8000	12.12	9.90	3.15
400	8600	10.11	9.90	3.74
400	8700	11.21	9.90	3.45
400	8800	9.22	9.90	3.40
400	8900	10.16	9.90	3.45
400	8950	12.64	9.90	3.50
400	9000	4.02	9.90	3.60

<b>Irradiance (W/m<sup>2</sup>)</b>	<b>Carrier Signal (Hz)</b>	<b>THDi (%)</b>	<b>Power (×10<sup>4</sup> )</b>	<b>Current (A)</b>
200	1000	726.21	2.30	6.00
200	2000	11.69	4.55	2.50
200	3000	59.01	4.70	3.55
200	4000	31.98	4.80	1.95
200	5000	31.50	4.80	2.10
200	6000	28.24	4.80	2.00
200	7000	18.82	4.80	2.24
200	8000	20.33	4.80	1.65
200	9000	18.33	4.80	2.00
200	10000	20.92	4.80	1.75
200	11000	16.52	4.80	1.90
200	11111	20.91	4.80	1.70
200	11950	12.87	4.80	1.88
200	11955	15.96	4.80	1.80
200	11956	18.11	4.80	1.72
200	11957	10.45	4.80	1.70
200	11958	13.99	4.80	1.70
200	11959	12.29	4.80	1.70
200	11960	16.49	4.80	1.70
200	11970	13.84	4.80	1.71
200	11980	15.76	4.80	1.77
200	11990	17.64	4.80	1.80
200	11999	15.90	4.80	1.70
200	12000	9.01	4.80	1.85
200	12001	11.17	4.80	1.85
200	12005	9.95	4.80	1.85
200	12010	12.38	4.80	1.80
200	12020	17.88	4.80	1.80
200	12030	14.93	4.80	1.78
200	12040	14.70	4.80	1.70
200	12050	14.66	4.80	1.70
200	12060	11.21	4.80	1.70
200	12070	14.31	4.80	1.70
200	12080	11.62	4.80	1.70
200	12090	14.74	4.80	1.70
200	12100	10.67	4.80	1.65
200	12200	11.84	4.80	1.75
200	12300	22.19	4.80	1.60
200	12400	28.53	4.80	2.15
200	12500	14.46	4.80	1.80

200	12600	18.82	4.80	1.70
200	12700	11.47	4.80	1.75
200	12800	14.65	4.80	1.75
200	12900	15.47	4.80	1.80
200	13000	17.19	4.80	1.82
200	13050	21.11	4.80	1.70
200	13500	8.64	4.80	1.75
200	13550	11.95	4.80	1.80
200	14000	16.35	4.80	1.89
200	14500	13.73	4.80	1.80
200	15000	11.56	4.80	1.86
200	15500	12.75	4.80	1.75
200	16000	15.62	4.80	1.68
200	16500	31.98	4.80	2.30
200	17000	14.65	4.80	1.82
200	17500	15.97	4.80	1.85
200	18000	21.19	4.80	2.50
200	18500	13.98	4.80	1.70
200	19000	10.46	4.80	1.68
200	19500	9.38	4.80	1.65
200	20000	18.48	4.80	1.50
200	20500	16.14	4.80	1.85
200	21000	13.31	4.80	1.60
200	21500	14.94	4.80	1.70
200	22000	38.04	4.80	3.00
200	22500	9.48	4.80	1.75
200	23000	9.03	4.80	1.70
200	23001	10.26	4.80	1.70
200	23002	9.46	4.80	1.75
200	23003	13.18	4.80	1.70
200	23004	8.37	4.80	1.75
200	23005	11.35	4.80	1.70
200	23006	9.03	4.80	1.70
200	23007	10.62	4.80	1.70
200	23008	9.93	4.80	1.80
200	23009	10.21	4.80	1.70
200	23010	8.97	4.80	1.67
200	23011	12.82	4.80	1.70
200	23012	12.67	4.80	1.70
200	23013	9.38	4.80	1.70
200	23014	8.12	4.80	1.70

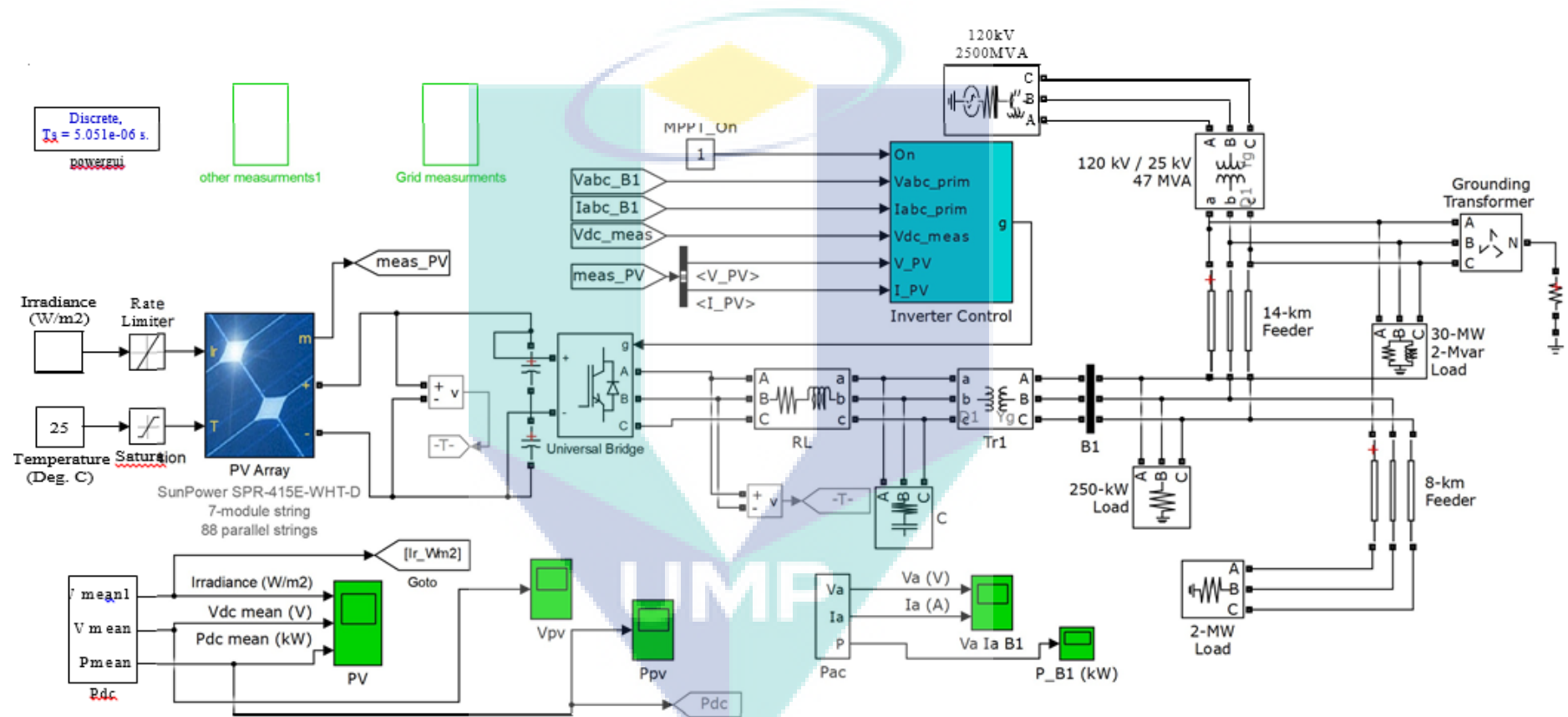
200	23015	10.26	4.80	1.70
200	23016	8.17	4.80	1.70
200	23017	8.60	4.80	1.70
200	23018	8.41	4.80	1.65
200	23019	9.69	4.80	1.65
200	23020	9.12	4.80	1.70
200	23021	9.71	4.80	1.75
200	23022	9.19	4.80	1.70
200	23023	10.56	4.80	1.70
200	23024	10.50	4.80	1.65
200	23025	9.45	4.80	1.65
200	23026	9.94	4.80	1.65
200	23027	9.58	4.80	1.65
200	23028	9.47	4.80	1.66
200	23029	8.88	4.80	1.64
200	23030	10.41	4.80	1.70
200	23031	11.57	4.80	1.70
200	23032	9.84	4.80	1.70
200	23033	7.97	4.80	1.65
200	23034	9.70	4.80	1.70
200	23035	11.79	4.80	1.70
200	23036	9.43	4.80	1.70
200	23037	13.02	4.80	1.70
200	23038	7.00	4.80	1.65
200	23039	8.27	4.80	1.70
200	23040	8.35	4.80	1.65
200	23045	11.18	4.80	1.65
200	23050	8.76	4.80	1.65
200	23055	9.40	4.80	1.70
200	23060	11.48	4.80	1.70
200	23065	12.45	4.80	1.00
200	23070	7.43	4.80	1.65
200	23075	8.19	4.80	1.65
200	23080	11.00	4.80	1.70
200	23085	7.51	4.80	1.70
200	23090	8.17	4.80	1.65
200	23095	8.72	4.80	4.65
200	23100	11.47	4.78	1.60
200	23150	16.79	4.80	1.70
200	23200	28.07	4.80	1.96
200	23250	17.02	4.80	1.80



200	23300	22.41	4.80	1.95
200	23350	19.50	4.80	1.85
200	23400	17.96	4.80	1.70
200	23450	9.91	4.80	1.65
200	23500	9.84	4.80	1.60
200	23510	9.83	4.80	1.65
200	23520	11.42	4.80	1.70
200	23530	11.64	4.80	1.70
200	23540	9.00	4.80	1.65
200	23541	8.78	4.80	1.70
200	23542	7.65	4.80	1.60
200	23543	9.15	4.80	1.73
200	23544	8.07	4.80	1.65
200	23544.5	8.06	4.80	1.70
200	23545	8.92	4.80	1.75
200	23545.1	8.92	4.80	1.73
200	23545.5	11.18	4.80	1.70
200	23546	12.12	4.80	1.70
200	23547	9.34	4.80	1.70
200	23548	8.90	4.80	1.70
200	23549	14.48	4.80	1.75
200	23549.5	11.02	4.80	1.65
200	23550	6.81	4.80	1.70
200	23551	8.81	4.80	1.69

UMP

## APPENDIX C GCPV SYSTEM MODEL MATLAB/SIMULINK CIRCUIT



## APPENDIX D INVERTER CONTROL WITH CPWM

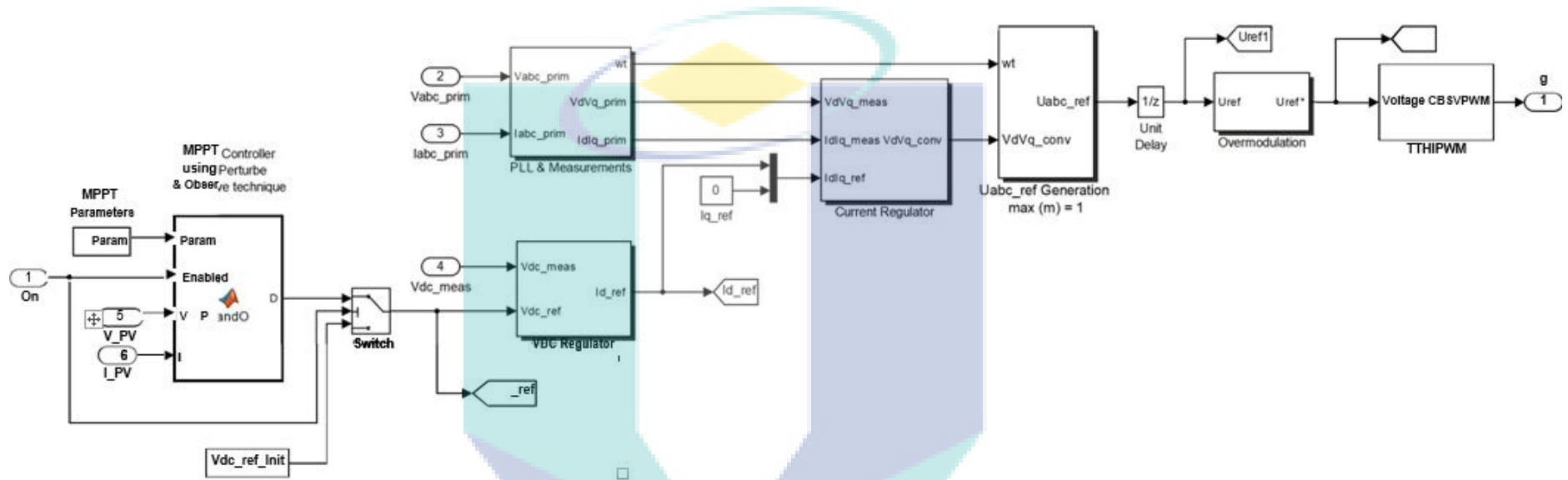


Figure D.1 Inverter control with CPWM MATLAB/Simulink circuit

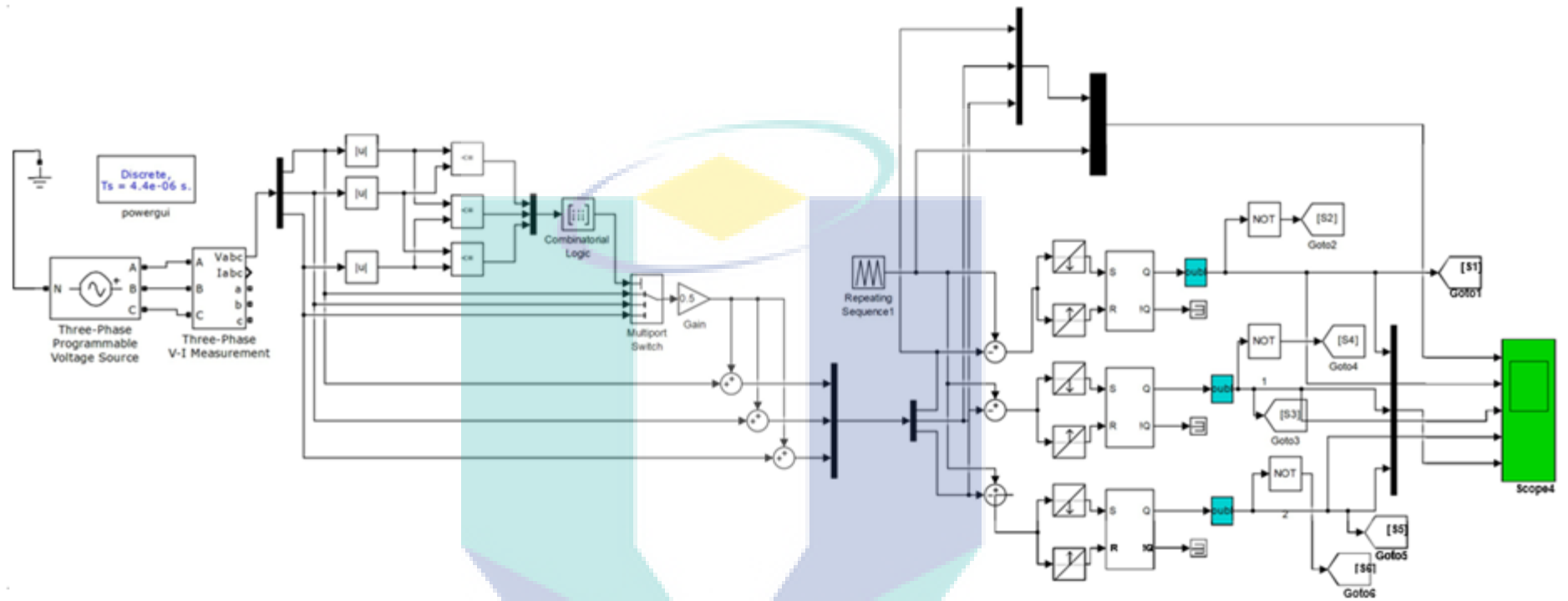


Figure D.2 CPWM MATLAB/Simulink circuit

UMP

## APPENDIX E INVERTER CONTROL WITH DPWM

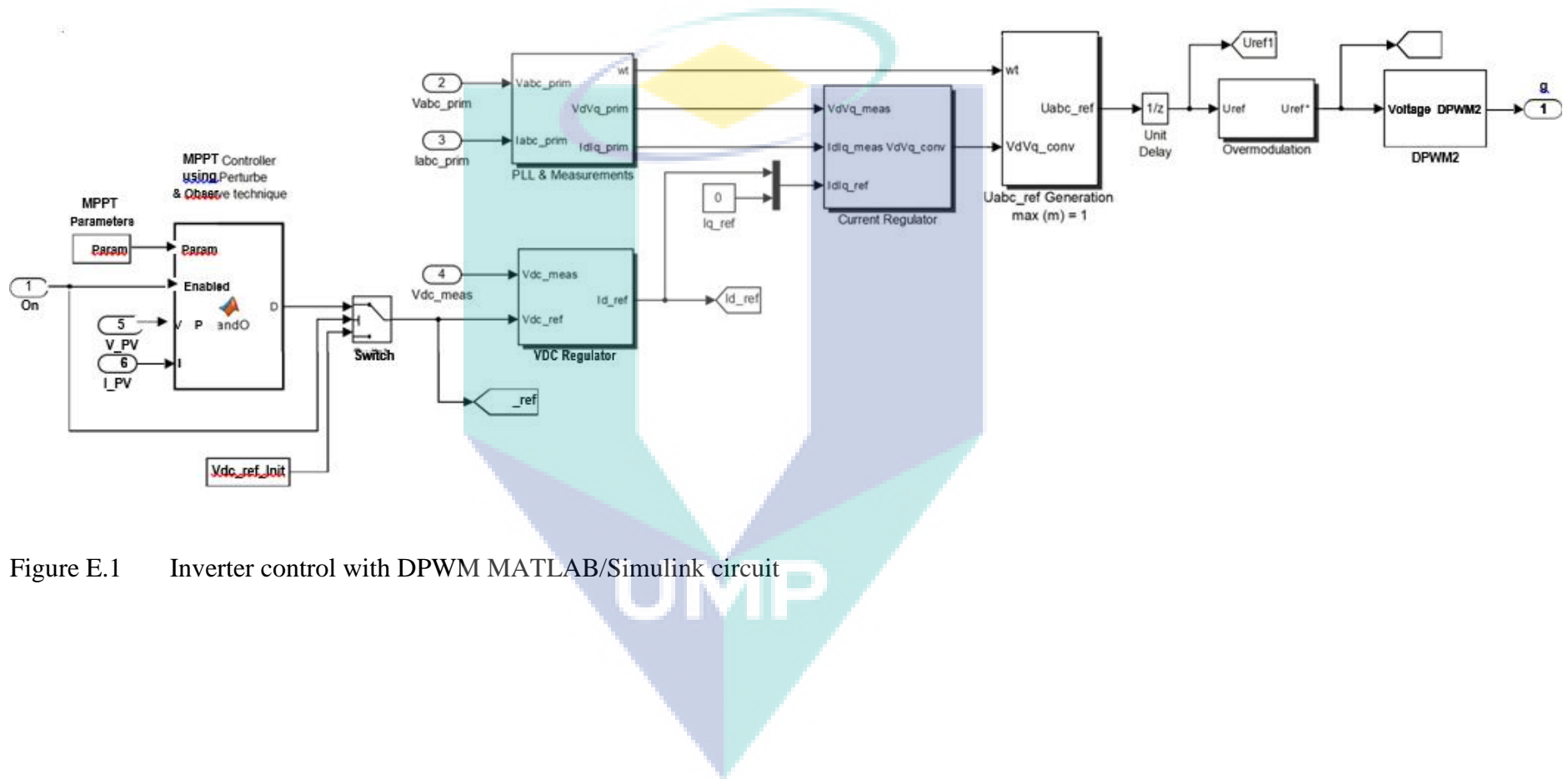


Figure E.1 Inverter control with DPWM MATLAB/Simulink circuit

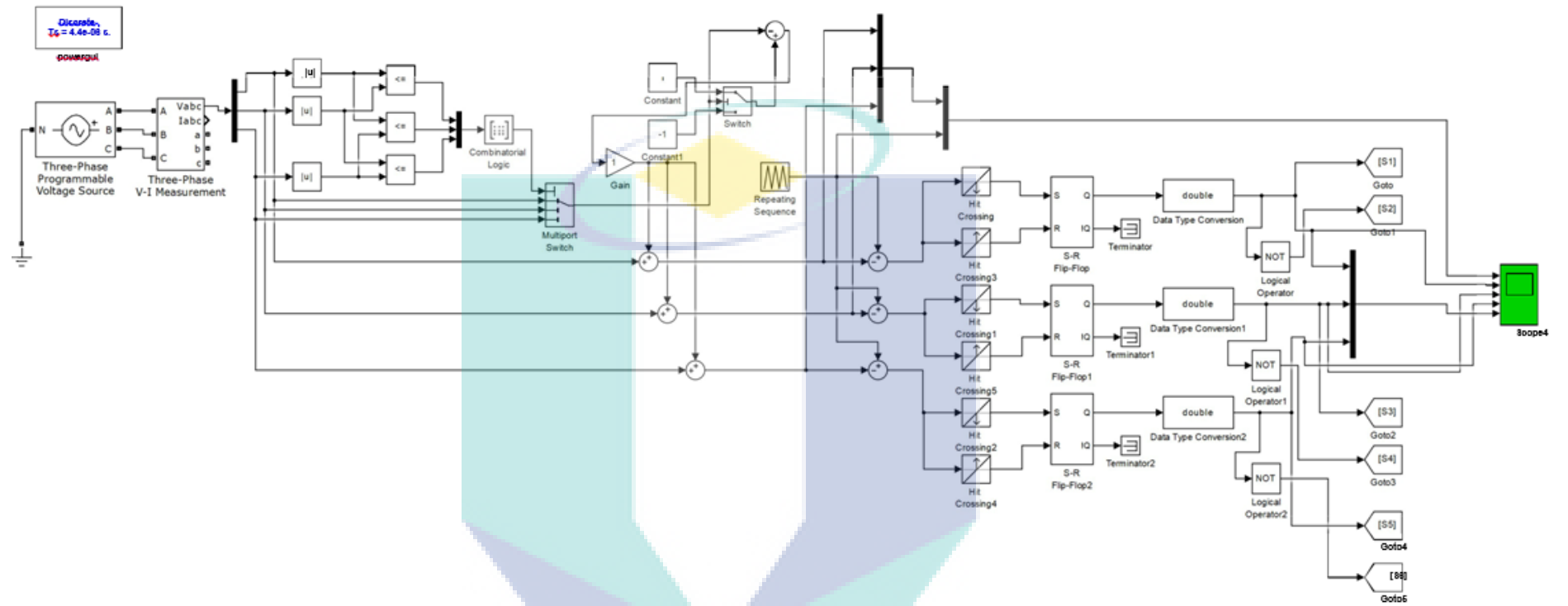


Figure E.2 DPWM MATLAB/Simulink circuit